공학박사학위논문

Study on the engine control using the in-cylinder pressure in Diesel engine

실린더 연소압을 이용한 디젤엔진의 실시간 제어에 관한 연구

2012년 8월

서울대학교 대학원

기계항공공학부

유 성 은

Study on the engine control using the in-cylinder pressure in Diesel engine

지도교수 민 경 덕

이 논문을 공학박사 학위논문으로 제출함

2012년 8월

서울대학교 대학원

기계항공공학부

유 성 은

유성은의 공학박사 학위논문을 인준함

2012년 5월

위 원 장 고 상 근 (인)

부위원장 민 경 덕 (인)

위 원 송 한 호 (인)

위 원 이 동 준 (인)

위 원 이 진 욱 (인)

Acknowledgements

First and foremost, I would like to express my respect and gratitude to my advisor, Professor Kyoungdoug Min. During the six years of graduate course, my knowledge and personality were grown up with his invaluable advices. He gave the inspirations of this study and his guidance and encouragement were the source of power overcoming many difficulties during the project.

I would like to special thanks to the project members who offered assistance, valuable discussions and beautiful memories of friendship. Junyong Lee gave many ideas to found an EGR rate estimation model, Seunghyun Lee and Seungha Lee assisted the engine test. This work would never have been achieved without their efforts and patients.

It was an honor to have the opportunity to work with Hyundai motor company and I appreciated the financial, material supports and comments from plentiful experiences on engine development.

I would like to present my deepest respect and gratitude to my family. My parents, Gwangyul Yu and Younghee Jung devoted themselves to me with great sacrifice, thoughtful consideration, unimaginable patience, and endless love. I extended my thanks to Jiyeon Yu and Minji Yu my lovely sisters for her thoughtful consideration. And my beloved fiancé was my emotional anchor and supported my long school days with infinite faith and boundless love. It was, it is, and it will be the greatest happiness in my life to be with her.

Abstract

Study on the engine control using the in-cylinder pressure in Diesel engine

Seungeun Yu
School of Mechanical and Aerospace Engineering
The Graduate School
Seoul National University

In these days, emission regulations have been becoming more severe and they remain a principal issue for vehicle manufacturers. Many engine subsystems and control technologies have been introduced to meet the demands of these regulations. For Diesel engines, combustion control is one of the most effective approaches to reduce not only engine exhaust emissions but also to cope with degradation of engine performance due to component deterioration. Moreover, thanks to the technology development and mass production, the cost of a pressure sensor can be lower.

In this study, cylinder-pressure-based engine control logic is introduced for a multi-cylinder Diesel engine. The time for 50% of the mass fraction burned (MFB50) and the IMEP are valuable for identifying combustion status. Maximum cylinder pressure is meaningful for extending engine durability. Also, an EGR rate is estimated by using the ECU information and in-cylinder pressure.

These in-cylinder quantities are measured and applied to the engine control logic. Main injection timing is controlled to adjust the operating MFB50 to the target MFB50 with PID control logic from low to medium load and it is controlled to suppress the maximum cylinder pressure below a certain level. Fuel injection quantity is controlled to adjust the measured IMEP to the desired IMEP. The effect of control logic is demonstrated at transient conditions and applied to an NEDC mode test. The emission peak at transient is minimized and emission level in transient state maintained that in steady state. Combustion control logic can also compensate the deterioration of fuel injector during the operation due to the aging or damaging.

Keywords: Direct injection Diesel engine, Model based control, Closed loop control, Exhaust emission Transient condition, Injector deterioration

Student Number: 2005-23445

CONTENTS

List of Tables

List of Figures

Acronym

A/F	Air to Fuel ratio
ASCET	Advanced Simulation/Software and Control Engineering Tool
ATDC	After Top Dead Center
BDC	Bottom Dead Center
BDF	Bio Diesel Fuel
BMEP	Brake Mean Effective Pressure
BTDC	Before Top Dead Center
CA	Crank Angle
CA50	Crank Angle of 50 % mass fraction fuel burnt
CAFE	Corporate Average Fuel Economy
CAI	Controlled Auto Ignition
CAN	Controller Area Network
CI	Compression Ignition
CPS	Crank Position Sensor
DI	Direct Injection
DPF	Diesel Particulate Filter
ECU	Engine Control Unit
EGR	Exhaust Gas Recirculation
EUDC	Extra Urban Driving Cycle
EVC	Exhaust Valve Close
EVO	Exhaust Valve Open
FS	Full Scale
FSN	Filter Smoke Number
GDI	Gasoline Direct Injection
GVWR	Gross Vehicle Weight Rating
HC	HydroCarbon
HRR	Hear Release Rate

HSDI	High Speed Direct Injection
HT	Heat Transfer
IMEP	Indicated Mean Effective Pressure
IQA	Injector Quantity Adjustment
IVC	Intake Valve Close
IVO	Intake Valve Open
LNT	Lean NOx Trap
LTC	Low Temperature Combustion
MFB10	Mass Fraction Burned 10 %
MFB50	Mass Fraction Burned 50 %
MFB90	Mass Fraction Burned 90 %
MIT	Main Injection Timing
MK	Modulated Kinetics
mpg	Miles Per Gallon
NDIR	Non-Dispersive InfraRed Sensor
NEDC	New European Driving Cycle
NOx	Nitrogen Oxide
NSC	NOx Storage Catalyst
PID	Proportional, Integral and Derivative
PM	Particulate Matter
RBFN	Radial Basis Function Network
RG	Residual Gas
RGF	Residual Gas Fraction
RPM	Revolution Per Minute
RSM	Response Surface Method
SCR	Selective Catalytic Reduction
SI	Spark Ignition
SoC	Start of Combustion
TDC	Top Dead Center
TDI	Turbocharged Direct Injection

THC	Total Hydrocarbon
TTL	Transistor-Transistor Logic
UEGO	Universal Exhaust Gas Oxygen
VGT	Variable Geometry Turbine

Chapter 1. Introduction

1.1 Research background

1.1.1 Emissions regulations

Direct-injection (DI) Diesel engines have advantages such as high fuel economy, affordable cost and excellent reliability compared to other internal combustion engines. Especially, a high speed direct injection (HSDI) Diesel engine is gaining recognition due to the potential for realization of low emissions and high fuel efficiency. Recent HSDI engines achieved higher specific power and fuel efficiency than the previous engines by using high injection pressure systems developed from an improved fuel injection system and an advanced air charging technology like a turbocharger and an intercooler. Moreover, the noise level was also improved due to an application of a common rail injection system. Therefore, an HSDI Diesel engine has been served in both light-duty and heavy-duty vehicles, and increased market share rapidly [1].

However, each country introduces tough emissions legislation annually and discusses even tougher emissions legislation roadmap for a long term view. This tougher legislation gives huge pressure on automotive companies. Figure 1.1 shows

the emissions regulations for light-duty diesel engines. For example, Tier2 Bin5 regulation in the US restricts NOx and soot emissions by 0.043 g/km and 0.006 g/km, respectively. Due to a characteristic of a Diesel engine, reducing both NOx and soot emissions requires intensive research since NOx and soot emissions have trade-off relationship. The current emission legislation in Europe, Euro 5, restricts the soot emission by 0.003 g/km and the new up-coming legislation, Euro 6 which will be executed in 2014, restricts the NOx emission by 0.08 g/km [2-4].

Along with the exhaust gas restriction, CO_2 emission regulation is also in enforcement as a new sort of legislation. The CO_2 emission regulation has the same effect as restricting fuel efficiency as the emission of CO_2 increases with an increase in fuel consumption. Automotive companies set their development target in accordance with American CAFÉ (Corporate Average Fuel Economy) and European CO_2 emission regulations. The 2007 Energy Independence and Security Act mandates a 40% increase in CAFE by 2020. The new law began to take effect in 2011. It specified annual increase in light duty vehicle fleet (<10,000 lbs GVWR) fuel economy with a final standard of 35 mpg (14.9 km/L). In Europe, CO_2 emission regulation is determined by the weight of car. The acceptable CO_2 emission is 130 g/km for every 1289 kg of the weight and, by 2020, the emission restriction is going to be tougher such that the acceptable CO_2 emission is 95 g/km for every 1289 kg [4,

5].

In order to reduce the tail-pipe emissions, several after-treatment systems have been developed these days. For example, a DPF (Diesel Particulate Filter) for collecting and removing soot, a storage type NOx reduction catalyst called an LNT (Lean NOx Trap) or an NSC (NOx Storage Catalyst) and a NOx reduction catalyst called a urea SCR (Selective Catalytic Reduction) were employed in addition to an oxidation catalyst as an after-treatment system that could be used on a lean burning diesel engine [6]. However, the application of these systems causes increase in the vehicle's weight, complicated system and high cost. Improvement in the fuel quality is another way to reduce emissions. The advanced countries are engaged in the reduction of sulfur content of diesel fuel, which is highly essential for introducing exhaust emission reduction technology. However, it is difficult to use in the developing countries because ultra-low sulfur diesel fuel is expensive. Also, several kinds of biofuel, which are renewable carbon neutral fuels, are studied and introduced all over the world. In Europe, a 5% mixture of rapeseed oil base and, in the U.S., a 20% mixture of soybean oil is accepted on the market as BDF (Bio Diesel Fuel). In the developing countries, especially some Asian countries, there are actual actions to introduce palm or coconut oil base BDF on the market. However, on the subject of manufacture of BDF, the balance between food and feed has to be

taken into consideration, so opinions to the effect that care should be exercised are starting to be voiced [7].

Thus, reducing engine-out emissions is the most effective way to decrease tail-pipe emissions. For reducing engine-out emissions, an accurate understanding of emission formation mechanisms is important. The reasons of the emission formation of the Diesel engine are high flame temperature and non-homogeneous distribution of AF ratio. Most of NOx emissions are produced by a thermal NOx reaction and the reaction rate depends on flame temperature. Since NOx reaction rate is slower than combustion reaction rate, NOx emission can be reduced with keeping combustion temperature low after combustion process. On the other hand, if fuel is injected continuously after ignition, rich regions ($\Phi = 4 \sim 5$) are formed by rapid vaporization in flame area, which causes soot formation. Meanwhile, soot oxidation rate also depends on flame temperature. For this reason, there is a trade-off relation between NOx and soot of existing HSDI engines [1].

An open-loop control system lacks at countering any changes occurred during production- such as variation in produced components- and running- such as aging of components characteristics of fuels and environmental changes. Also, at the moment, it takes a long time for calibration and mapping to maximize the performance of a newly developed engine. Unlike open-loop systems, a closed-loop

control is more flexible at coping with unexpected changes imposed on the system which helps to reduce cost and time spent on engine development. In addition, it allows an easier approach for pre-mixed fuels such as bio-diesel. Combustion control can be one of solutions to reduce both emissions simultaneously [8, 9].

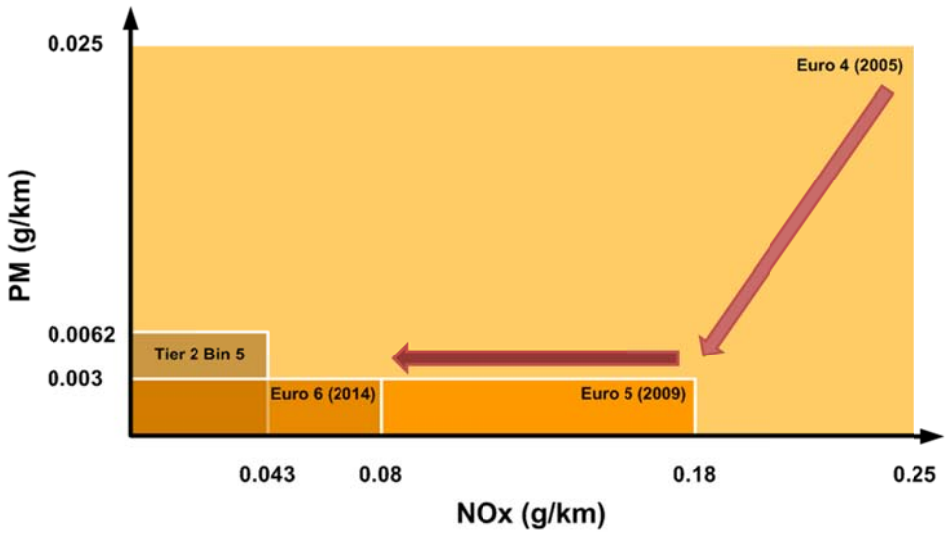

Figure 1.1 Emissions Regulations [2]

1.1.2 Emissions characteristics in transient condition

A transient engine operation is a significant source of regulated exhaust emissions and the nature of emission formation during a transient engine operation must be more closely investigated. These days, many exhaust gas measurement systems are developed to cope with not only in steady state but also transient state. These

advanced measurement systems give circumstances to investigate the impact of a dynamic engine operation on emissions. Both NOx and soot emissions are characterized by a significant increase in instantaneous emission levels as the ramp-up time became shorter. Peak level of NOx emissions occurs when a step load change is applied for constant speed and constant torque cases, especially at low EGR levels. Peak level of soot emission is an order of magnitude greater than steady state values during the step change in torque. In the case of NOx, it is primarily the lag between increased fueling and the response of the air-charging system, as well as the EGR starvation during the first instances. The injection pressure and exhaust pressure history have a secondary impact. When it comes to soot, the very first part of the transient initiated by a step change of fueling command seems to be critical. Lack of air due to turbo lag, poor mixing, increased wall impingement and the surplus of EGR at the very beginning of the event are to blame. The overall emissions of an engine can clearly be reduced by limiting the rate at which the engine load is applied, however this would come with a drivability penalty. However, it can be overcome with the injection control through the in-cylinder pressure monitoring which contains information of combustion status. Kirchen *et al.* revealed that soot emissions was seen to increase with decreasing transient duration and was less evident at the higher engine speed [10]. Soot emission during different tip-in duration is shown in Figure 1.2. Similar to the acceleration transients, a large

variability of up to ±50% in the soot emissions was seen from one repetition of the transient to the next. Hagena *et al.* analyzed diesel emissions during a tip-in transient condition [11]. Figure 1.3 shows that as the rate of pedal position change increases, the emissions of NOx and particulates are affected dramatically. An instantaneous load increase was found to produce peak NOx values 1.8 times higher and peak particulate concentrations an order of magnitude above levels corresponding to a smooth ramp-up. Kang *et al.* focused on NOx and HC emissions at transient engine operating conditions [12]. The highest peak NOx emissions occurred for a step load change. HC was increased a little at advanced injection timings and increased substantially for increased EGR valve opening for the constant torque case. However, there were small effects on HC and NOx of a step load change when the EGR valve was set to a large opening for the constant speed case.

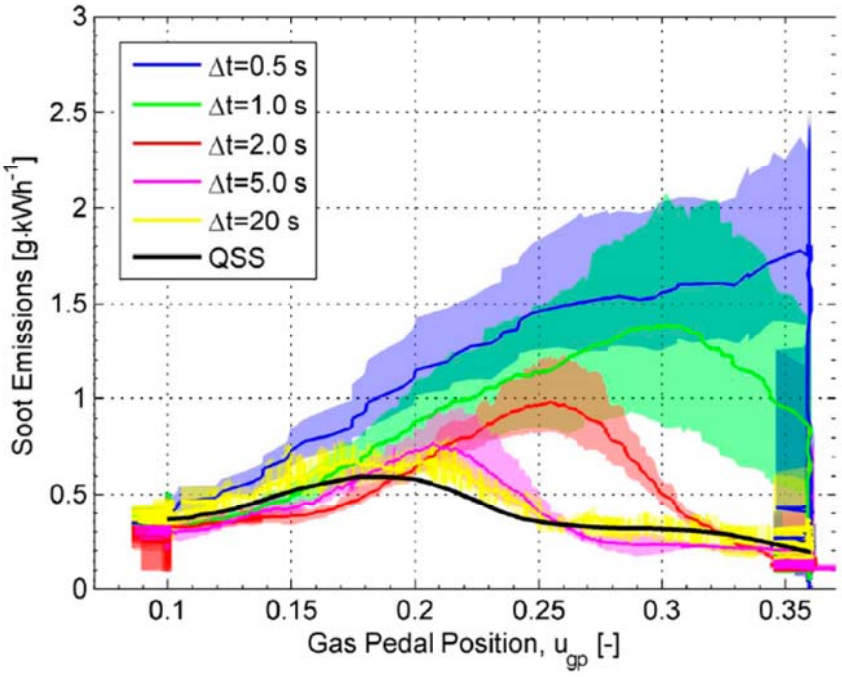

Figure 1.2 Measured soot emissions at exhaust stream during tip-in and transients of different durations [10]

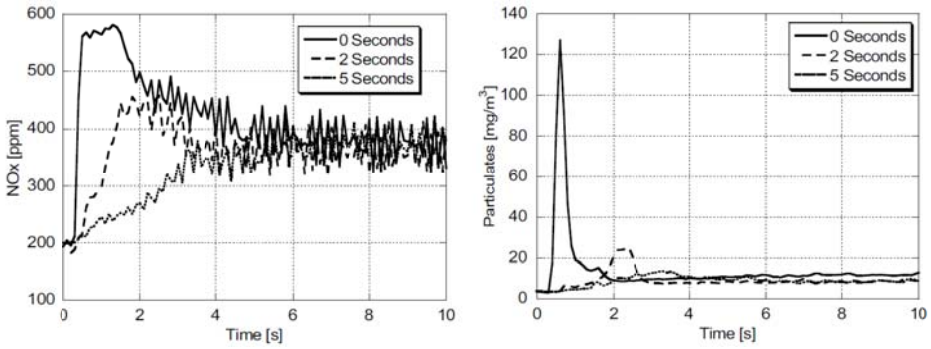

Figure 1.3 NOx and PM emission during transient load step at 2000 rpm [11]

1.1.3 Real-time EGR estimation

It is essential for the real-time engine control to know the state of in-cylinder cycle-by-cycle. One of the most important in-cylinder information is composition of induced gas, the EGR rate, because it affects in-cylinder combustion significantly. Therefore, there were many researches to estimate the EGR rate in offline and online, in real-time.

Youssef *et al.* suggests a new method for in-cylinder trapped mass estimation, using instantaneous cylinder pressure measurements as an input [13]. The method is based on a graphical signature generation tool, proposed for diagnosis and parametric estimation of nonlinear systems. Figure 1.4 shows the example plot of signature generated from cylinder pressure measurement. A two dimensional graphical signature is generated from measured cylinder pressure. It is shown that generated signature is correlated with the value of trapped mass. Worm examined several methods by which the air mass trapped within the cylinder could be computed on a cycle by cycle basis during a transient operation of the engine [14]. The strengths and weaknesses, relative to transient analysis, were pointed out for each method. Application of the ideal gas law to both inside the cylinder and the intake manifold has the potential to provide very accurate results with minimal computational effort. Although computationally the simplest, the A/F method's

major weakness is in knowing how much of the injected fuel was ingested into the cylinder. The iterative approach of Mladek and Onder has the potential to be not only very accurate on a cylinder by cylinder basis but requires virtually no pre-work to use the method [15]. Figure 1.5 shows the comparison between the residual gas fraction of the first estimation results and the iteration results. Its largest disadvantage is that it is computationally the most intensive. The Delta P method is computationally very simple. The delta P method should be avoided for general usage with a cam phaser and EGR equipped engines. Colin *et al.* proposed an algorithm to estimate the fresh air mass, based on physical equations, which estimates the in-cylinder total mass based on cylinder pressure in a gasoline engine [16]. They applied the delta p method to estimate the mass of in-cylinder gas. A residual gas model, which computes the burned gas fraction, is then used to determine the fresh air mass. Desantes *et al.* applied the delta p method in a turbo charged diesel engine [17]. However, an EGR rate is measured by the NDIR-based CO_2 concentration measurement tool. Klein *et al.* developed an empirical model that calculates the EGR ratio as a function of the engine speed, the engine load and special characteristics of the heat release rate [18]. The ignition delay, the premixed combustion ratio and the mixing-controlled combustion ratio correlate with the EGR ratio. The empirical function is a 2^{nd} order correlation equation using above parameters. Chauvin *et al.* developed an air path estimation model on a HCCI

engine [19]. Mass balance, energy balance equations and ideal gas law are used basically. Mass flow rate of EGR gas is estimated with an effective flow area of EGR valve and a constant. The constant is depending on the exhaust temperature, the pressure ratio between intake and exhaust manifold, and the behavior of the EGR cooling system. Park *et al.* proposes a cylinder air charge estimation algorithm for a diesel engine equipped with variable geometry turbocharger, exhaust gas recirculation and swirl control valve [20]. The estimation algorithm predicts the cylinder air charge by using a mean value air path model. The EGR mass flow was derived from the intake manifold energy balance equation. Lee *et al.* introduced a mean value engine model, using an empting and filling model [21]. They used the variables that measured in mass-produced engines. However, variables that are not measured are estimated by an engine model. Wahlstrom *et al.* introduced a mean value model of a diesel engine with VGT and EGR [22]. They calculated EGR gas flow rates by using orifice flow equations. However, a theoretical equation could not reflect an EGR flow rate status because of unstable flow condition and influence of EGR cooler. To simplify the model, the approximating equation is introduced. Park et al. also applied the orifice flow equation [23]. However, he adapted the effective flow area of EGR valve to compensate the difference between ideal EGR mass flow rate and real EGR mass flow rate. Eck *et al.* proposed a fault detection system for the air path of a diesel engine, using low pressure EGR [24]. As the first step of the

system, a model was developed to detect and isolate typical faults in the air path of common rail diesel engines with high as well as low pressure exhaust gas recirculation. Mass flow rate of EGR gas is calculated by the orifice flow equation and he also applied a correlation factor to match the estimated value to the measured value. Darlington *et al.* developed a sampling valve system using a modified injector from a GDI engine [25]. A sample of the compression gas from one of the cylinders was extracted on a cycle-by-cycle basis. The CO_2 concentration of this sample was then measured by using a fast gas analyzer. Welling *et al.* introduced UEGO sensor modified for fast response to measure EGR and RGF rate [26]. Figure 1.6 shows the EGR fraction measurement comparison for NDIR and UEGO method. UEGO sensor is installed at both intake manifold and exhaust manifold, and EGR rate is calculated by using the measured relative A/F ratio of two UEGO sensors. Han *et al.* introduced the temperature based EGR rate measuring system and the technique is based upon the law of conservation of energy [27]. Figure 1.7 shows the measured EGR rate from temperature based system. When the heat losses are neglected, all the energy lost from the EGR gas has been transferred to the intake air. To measure the temperature in transient state, a fast response thermocouple which has 5 ms of response time is introduced. Molar specific heat of fresh air and EGR gas are approximately equal and, hence, EGR rate calculation could be simplified.

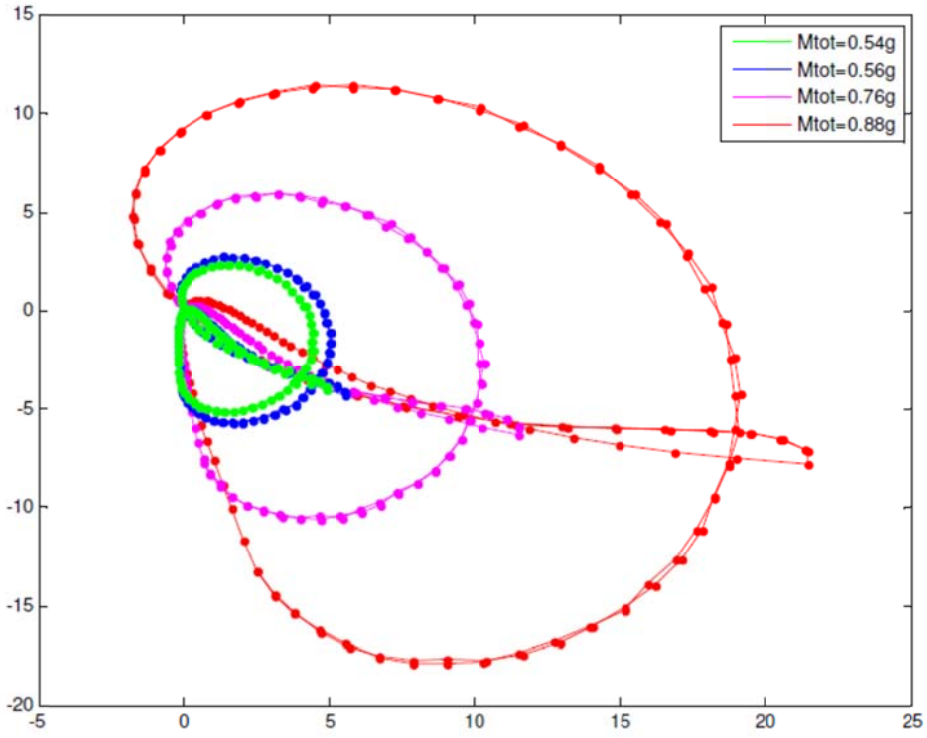

Figure 1.4 Signature generated from cylinder pressure measurement [13]

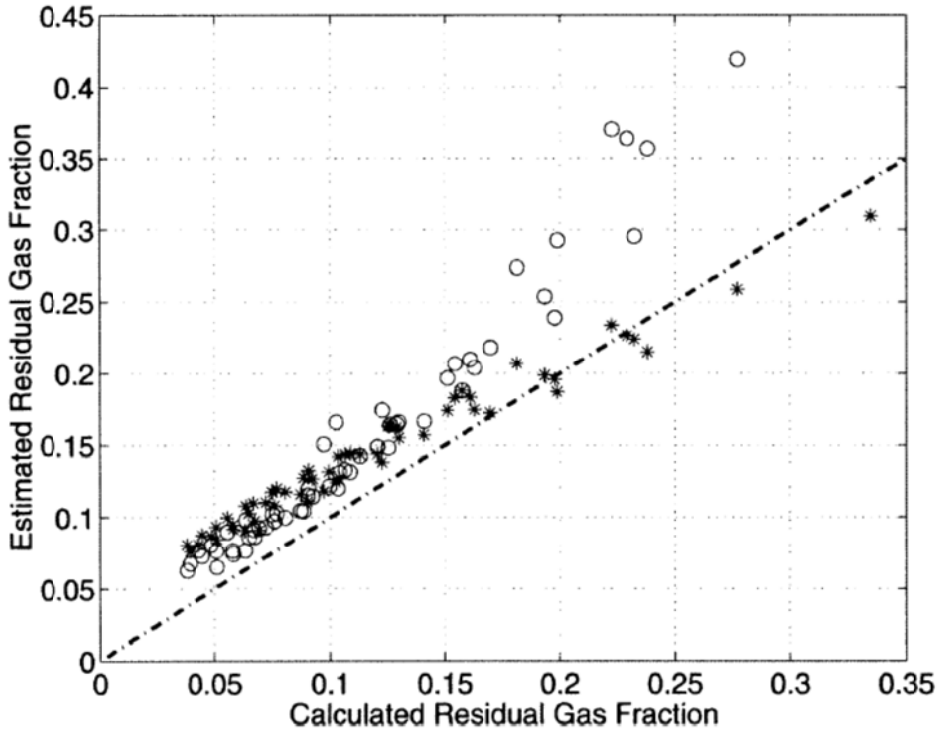

Figure 1.5 Estimated residual gas fraction (first estimation results <marked 'o'> and iteration results <marked '*'>) [15]

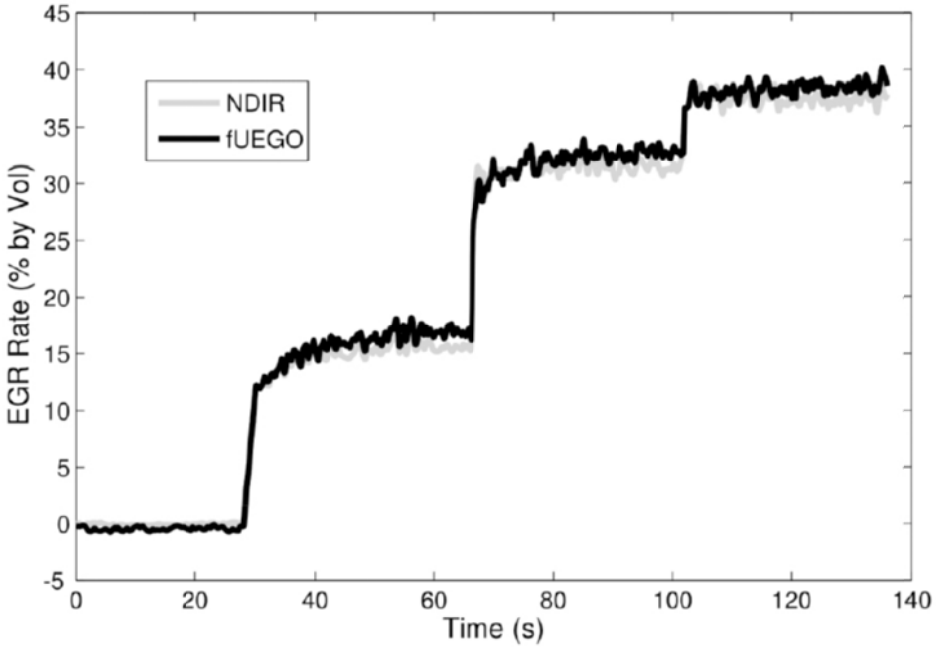

Figure 1.6 EGR fraction measurement comparison for NDIR and fUEGO methods [26]

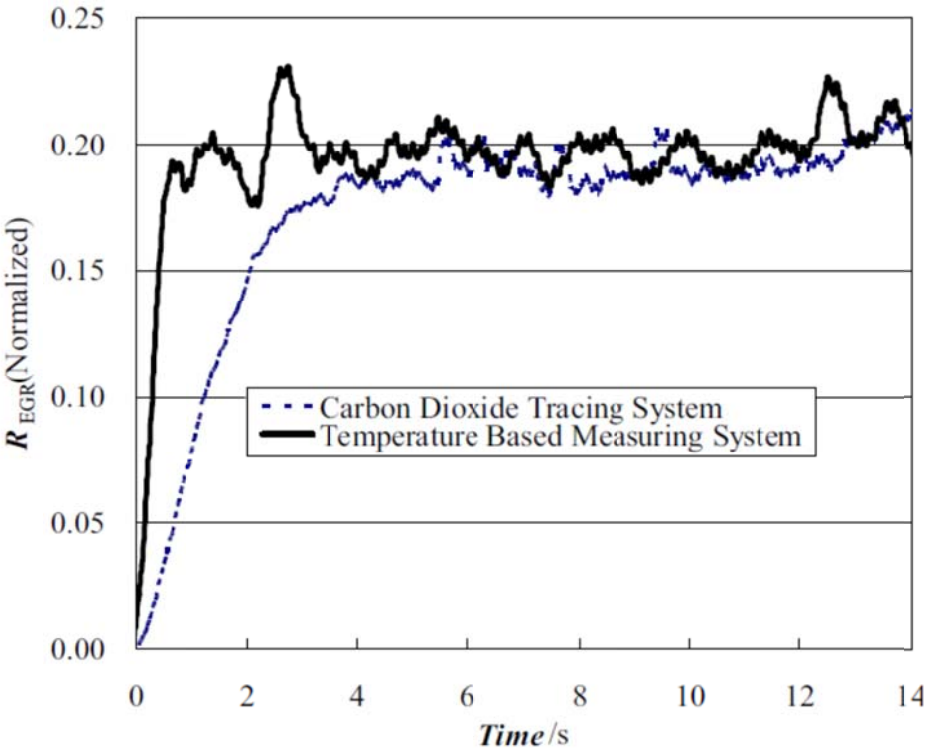

Figure 1.7 Measured EGR rate from temperature based system [27]

1.1.4 Application of combustion control

An Open-loop control method has been selected to adjust parameters related with operating variables in the previous control system of Diesel engines. However, fluctuation of combustion characteristics which are ignition timing and IMEP, etc. is rather bigger than a gasoline engine due to the feature of compression ignition [28]. Furthermore, open-loop control systems have no inherent potential to compensate for variations from mass production, aging, fuel properties and environmental factors, such as the humidity and temperature of the intake air [29]. Additionally, they require a time-consuming calibration and mapping procedure at the development stage and recalibration for newly developed engines. However, a closed-loop control system that measures the results of the actual combustion has adaptability to environmental factors and advantages for on-board diagnostics.

Ignition criteria can be divided into direct measurement and indirect measurement. The most well known method of indirect measurement is detecting the vibration signal of engine block so as to analyze singular points in the achieved signal. Combustion noise in compressed ignition engines is produced by the pressure rising rate and mechanical forces inside the cylinder. These forces cause the engine block to vibrate and radiate noise shown in Figure 1.8. The engine vibration signal is complex data and includes vibration from many noise sources; it also contains the

effect of combustion. Utilizing the accelerometer to detect the engine block vibration signal is a cheaper and a highly durable method compared to the use of a pressure transducer. However, analyzing the vibration signal cannot show the overall combustion phenomenon compared to HRR calculation. In addition, the engine has many vibration sources which are included in the raw signal of the engine block vibration. Therefore, transformation of the vibration signal of the engine block is required to analyze combustion [30-34].

Assanis *et al.* and Heywood indicated that pressure-based diagnostics are reliable compared to other direct measurement methods [35, 36]. Since pressure changes in the combustion chamber project the overall reaction occurred by combustion, the heat release rate calculated from in-cylinder pressure can describe the overall combustion process such as start of combustion, combustion duration and 50% burning rates with a great deal of accuracy. Pressure sensors for an experimental purpose usually have burdensome price. Most of all, pressure and temperature of combustion chamber rise very high when an engine is working and durability of these directly exposed sensors are low. However, advances in technology and mass production allow not only decline of price but also extended life-time [37-40].

Researches about combustion control of a diesel engine by closed-loop control have been conducted actively since 2000s and followings are examples of the

researches:

There are efforts to apply closed-loop control without using a pressure sensor. Other type of sensors are used which can reflect combustion characteristics indirectly. Glavmo *et al.* used an ionization sensor for detecting SoC of a diesel engine in real time and suggested that detecting SoC can be used effectively for closed-loop control of an injection system [39]. Smith *et al.* suggested removing cylinder imbalance using the signal of an air-fuel ratio sensor [41]. They extracted cylinder imbalance information from one oxygen sensor and the analyzed signal of the oxygen sensor is processed into separate virtual oxygen sensors-one for each cylinder. The feedback controller is then applied to drive those imbalances to zero. Rackmil *et al.* proposed a by cylinder IMEP estimator which operates without direct cylinder pressure sensor measurement and it was coupled with associated closed loop torque controller [42]. Guillemin *et al.* illustrated the functionalities of the platform through an example of combustion parameters estimation from a knock sensor [43]. The measurement platform is applied on HCCI and CAI engines. Byttner *et al.* proposed two virtual sensors that use the spark-plug based on a current sensor for combustion engine control [44]. The first sensor estimates combustion variability for the purpose of controlling exhaust gas recirculation and the second sensor estimates the pressure peak position for control of ignition timing. The

combustion variability sensor is demonstrated in a closed-loop control experiment of EGR on the highway and the pressure peak sensor is shown to handle both normal and an EGR condition. Thomas *et al.* developed a model base control system with the mean value engine model [45]. The mean value engine model for air-fuel ratio control, idle speed control and the cyclic engine model for knock control are suggested.

Many automotive manufactures are interested in the engine control based on the in-cylinder pressure. Audi is trying to apply in-cylinder pressure control in 3.0 L TDI diesel engine [46]. They expect a significant development; permitting models to undercut the U.S. Bin 5 standards for all states and the limits are likely to constitute Euro 6. Honda diesel engine engineers focused on reducing engine-out emissions through advanced combustion control for 2.2 L i-DTEC engine, coupled with after-treatment technology [47]. 2.9 L V6 diesel engine of GM uses cylinder-pressure feedback loops to address combustion variation and achieve smooth transitions between premixed charge compression ignition mode and conventional combustion mode [48]. Volkswagen introduced unique in-cylinder pressure sensors to the 2.0 L TDI diesel engine that allow combustion control based individual cylinder pressure [49].

Haraldsson *et al.* changed the compression ratio variously and examined the

change of CA50 and IMEP [50]. Also, step experiments of CA50 using closed-loop control were performed. The effectiveness of the RSM as a part of an engine control system was also demonstrated. Results obtained from the engine control experiments indicate that the RSM can be used successfully in an engine control algorithm, which would be especially useful when compensating for changes in operating conditions. The tests demonstrated that modest changes in operating conditions could be compensated for using the RSM in a control strategy [51]. Hasegawa *et al.* investigated a system that addresses these issues by detecting the ignition timing with in-cylinder pressure sensors and by controlling the fuel injection timing and the amount of EGR for optimum combustion onboard [52]. Yoon *et al.* suggested difference pressure (DP) to represent the combustion characteristics in the cylinder, DP is the difference between the in-cylinder firing pressure and motoring pressure [53]. They applied an adaptive feedforward controller in order to improve the performance of the feedback controller. The feedforward controller consists of the radial basis function network (RBFN) and the feedback error learning method that is for training of the network. They made closed-loop algorithm for combustion control and performed step experiments at steady and transient states. Schnorbus *et al.* used closed-loop control for diesel combustion control in transient cycles and NEDC mode shown in Figure 1.9 [54]. However, the results of emissions were not good at transient conditions and NEDC

mode, so additional method of pilot injection strategy had been added during the control. Liebig *et al.* shows that cylinder pressure based on closed loop control levels out the influence of fuel ignition quality [55]. They considered three kinds of fuel characteristics, cetane number, volatility and energy density. Even the MFB50 is maintained constant under varied cetane number, there remained small effect on emission level. Volatility and energy density showed weaker correlation with engine behavior. In addition, IVC timing and fuel octane were used to control combustion timing and the efficiency of closed-loop control was examined [56]. Willems *et al.* examined the potential of in-cylinder pressure based control in a heavy-duty engine for late DI diesel combustion with high EGR rates shown in Figure 1.10 [57]. To demonstrate transient performance and robustness of the controller, fuel steps and experiments with uncalibrated injectors and different fuels, such as US diesel, EN590 and Biodiesel, are performed.

Various versions of LTC have been intensely investigated for last decay such as the homogeneous charge compression ignition (HCCI) combustion, the smokeless-rich diesel combustion, the modulated kinetics (MK) combustion and etc, because of their potential for generating reduced PM and NOx emissions shown in Figure 1.11 [58-60]. However, the biggest challenge in implementing LTC widely is that it is less stable and more difficult to control than conventional diesel and spark ignition

combustion, especially at high loads where engine efficiencies are high. Several modes of LTC are also apparently sensitive to small changes in fuel properties. While some LTC engine experiments have apparently demonstrated peak net indicated efficiencies in excess of 55%, this has been achieved under idealized laboratory conditions. There were controversial opinions regarding how well these results would translate to actual drive cycle conditions.

To overcome these issues, closed-loop control through combustion monitoring could be a critical key solution. A closed-loop control system is used to monitor the combustion process with real-time and has such a device that can contribute to the engine control, hence, it would be possible to enlarge the operating range. Olsson *et al.* researched closed-loop control of a HCCI engine using two kinds of fuel [61]. They used CA50, which is almost the same meaning as MFB 50 to detect combustion of a HCCI engine. Ramp experiments were performed with changing engine load artificially. However, the calculation time of closed-loop algorithm was not fast enough, so it cannot support real time responses. In other research, the change of combustion phasing in HCCI engine with various internal and external EGR was examined, and also only the step experiments of CA50 were performed [62]. Kumar *et al.* performed empirical tests to enable smooth transition from high temperature to low temperature combustion regions with adaptive fuel injection

control shown in Figure 1.12 [63]. Husted *et al.* suggested that closed-loop combustion phasing and cylinder balancing are both effective in helping control of low-temperature and pre-mixed diesel combustion, especially during transient operation [64]. The cylinder-to-cylinder variation was greatly improved for both MFB50 and BMEP by closed-loop control of combustion.

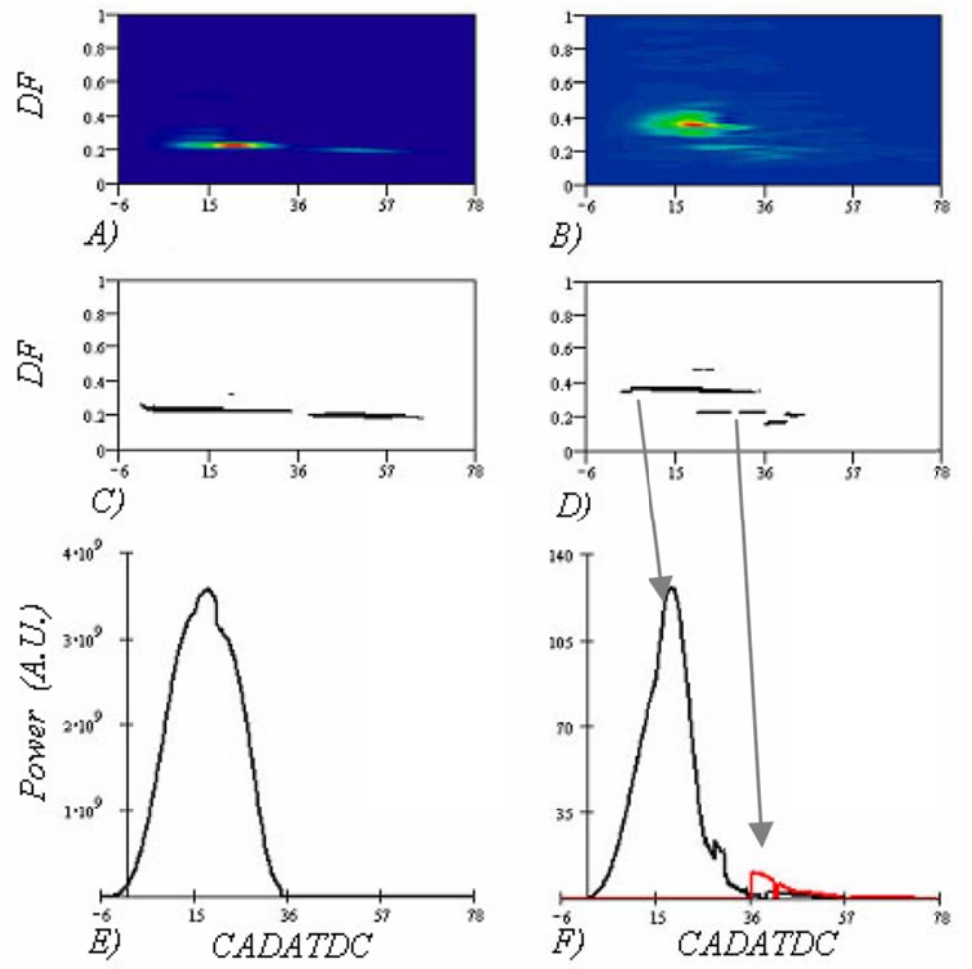

Figure 1.8 Time frequency analysis of the in-cylinder pressure signal (left) and block vibration signal (right) [30]

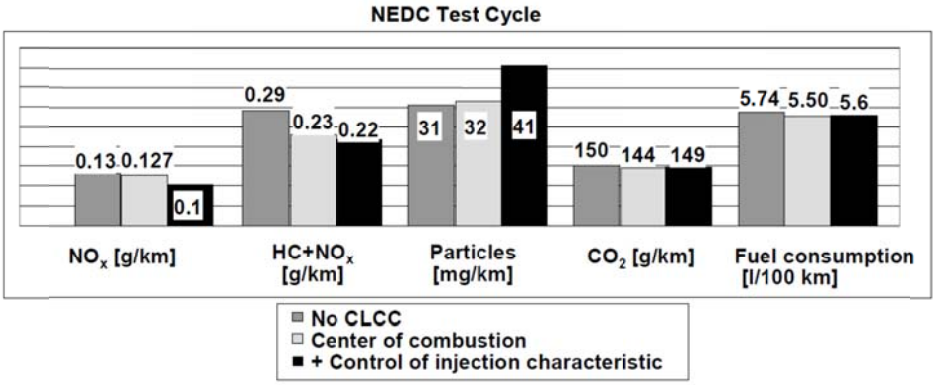

Figure 1.9 NEDC test results with different combustion control strategies [54]

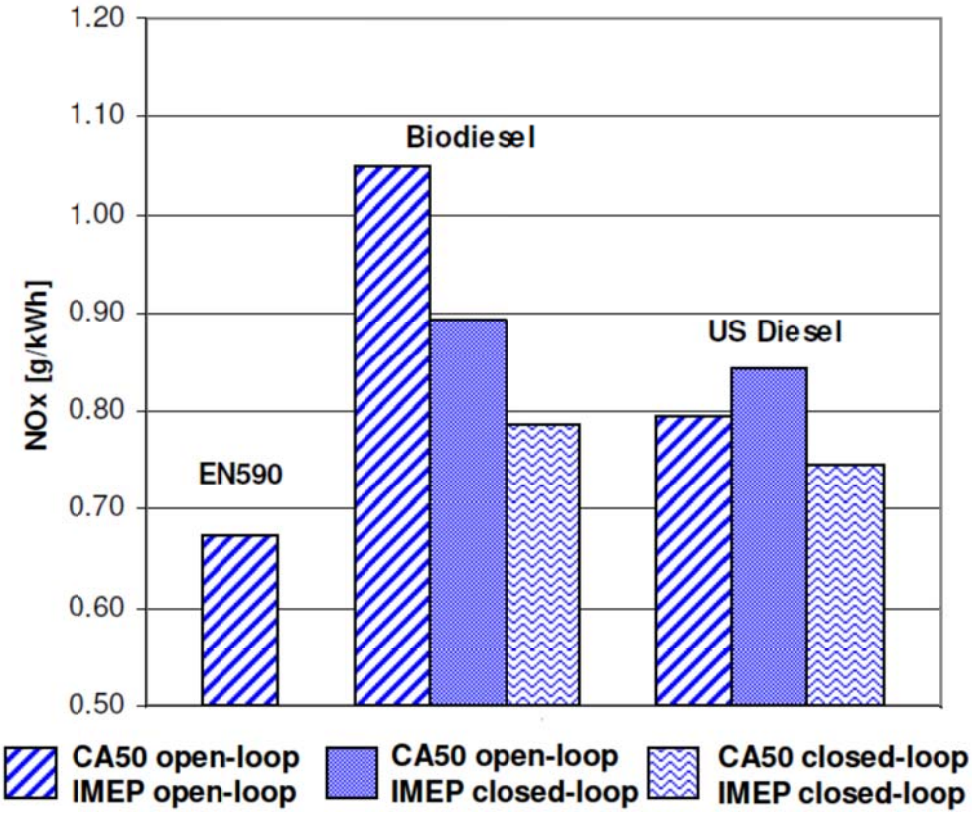

Figure 1.10 Effect of closed-loop CA50 and IMEP control on brake-specific engine-out NOx emissions for Biodiesel and US Diesel (1200 RPM, l=1.5, 46% EGR), CA50desired=5°CA ATDC, IMEPdesired=8.2bar. [57]

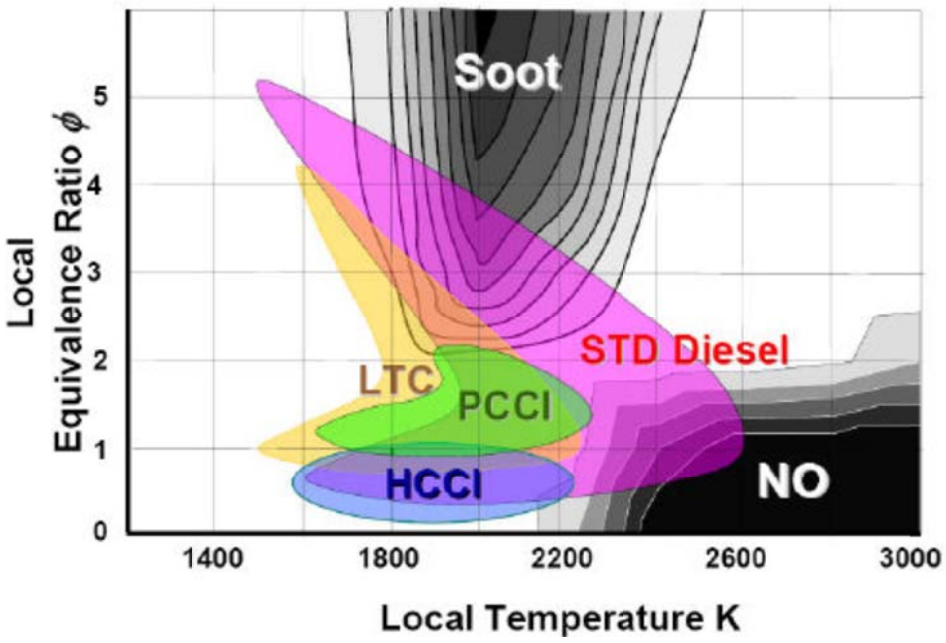

Figure 1.11 Possible classification of different combustion concepts [57]

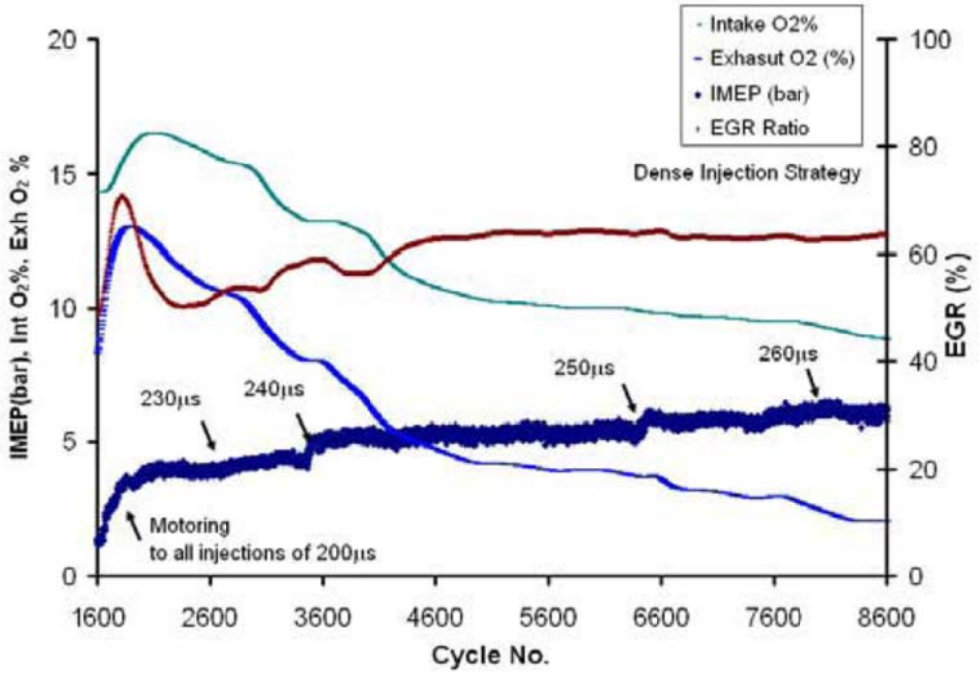

Figure 1.12 The mode transition from diesel to HCCI combustion mode [63]

1.2 **Objectives**

In this study, in-cylinder combustion control logic is developed to control MFB50 and IMEP. It is evaluated that the designed logic has an effect on reducing the exhaust gas emissions and compensating the reduced performance caused by deterioration of engine components.

The detailed objectives of this study are :

1. Developing real-time combustion analyzer algorithm to predict cycle-by-cycle combustion status

2. Building real-time EGR rate estimation algorithm to indicate intake air composition

3. Constructing cycle-by-cycle and cylinder-to-cylinder closed-loop MFB50 and IMEP control logic

4. Verifying the effect of combustion control logic to engine out emissions characteristics in transient operating conditions

5. Applying the combustion control logic to compensate deteriorated engine operating conditions due to the degradation of engine component

1.3 **Expected benefits**

Engine-out emissions are already stable and maintained at low level under the open-loop control system, currently being used, due to the optimization during engine development state. Real-time engine control based on in-cylinder pressure is a pretty well-known method as introduced in the previous chapter and the potential of emissions reduction with combustion control in steady state was evaluated. However, when the engine is operated in transient state, engine control map developed by steady state experiment has difficulties to suppress generating emissions. The emissions performance with combustion control was analyzed while driving under the NEDC mode. However, the analysis focused on the total amount of engine out emissions during the entire cycle. There was little analysis in a short period as a microscopic view for one state of acceleration or deceleration. While driving under NEDC mode, difference of engine out emissions between open-loop and closed-loop control system occurs at transient period. It is needed to focus on the emissions characteristics in transient state. Moreover, there has been no consideration of in-cylinder gas composition and EGR rate when applying combustion control. According to the researches about engine-out emissions characteristics in transient condition, the time gap between air supply system and fuel injection system could cause potential emissions peaks. Therefore, in-cylinder

gas composition is essential information to control the in-cylinder combustion and engine-out emissions cycle-by-cycle in transient states. Combustion control is effective to compensate external factors such as fuel variations but there was no consideration to apply the combustion control for hardware failure.

In this study, the effect of combustion control is analyzed, especially focusing on transient states. Modified injection strategy by combustion control and real-time EGR rate estimation are expected to offer the cause of emission reduction. In addition, combustion control algorithm is able to be a solution to compensate for the wear and aging of injection system.

The expected benefits by real-time cylinder pressure based combustion control can be explained as:

A. Reduction of emissions in transient condition 1 : Modified main injection strategy effects on the emission characteristics

B. Reduction of emissions in transient condition 2 : Main injection strategy controlled according to the EGR rate at transient state effects on the emission characteristics in transient state.

C. Compensating wear of injection system : Deterioration of emission performance is mitigated by controlling main injection strategy.

Chapter 2. Experimental Apparatus

2.1 Overall configuration

In this part, test and measurement equipment for the target engine will be introduced. The schematic diagram of test and measurement equipment is shown in Figure 2.1.

2.1.1 Engine test equipment

The engine experiment was coupled with a 190 kW AC dynamometer for engine speed control and torque measurement. The specifications of the dynamometer is shown in Table 2.1. Coolant temperature was controlled during the engine test using the coolant temperature controller (SAMBU, SWC-1200). The quality of diesel fuel was preserved from a large capacity fuel tank during the entire experiment period and fuel temperature was maintained at 40 °C by using the fuel temperature controller (SAMBU, SFTC-1400). The temperature of the engine test cell was controlled to 25 °C by an air-conditioning system. In addition, a duct for supplying fresh air is installed near the engine air inlet.

2.1.2 Measurement of fuel flow rate

Fuel mass flow rate was measured by OVAL ULTRA mass MK II coupled with CT9401 transmitter. OVAL flow meter measures the flow rate of fluid using a Coriolis force. The flow meter does not require the fuel to be stored in the equipment, so it is easy to measure the flow rate in transient engine operating condition. The specification of fuel flow meter is shown in Table 2.2

2.1.3 Measurement of exhaust gas emissions

Exhaust gas composition of O_2 and CO_2, and emissions of NOx, THC, CO, and PM were measured during the test. Exhaust gas was sampled at each corresponding device as shown in Figure 2.1. PM was measured in FSN (Filtered Smoke Number) by a smoke meter for steady state and an opacimeter was used to measure the PM emission when the engine in transient test conditions. The specification of smoke meter and opacimeter are shown in Table 2.3 and Table 2.4, respectively. NOx, THC, CO, CO_2, and O_2 were measured by the exhaust gas analyzer (HORIBA, MEXA-7100DEGR). All species are measured in volume fraction (vol % / ppm) in wet condition. The measured principles of each emission are listed in Table 2.5.

In case of NOx emission, it was needed to be measured not only in steady state but also in transient state because of verifying MFB50 control correction factor by EGR rate. In this study, fast response NOx analyzer (Cambustion, CLD-500) was

applied to real-time measurement. The specifications of fast response NOx analyzer are shown in Table 2.6.

Table 2.1 Specifications of dynamometer

Item	Specification
Manufacturer	AVL ELIN
Model	MCA-231
Capacity	190 kW
Type	AC
Maximum rpm	6980 rpm
Cooling	Air cooling

Table 2.2 Specifications of fuel mass flow meter

Item	Specification
Manufacturer	OVAL
Type	Coriolis type
Model	ULTRA mass MKII CN-003
Transmitter	CT9401
Range of measurement	0 ~ 20 g/sec
Minimum range	1 g/s
Accuracy	± 0.1 %
Allowable measuring density	0.3 ~ 2 g/mL

Table 2.3 Specifications of smoke meter

Item	Specification
Manufacturer	AVL
Model	AVL 415S
Measurement range	0 ~ 10 FSN / 0 ~ 32,000 mg/m³
Resolution	0.001 FSN / 0.01 mg/m³
Repeatability (as standard deviation)	$\sigma \leq \pm$(0.005 FSN + 3 % of measured value)
Reproducibility (as standard deviation)	$\sigma \leq \pm$(0.005 FSN + 6 % of measured value)

Table 2.4 Specifications of opacimeter

Item	Specification
Manufacturer	AVL
Model	AVL 439
Measurement range	0 ~ 100 % / 0 ~ 10 m^{-1}
Resolution	0.01 % / 0.0025 m^{-1}
Response time	0.1 s
Zero stability	0.1 % / 0.0025 m^{-1} for 30 min

Table 2.5 Measurement principle of emission analyzer (MEXA-7100DEGR)

Emissions	Measurement principle
NOx	Chemiluminecent Detector
THC	Flame Ionization Detector
O_2, CO_2, CO	Non Dispersive Infrared Rays

Table 2.6 Specifications of fast response NOx analyzer

Item	Specification
Manufacturer	Cambustion
Model	CLD-500
Measurement range	0 ~ 100 ppm to 0 ~ 20,000 ppm
Linearity	±1 % FS to 5,000 ppm ±2 % FS to 10,000 ppm
Response time	2 ms (10 ms with NO_2measurement)
Zero stability	5 ppm for 1 hour

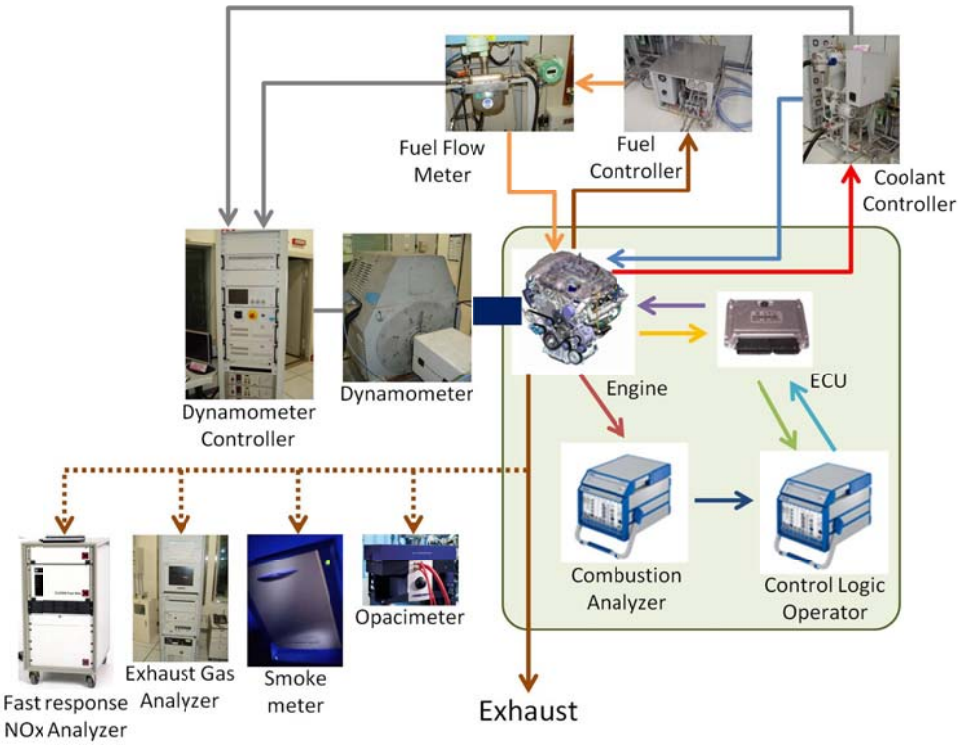

Figure 2.1 Schematic diagram of engine test and measurement equipment

2.2 **Multi-cylinder Diesel engine**

For this research, an in-line 4 cylinder 2.2 L Diesel engine was chosen for the development. Figure 2.2 shows the target engine in this study. This engine has fuel injection equipment including piezoelectric type injector, common rail and high pressure pump, which enable injection pressure up to 1600 bar. The engine is controlled by Bosch ECU version of EDC 17C, which allows variable bypass. Detailed specifications of the engine is shown in Table 2.7.

Table 2.7 Specifications of engine

Criteria	Specification
Layout	In-line 4 cylinder 2.2 L
Max power	200 hp / 3800 rpm
Max torque	44.5 kgm / 1800 rpm~2500 rpm
Bore	85.4 mm
Stroke	96 mm
Displacement volume	550 cc
Connecting rod	145 mm
Compression ratio	16
Valve timing	IVO : 10° BTDC
	IVC : 28° ABDC
	EVO : 54° BBDC
	EVC : 4° ATDC
Fuel injector type	Piezoelectric type
ECU version	EDC 17C

Figure 2.2 In-line 4 cylinder 2.2 L Diesel engine

2.3 **Combustion control system**

Figure 2.3 shows the core components for combustion control. 2.2 liter Diesel engine was coupled with ECU, and, combustion analyzer and control logic operator were installed. The combustion gas pressure was measured by using a pressure sensor installed for each cylinder and, at the same time, CPS signal was also sent to a combustion analyzer. Based on the two signals received, the combustion analyzer calculated MFB50, IMEP and extracted other analyzed combustion data for real-time control. The analyzed results were then passed on to the combustion-control logic, and, the control logic determines the main injection timing and the fuel injection quantity. The ECU used for the research was able to bypass some of the parameters which means that the fuel injection value extracted from the combustion control logic can be written over the existing value of the ECU. As a result, the engine operated in accordance with the new fuel injection control value.

2.3.1 ES-1000

ES-1000, shown in Figure 2.4, was a platform that is possible to be composed of several boards for the desired function. For the case of combustion analysis, simulation controller board, analog input board and CAN communicating board were installed. Simulation controller board was designed for rapid prototyping

applications in ES-1000 systems and combustion analyzing algorithm was loaded in this case. Analog input board acquired pressure sensor signals and CPS signal. CAN communicating board sends analyzed results to the combustion control operator. For the case of combustion control, simulation controller board, ETK communicating board and CAN communicating board were installed. Simulation controller board operates control logic. ETK communicating board received the engine operating parameters and sends the modified injection strategy. CAN communicating board received the combustion analyzed results from the combustion analyzer. Tables 2.8,Table 2.9 are the specifications list for the combustion analyzer and the combustion control operator, respectively.

2.3.2 Pressure sensor

The cylinder pressure sensor was a very important part of combustion control. It measured the in-cylinder pressure in each cylinder and sent this signal to the combustion analyzer where indicates torque and the midpoint of combustion represents the cylinder pressure characteristics and it was calculated for each individual cylinder. Therefore, the quality of the combustion control was determined by a great extent of the quality of the measured in-cylinder pressure signal and, thus, by the cylinder pressure sensors.

In order to measure the in-cylinder pressure by real-time in this study, an in-body glow-plug pressure sensor, manufactured by Beru shown in Figure 2.5, was used. The structure of the pressure sensor is shown Figure 2.6 and the specifications of the pressure sensor are listed in Table 2.10. The method of the pressure measurement was piezoresistive and it has a measuring range of 0~200 bar. The input operating voltage was 5 V and its accuracy is ±2 %. Output signal type was ratio metric and bandwidth of sensor is 0 to 5 kHz. This sensor has a glow function. Temperature after 60 seconds was higher than 980 ℃ and maximum temperature is 1100 ℃. However, in this study, the glow function was deactivated. It had a flexible heating rod for pressure transmission. In this study, pressure sensors were placed on all four cylinders to measure the in-cylinder pressure.

2.3.3 ASCET

ASCET is a graphic based language using block diagrams, state machine and C code shown as Figure 2.7. ASCET enables model-based development of application software and automatic code generation, and it supports embedded software with real-time shown as Figure 2.8. ASCET enables the initial component design with block diagrams and automatic generation code for micro-controller target.

The most important function of ASCET in this study is bypassing the ECU pre-set

values. Bypass development is usually suitable for early testing of an additional or modified software function of the control unit in the vehicle. The new or modified software function is specified by a model and executed on the experimental system. It makes that a control unit that has the basic functionality of the software system can be used- that all required set-point generators, sensors and actuators are supported, and that a so-called bypass interface to the experimental system is available. The new or modified software function is developed using a rapid prototyping tool and executed on the experimental system

This approach is suited for enhancing the existing functions on the control system. The existing functions in the control unit are often still calculated, but modified, so that the input values are sent via the bypass interface and the output values from the new bypass function are used. Required host system and calculation specifications for ASCET are shown in Table 2.11.

Table 2.8 Specifications of combustion analyzer

Criteria		Specification
Simulation Board	CPU	1 GHz
	RAM	256 MB SDRAM
A/D board		16 CH, 100 kHz/CH
D/A board		8 CH
Digital and PWM I/O board	Channel	16 CH input, 16 CH output 2 external trigger
	Frequency	1 Hz to 60 kHz
CAN Communication		4 CAN signal

Table 2.9 Specifications of combustion control logic

Criteria		Specification
Simulation Board	CPU	1 GHz
	RAM	256 MB SDRAM
CAN Communication		4 CAN signal
ETK Communication		1 CH, 100 MBit/s

Table 2.10 Specifications of piezoresistive type pressure sensor

Technical data	
Operating temperature	-40 – 140°C (max. 150°C)
Pressure range	0 – 200 bar (max. 210 bar)
Sensor	
Power supply (Vdd)	5,0 V or 3,3 V
Output signal	ratio metric
Bandwidth	0 to 5 kHz
Accuracy	± 2%
Glow function	
Current 60sec	< 10 A
Temperature after 60sec	> 980°C
Max. temperature	1100°C

Table 2.11 Required specifications of host system for ASCET and calculation

Item	Specification
CPU	1 GHz Pentium
RAM	512 MB
Operating System	Windows 2000 Windows XP Windows Vista
HDD	1 GB
Calculation clock	50 ms (20 kHz)

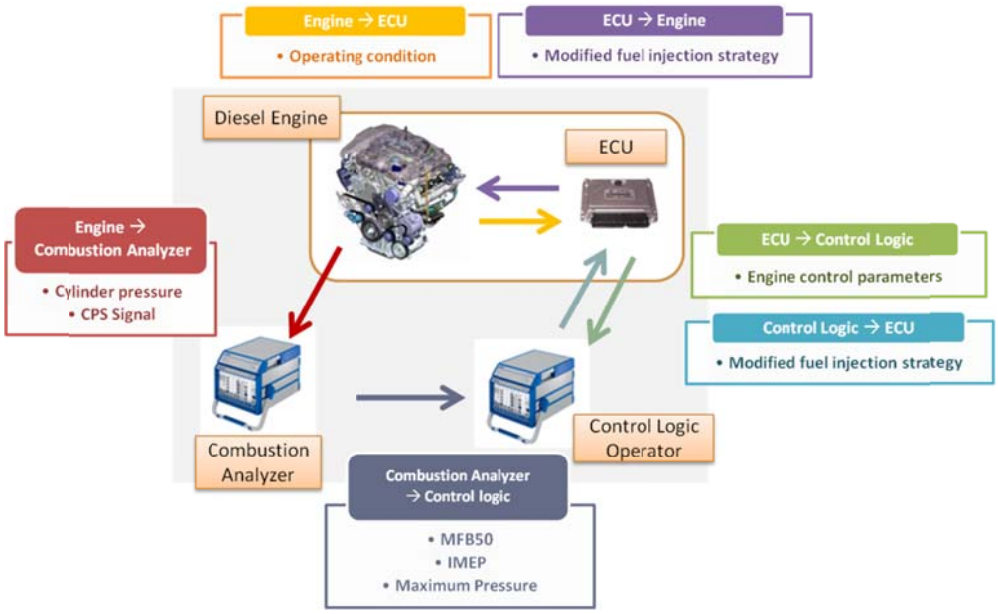

Figure 2.3 Schematic of experiment components

Figure 2.4 ES-1000 module

Figure 2.5 Glow-plug in-body pressure sensor

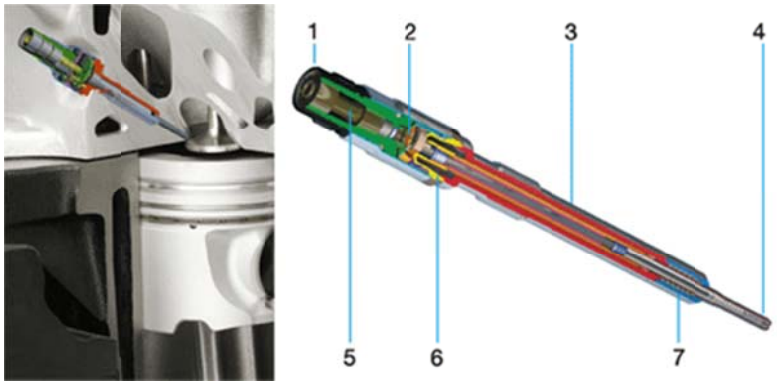

Figure 2.6 Cross section of pressure sensor.

(1.Plug 2.Circuit board with electronics 3.Glow plug body 4.Glow plug heating rod 5.High voltage connection 6.Measuring diaphragm 7.Gasket)

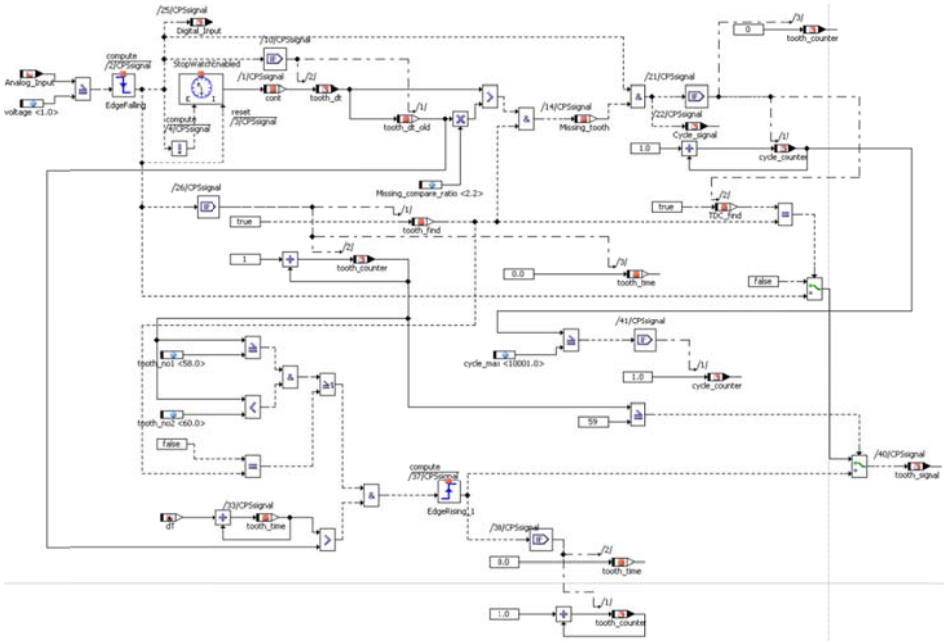

Figure 2.7 ASCET code

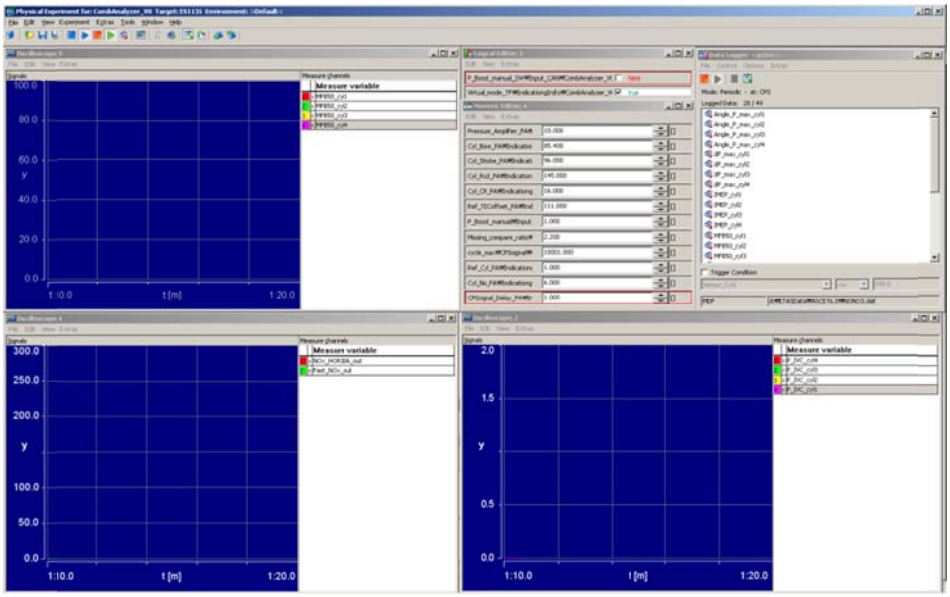

Figure 2.8 Physical experiment – operating code in real-time

Chapter 3. Algorithm for real-time estimation of in-cylinder pressure based engine operating conditions

3.1 Combustion analyzer

3.1.1 Overall logic description

In order to extract information from combustion data in real-time, various combustion reaction parameters related with the pressure signals must be calculated in sequence with the plan shown in Figure 3.1. Most of all, controlled injection strategy should be prepared before BDC and just before the firing TDC because of overwriting time. Considering the time of control logic calculation and data transfer, combustion analysis should be completed by the end of each cycle. To overcome the lack of time, calculation window for heat release rate is narrowed and the starting of calculation is advanced. Heat release analysis is progressed with the pressure data between 40° BTDC compression and 90° ATDC, and the calculation is started just after the 90° ATDC. The heat release rate calculations operate from 90° ATDC to 270° ATDC. After that MFB50 is derived during 90° CA period. IMEP calculation is operated between 180° ATDC and TDC at valve overlap.

The calculation scheduling is used, when the cycle terminates, so that all the analyzed combustion parameters are prepared until the end of cycle to be used for the next cycle. It is verified that the combustion control logic works until 3800 rpm which is the full load.

Figure 3.2 shows the flow chart of combustion analyzer. Combustion analyzer receives CPS and pressure sensor signals with a frequency of 20 kHz. Time based pressure data is converted into crank angle based data using linear interpolation. Moving average method is introduced to filter the noise of pressure signal. In a combustion analyzing algorithm, MFB10, MFB50, MFB90, pressure signal at intake valve closing, maximum cylinder pressure, crank angle at maximum cylinder pressure, maximum pressure gradient, crank angle at maximum pressure gradient, maximum heat release rate per crank angle, the timing of maximum heat release rate per crank angle, and IMEP are calculated for each cylinders, and, exported. The exported results are then passed on to the control logic operator through a CAN communication.

3.1.2 Input signal treatment

In a combustion analyzer, the cylinder pressure and the CPS signal is used. - For the CPS signal, a TTL signal is produced in every 6 degree and it also has a missing

tooth; 60-2 signal type to determine one complete rotation as shown in Figure 3.3.

Interference is caused by a noise for the measured pressure signal and, for the low pressure range, the interference effect becomes more important since the signal-to-noise ratio is small. Also, when logic is applied to a real vehicle, there might be an extra interference due to sub-components which are not used for an engine experiment. Therefore, it is necessary to remove the noise because a distortion of the pressure signal affects the reliability issue of the analyzed combustion data.

In this study, a process which removes the noise by using a moving average technique for the pressure signal is added for a faster signal processing. The moving average technique is a method that derives the current signal value by averaging signals around the current signal, before and after the current value. The noise cancellation and the signal distortion depend on the number of signals used before and after the moving average. 5 signals are used, 2 before and 2 after the current signal, to get the average for this particular combustion analyzer logic as shown in equation 3.1. The averaged signal of 5 uses 20 kHz which is similar to using a 4 kHz filter.

For the logic, there is a delay in pressure signal in accordance with the applied average signal. Hence, logic is added to initialize the CPS signal by having the same delay step.

$$P_{filtered} = \frac{P_{n-k}+P_{n-k+1}+\cdots+P_{n+k-1}+P_{n+k}}{2k+1} \quad (3.1)$$

Where k is 2 : Average of the 5 data

Also, there is a selection switch of reference cylinder and pressure data of reference cylinder is used to find the piston position of each cylinder. Time gap between missing tooth of CPS signal and firing TDC of reference cylinder is measured.

3.1.3 CPS signal processing, TDC detection

In case of rapid prototyping machine used in this study, due to its characteristics, when it processes data acquisition from an external trigger, all the internal calculation processes are interrupted by the trigger signal causing malfunction of the logic. Therefore, in this study, obtaining a 6 degree unit CPS signal and forming a 1 degree unit pressure signal are processed after measuring the one term of CPS signals. Figure 3.4 shows the concept diagram of CPS signal processing. At the missing tooth part, 2 virtual CPS signals are formed which have the same time period with the CPS signal detected just before the missing tooth. Also, at the same time, a signal is produced to indicate one complete revolution whenever the missing tooth is identified. The signal is generated where the falling edge is detected again.

Period of CPS signal is the time between two falling edges of the CPS signal. Missing tooth is detected where the period of two falling edge is 2.2 times larger than normal period.

In order to give crank angles for CPS signals and pressure data of each cylinder, logic is formed to add angles to the CPS signal after TDC calibration. TDC calibration is done, between the max pressure position- at which the reference cylinder is on motoring- and the one revolution signal, by inputting the angles. It must be done when a combustion analyzer is applied to a new engine.

3.1.4 Angle calculation

After the TDC calibration, a process is made to convert the crank angles of each cylinder to 360° CA at Firing TDC. The process initiates from the number 1 cylinder and follows the firing order of an engine by adding 180° CA each time. The firing order for the used engine is number 1-3-4-2 cylinder which is then applied to the angle calculation.

3.1.5 Formation of 1° CA unit pressure data

As it was mentioned before, it is impossible to obtain a combustion pressure signal from the trigger signal, so logic is required to obtain every 1 degree

combustion pressure. In this study, a combustion pressure sensor signal is obtained first with the maximum speed of this platform that an analog signal of 20 kHz. However, the pressure signal is divided into every CPS signal and saved in an array. A pressure signal in an array is equivalent to 6 degree crank angle and, by using the signal, 6 pressure values can be obtained with the same steps. There are two pressure signal array equivalent to 6 degree crank angle and receiving array is changed alternately to reduce the array data generation.

Figure 3.5 shows interpolation of the pressure for the research. For example, 10 pressure signals are detected in 1 period of CPS signal and then the array measures until the first signal of the next period. In addition, every 1 degree, interpolation is performed to convert the pressure signal. For example, to obtain 2 degree pressure signal, a linear interpolation process is done between the 2^{nd} and the 3^{rd} pressure signal.

3.1.6 Pegging of pressure signal by boost signal

The combustion pressure sensor measures relative pressure and, hence, it requires pegging based on the absolute pressure. In this study, a reference pressure was calculated around the ±10° BDC while the intake valve is opened. Then, the calculated pressure becomes the boost pressure or the other pressure value which is

manually selected, by the equation 3.2. Pressure data pegging is calculated when the data are extracted from pressure array to calculation process.

$$P_{pegged} = P_{raw} - P_{BDC,averaged} + P_{boost} \quad (3.2)$$

In this study, the intake pressure used in the ECU is taken as the boost pressure. However, the control logic operator controls ETK communication with the ECU, so the value from the control logic operator was sent back to the combustion analyzer via CAN communication.

3.1.7 Calculation of heat release rate, maximum pressure

HRR is calculated by using equation 3.3, which does not consider the heat transfer [36].

$$\frac{dQ}{d\theta} = \left[1 + \frac{C_v}{R}\right] p \frac{dV}{d\theta} + \left[\frac{C_v}{R}\right] V \frac{dp}{d\theta} \quad (3.3)$$

In this study, to minimize the calculation load, Cv and R, are assumed as a constant. Then, the amount of heat release is calculated for each crank angle and they are integrated until the specified crank angle to calculate the total released thermal energy. Finally, they are saved in an array and, after that, the array is scanned to obtain the maximum value and the crank angle information for that value. Figure 3.6 shows the sample case of heat release calculation.

In this study, the calculation window for thermal energy was set between 40° BTDC to 90° ATDC for a rapid calculation. Except IMEP, all values such as Pmax, dP/dθ and etc are extracted from the set-range. The calculations take place between 90 ° ATDC and 270 ° ATDC.

3.1.8 MFB50 determination

The amount of heat release for MFB10, MFB50 and MFB90 are calculated by multiplying the maximum Q value obtained from the HRR calculation with the required constant of heat release rate. Figure 3.7 shows the sample case of calculating MFB50 from the result of heat release rate. Then, they are found from the integrated heat release array and, a linear interpolation technique is used to find the exact position as indicated in equation 3.6.

$$Q_\theta = \sum_{CA=-40}^{\theta} \left(\frac{dQ}{d\theta}\right)_{CA} \tag{3.4}$$

Find n of (the case of MFB50, Figure 3.7)

$$Q_n < Q_{max} \times \frac{50}{100} < Q_{n+1} \tag{3.5}$$

$$MFB50 = n + \frac{Q_{max} \times \frac{50}{100} - Q_n}{Q_{n+1} - Q_n} \tag{3.6}$$

The calculation takes place between 270 ° ATDC and TDC.

3.1.9 IMEP calculation

In case of IMEP calculation, the calculation is conducted using the pressure data from BDC of the previous cycle to the BDC after the firing of the present cycle. Unlike MFB50, IMEP requires pressure signals from the complete cycle but the real calculation processes take a place between 180 ° CA (BDC) and 360 ° CA (TDC) . To minimize the calculation time, 10 crank angles of pressure data are calculated in one calculation loop.

If the pressure signal of the present crank angle is used to calculate IMEP, it could be an error source due to the principle of measurement by division [36]. Therefore, the pressure signal of the present crank angle and the previous crank angle are averaged as shown in Figure 3.8.

$$\mathrm{IMEP} = \int \mathrm{pdV} = \sum_{\mathrm{CA}=-540}^{180} \frac{\mathrm{p_{CA+1}} + \mathrm{p_{CA}}}{2} \times (\mathrm{V_{CA+1}} - \mathrm{V_{CA}}) \qquad (3.7)$$

The pressure signals from the previous cycle between BDC at exhaust stroke and TDC at valve overlap (180 ° CA) are used for the calculation.

3.1.10 Verification of combustion analyzer

Calculated MFB50 was compared to the MFB50 from the commercial combustion analyzer in Table 3.1. According to MFB50 results, except the idle state, under the part or the full load, the difference in MFB50 value was within 0.5 degree. It means that the results are within the error range since the smallest measurement unit is 1 degree.

Calculated IMEP was compared to the results of commercial combustion analyzer in various engine operating conditions. Figure 3.9 shows the results of IMEP calculation, maximum deviation between two results is 0.15 bar which is 3 %. By comparing the data, the performance of the combustion analyzer is reliable.

Table 3.1 Comparison of measured MFB50 performance

	Cyl1	Cyl2	Cyl3	Cyl4	AVG
IDLE	-0.73	-0.57	-0.86	-2.83	-1.25
1000rpm3bar	-0.12	-0.06	-0.08	0	-0.06
1500rpm4bar	-0.25	-0.23	0.05	-0.31	-0.18
1500rpm6ar	-0.79	-0.24	-0.07	-0.32	-0.36
1750rpm6bar	-0.4	-0.22	-0.51	-0.39	-0.38
1750rpm8bar	-0.42	-0.42	-0.45	-0.48	-0.44
2000rpm6bar	-0.39	-0.13	-0.2	-0.38	-0.27
2000rpm8bar	-0.42	-0.03	-0.25	-0.43	-0.28
2000rpm10bar	-0.4	0.03	-0.21	-0.3	-0.22
2500rpm10bar	0.13	0.43	0.3	0.02	0.22
1000rpmFull	0.47	0.35	0.38	0.39	0.4
1500rpmFull	0.33	0.27	0.41	0.26	0.32
2000rpmFull	0.02	0.2	0.11	0.06	0.1
2500rpmFull	-0.2	0.08	0.02	-0.16	-0.07
3000rpmFull	-0.33	-0.17	-0.03	-0.17	-0.18
3500rpmFull	-0.45	-0.21	-0.16	-0.28	-0.28
3800rpmFull	-0.32	-0.05	0.12	-0.12	-0.09

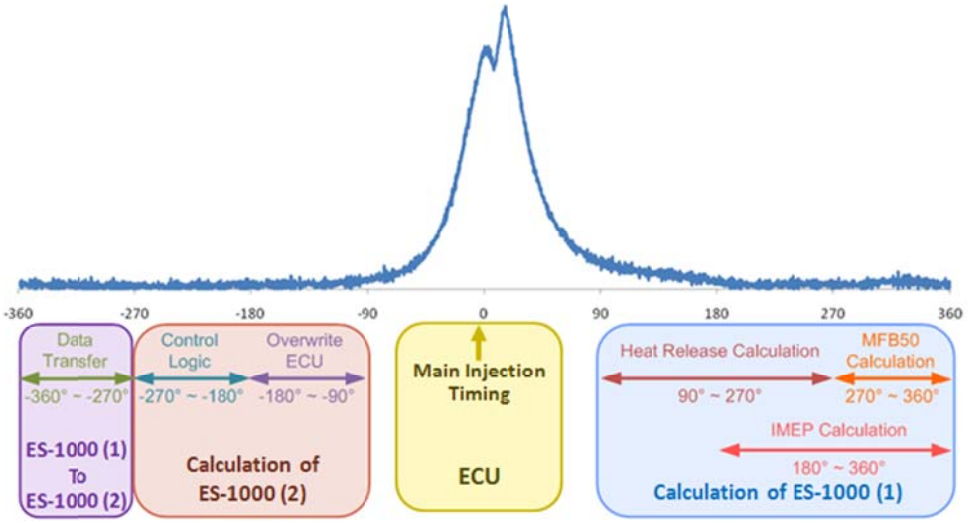

Figure 3.1 Combustion analyzer time scheduling

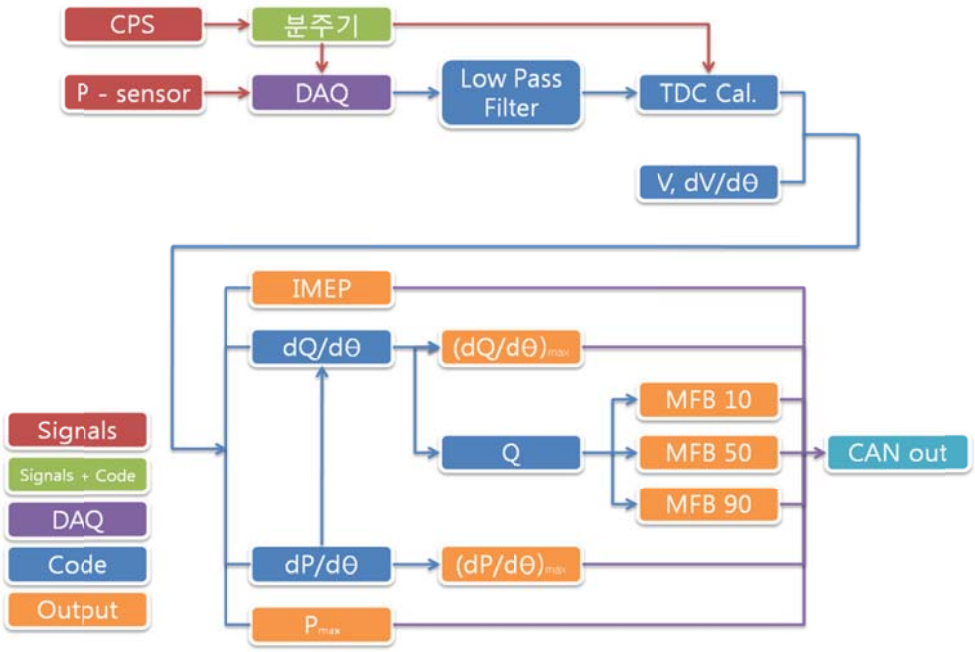

Figure 3.2 . Combustion analyzer algorithm

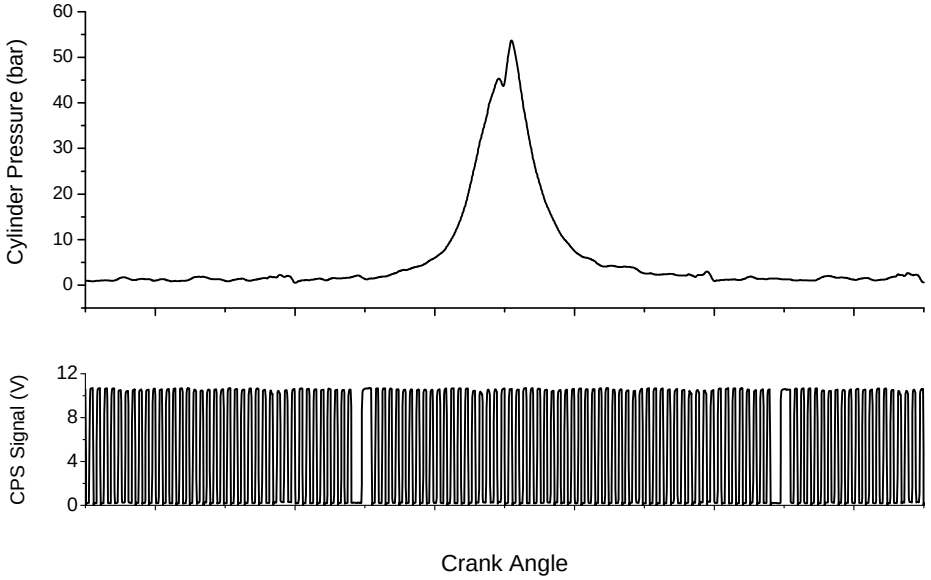

Figure 3.3 CPS Signal and cylinder pressure signal

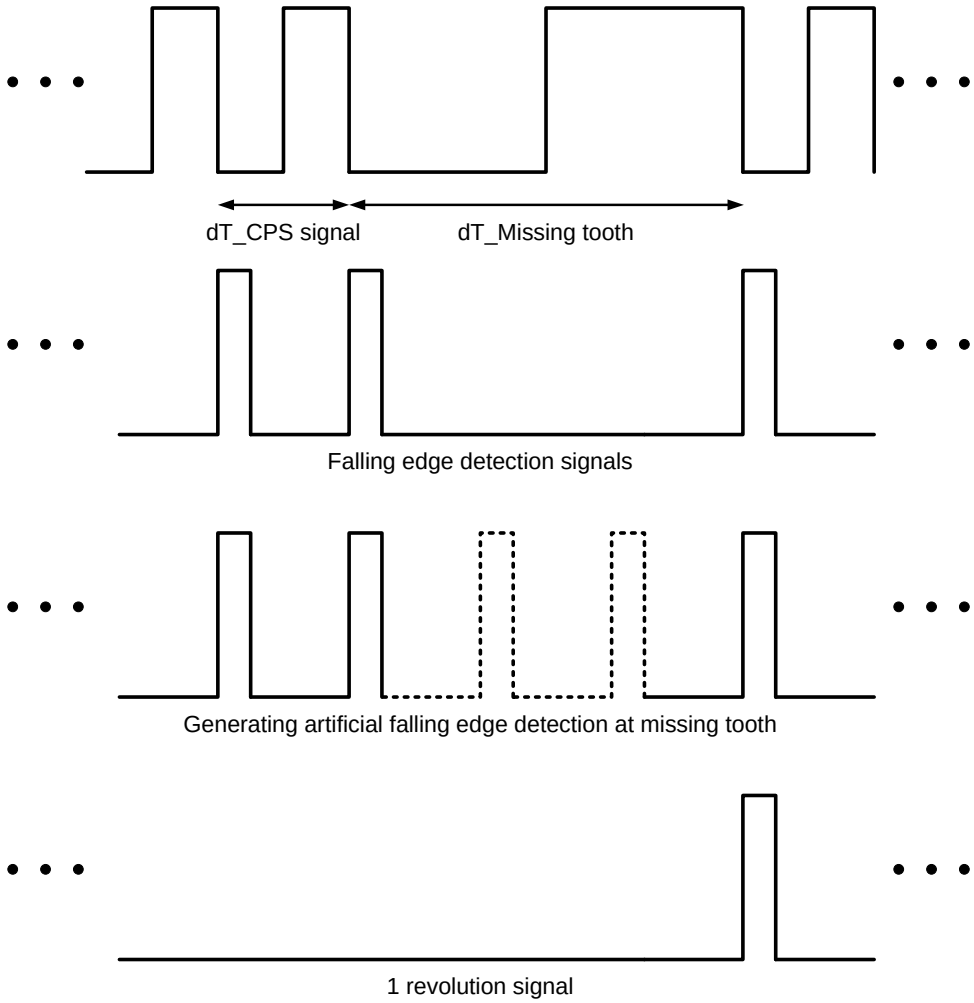

Figure 3.4 Detecting CPS signal and generating 1 revolution signal

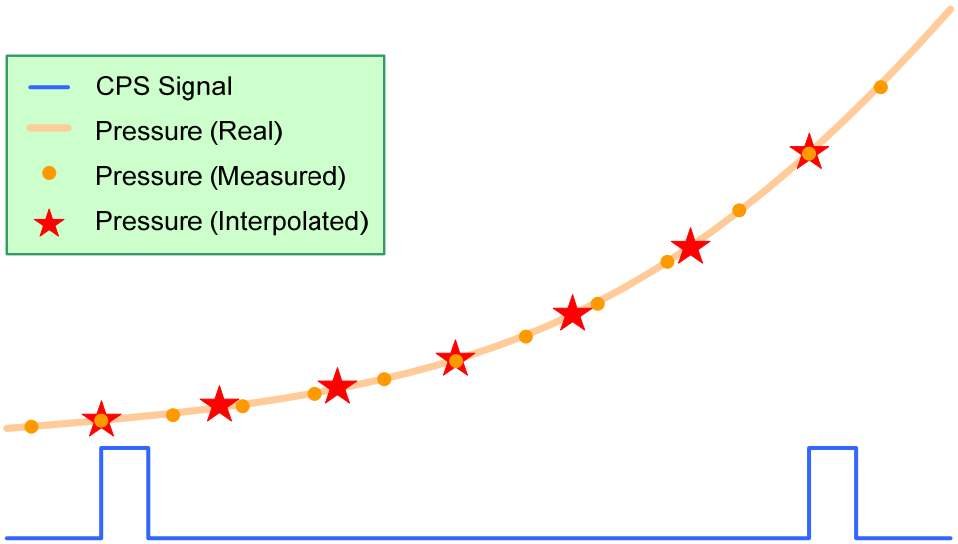

Figure 3.5 Formation of 1 degree unit pressure signal

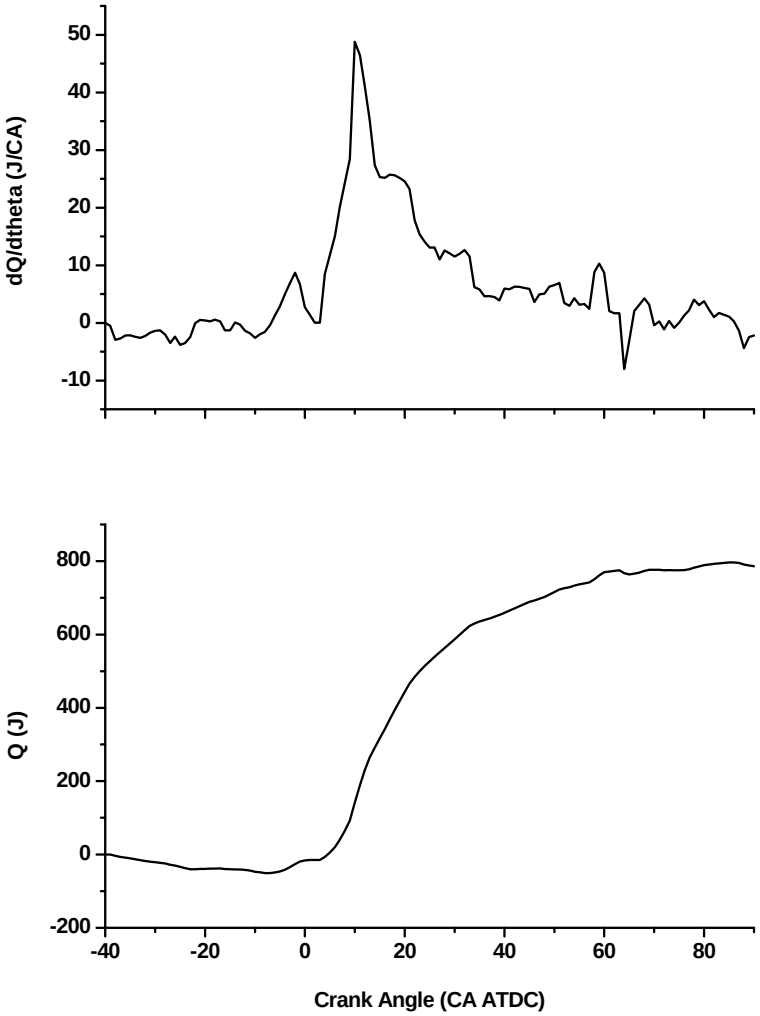

Figure 3.6 Hear release rate calculation (2000 rpm, BMEP 6 bar)

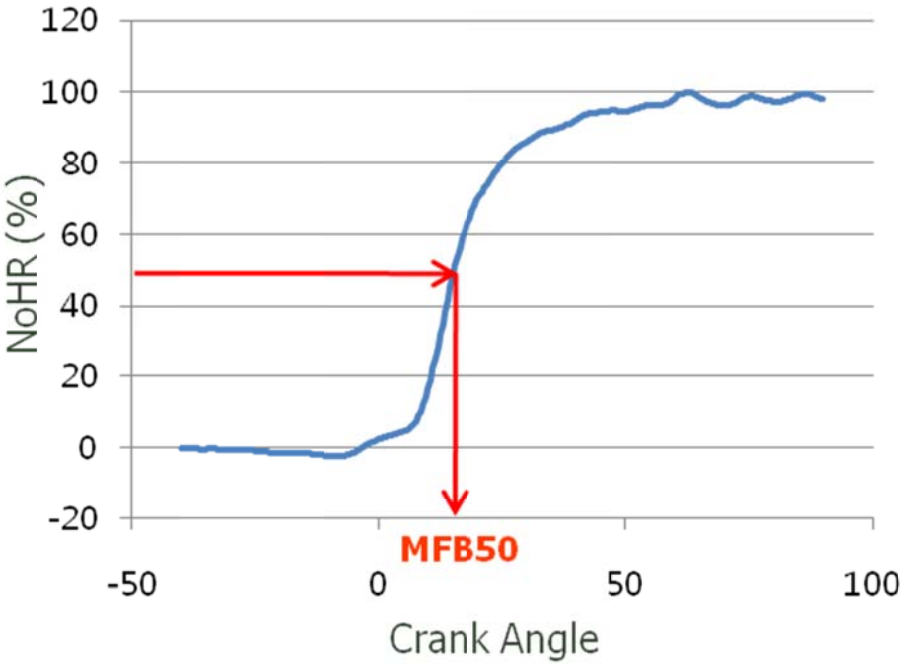

Figure 3.7 MFB50 calculation

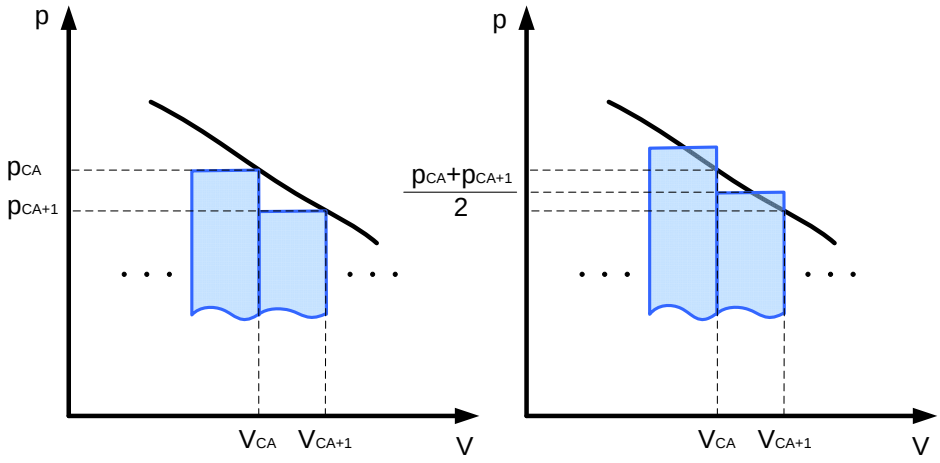

Figure 3.8 IMEP calculation

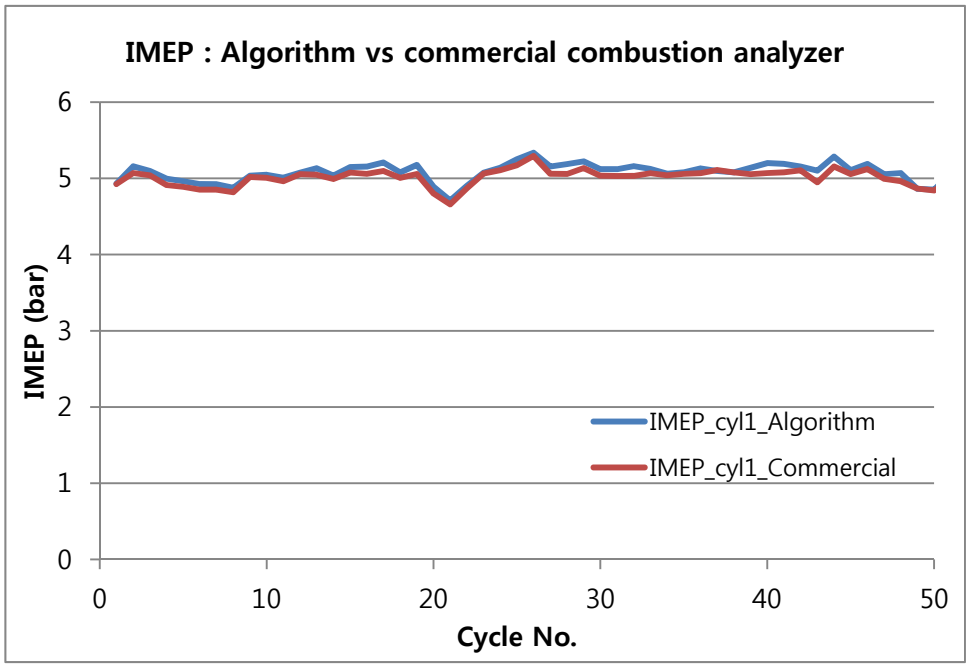

Figure 3.9 Comparison of measured IMEP performance

3.2 **EGR prediction model**

3.2.1 Overall model description

The EGR prediction model is based on the ideal gas equation of state. Total mass of the in-cylinder gas at IVC can be derived with the pressure, volume, gas constant and temperature of in-cylinder gas. Then, the mass of EGR gas can be calculated if the mass of fresh gas per cycle and the mass of residual gas are known. Figure 3.10 shows the gas composition of in-cylinder gas. In-cylinder pressure is measured by the pressure sensor for the combustion analyzing and in-cylinder volume at IVC can be calculated easily. Also, the mass of fresh air per cycle is measured by the ECU. Control logic and ECU is communicating with each other by ETK communication, and EGR model receives the mass of fresh air from ECU.

The temperature of in-cylinder gas at IVC should be derived to calculate ideal gas equation. The temperature is derived using the energy conservation equation without considering heat transfer from cylinder walls to gas. However, heat transfer is not negligible. Previous researches use a correction factor to remove the error, however these assumptions are not based on thermodynamics or fluid dynamics. In this model, main error source is the increase of gas temperature due to the heat transfer and it is needed to be calculated with some assumptions.

The assumptions applied in this study are:

A. There is no heat transfer in the intake manifold.

B. Residual gas fraction is fixed as a constant.

C. The cooling efficiency of EGR cooler is constant.

3.2.2 Overall model

According to the gas equation of state, mass of in-cylinder gas at IVC, m_{IVC}, is calculated as [17]:

$$\frac{P_{IVC}V_{IVC}}{RT_{IVC}} = m_{IVC} \quad (3.8)$$

Where P_{IVC} is the cylinder pressure at IVC, V_{IVC} is the cylinder volume at IVC, R is gas constant of in cylinder gas, and T_{IVC} is the in-cylinder gas temperature at IVC.

Pressure at IVC is measured by the installed in-pressure sensor. Pressure signal at this range is easy to be interrupted by noise. Therefore, weighted average with 3 previous cycles is applied.

$$P_{IVC,averaged} = 0.4 \times P_{IVC,n} + 0.3 \times P_{IVC,n-1} + 0.2 \times P_{IVC,n-2} + 0.1 \times P_{IVC,n-3} \quad (3.9)$$

In-cylinder volume at IVC,V_{IVC}, is derived as [17]:

$$V_{IVC} = Vc\left[1 + \frac{1}{2}(r_c - 1)\left(\frac{r}{a} + 1 - \cos\theta_{IVC} - \sqrt{\left(\frac{r}{a}\right)^2 - \sin^2\theta_{IVC}}\right)\right] \quad (3.10)$$

Where Vc is the clearance volume, r_c is the compression ratio, r is the length of connecting rod, a is the half of the stroke, and Θ_{IVC} is the crank angle at the IVC.

Mass of in-cylinder gas at IVC, m_{IVC}, is calculated with mass of fresh air, mass of EGR gas and mass of residual gas [17].

$$m_{IVC} = m_{air} + m_{EGR} + m_{RG} \quad (3.11)$$

Where m_{air} is the mass of fresh air at IVC, m_{EGR} is the mass of EGR gas at IVC, and m_{RG} is the mass of residual gas at IVC.

In this study, fresh air flow rate per cylinder is measured by the air flow sensor in ECU and the measured value is imported to this model in real time.

Mass of residual gas is removed by below equation where RGF is the ratio of residual gas in the trapped mass in the cylinder.

$$RGF\ (\%) = \frac{m_{RG}}{m_{air}+m_{EGR}+m_{RG}} \times 100 \quad (3.12)$$

$$m_{RG} = \frac{RGF}{100-RGF}(m_{air} + m_{EGR}) \quad (3.13)$$

If the heat losses are neglected, law of conservation of energy is applicable to consider the temperature at IVC.

$$C_{IVC}T_{IVC,no\ HT}m_{IVC} = C_{air}T_{air}m_{air} + C_{EGR}T_{EGR}m_{EGR} + C_{RG}T_{RG}m_{RG} \tag{3.14}$$

Where C_{IVC}, C_{air}, C_{EGR}, and C_{RG} are the molar specific heat of in-cylinder gas, fresh air, EGR gas, and residual gas at IVC, respectively. $T_{IVC,no\ HT}$ is the in-cylinder gas temperature without considering heat transfer from cylinder wall.

Molar Specific heat of fresh air, EGR gas and residual gas are approximately equal, so molar specific heat is removed [27].

$$T_{IVC,no\ HT} = \frac{T_{air}m_{air}+T_{EGR}m_{EGR}+T_{RG}m_{RG}}{m_{air}+m_{EGR}+m_{RG}} \tag{3.15}$$

However, heat transfer from cylinder wall to in-cylinder gas is not negligible. A term considering increased gas temperature caused by heat transfer is applied to the equation.

$$T_{IVC} = T_{IVC,no\ HT} + \Delta T_{IVC,HT} = T_{IVC,no\ HT} \times \eta_{HT} \tag{3.16}$$

$$\eta_{HT} = \frac{T_{IVC}}{T_{IVC,no\ HT}} = 1 + \frac{\Delta T_{IVC,HT}}{T_{IVC,no\ HT}} \tag{3.17}$$

Substituting the equations, the mass of EGR gas is calculated as:

$$m_{EGR} = \frac{\frac{P_{IVC}V_{IVC}}{R\eta_{HT}} - m_{air}\left(T_{air} + T_{RG} \times \frac{RGF}{100-RGF}\right)}{T_{EGR} + T_{RG} \times \frac{RGF}{100-RGF}} \quad (3.18)$$

Then, EGR rate is calculated as:

$$\text{EGR}\ (\%) = \frac{m_{EGR}}{m_{air} + m_{EGR}} \times 100 \quad (3.19)$$

EGR rate calculation is scheduled to finish by the middle of intake stroke. Then, the calculated EGR rate is used to control injection strategy.

3.2.3 Sub-part calculation

The variation range of residual gas in a CI engine is relatively narrower than that in a SI engine and the average level of residual gas in a CI engine is lower than that in a SI engine. In this study, residual gas fraction, RGF, is fixed to 3.11 % [17].

$$\text{RGF} = 3.11\ (\%) \quad (3.20)$$

Using the variable EGR and RGF, equation 3.15 is re-defined as:

$$T_{IVC,\text{no HT}} = \frac{T_{\text{intercooler}} \times (100 - EGR_{n-1}) + T_{EGR} \times EGR_{n-1}}{100} \times \frac{100-RGF}{100} + T_{RG} \times \frac{RGF}{100} \quad (3.21)$$

Convective heat transfer from cylinder wall to in-cylinder gas is calculated as [65]:

$$\frac{dQ}{dt} = h_c \sum A_{eff}\left(T_{wall} - T_{cyl}\right) = h_c\left[A_{piston}\left(T_{piston} - T_{cyl}\right) + A_{liner}\left(T_{liner} - T_{cyl}\right) + A_{head}\left(T_{head} - T_{cyl}\right)\right] \quad (3.22)$$

Area of liner is considered as averaged liner area of every crank angle from BDC to IVC. Area of piston is considered as 1.3 times larger than area of head.

Convection coefficient, hc, is assumed by Woschni's correlation [36].

$$h_c = 3.26B^{-0.2}p^{0.8}T^{-0.55}w^{0.8} \quad (3.23)$$

Where B is the bore of the target engine. Pressure at intake stroke, p, is assumed to be boost pressure and temperature at intake stroke, T, is estimated to be the intake manifold temperature.

Averaged cylinder gas velocity, w, determined for a 4-stroke direct injection CI engine was expressed as [36]:

$$w = \left[C_1\bar{S}_p + C_2\frac{V_d T_r}{p_r V_r}(p - p_m)\right] \quad (3.24)$$

Where V_d is the displacement volume, p is the instantaneous cylinder pressure and p_r, V_r and T_r are the working fluid pressure, volume and temperature at some reference state, respectively. Lastly, pm is the motored cylinder pressure at the same

crank angle as p. For the gas exchange period, C_1 is 6.18 and C_2 is 0. Thus, the above equation at intake stroke can be simplified as below.

$$w = C_1 \bar{S}_p \tag{3.25}$$

Then, total convective heat transfer in intake stroke is calculated as:

$$Q = \frac{dQ}{dt} \times T_{BDC\sim IVC} \tag{3.26}$$

Duration of heat transfer $T_{BDC\sim IVC}$ is considered as the time from BDC to IVC.

Transferred heat is used to increase in-cylinder gas. Increased temperature due to the heat transfer is calculated as

$$\Delta T_{IVC,HT} = \frac{Q}{C_v m_{in-cylinder}} \tag{3.27}$$

Where C_V is the specific heats at constant volume and m is the mass of in-cylinder gas at IVC.

Temperature of fresh air after the intercooler is calculated by 2-D map and the temperature is exported in accordance with the engine speed and total injected fuel mass per cycle [23].

$$T_{air} = f(RPM, m_{fuel}) \tag{3.28}$$

Temperature of exhaust gas is calculated by 1-D curve where the temperature is derived by the 2nd order of total injected fuel mass and measured exhaust gas temperature shown as Figure 3.11 [23].

$$T_{exhaust} = C_1 \cdot {m_{fuel}}^2 + C_2 \cdot m_{fuel} + C_3 \quad (3.29)$$

Temperature of EGR gas after the EGR cooler is derived as:

$$\eta_{EGR\ cooler}(\%) = \frac{T_{exhaust} - T_{EGR}}{T_{exhaust} - T_{coolant}} \times 100 \quad (3.30)$$

$$T_{EGR} = T_{exhaust} - \frac{\eta_{EGR\ cooler}}{100} \times (T_{exhaust} - T_{coolant}) \quad (3.31)$$

$\eta_{EGR\ cooler}$ is the cooling efficiency of the EGR cooler. In this study, the efficiency is fixed to 88 % which is averaged result with the representative engine operating at conditions where the EGR is activated. Figure 3.12 shows the test condition of EGR cooler efficiency and the result is shown in Figure 3.13.

3.2.4 Verification of EGR rate model

EGR rate model was verified at various engine operating conditions. EGR rate was measured at steady engine operating conditions where exhaust gas temperature and engine oil temperature reach the steady state. EGR rate model was tested at the most of the ranges where EGR gas supplying is activated.

Measured EGR rate and estimated EGR rate was compared using the coefficient of determination. Coefficient of determination uses the prediction of future outcomes on the basis of other related information in statistics. It provides a parameter of how well real values are likely to be predicted by the model

Figure 3.14 indicates the test cases to verify the EGR rate model where x axis is engine speed and y axis is engine BMEP. Then, the measured EGR rate and estimated EGR rate is compared as shown in Figure 3.15 where x axis is measured EGR rate and y axis is estimated EGR rate. The coefficient of determination is derived as 0.9397 and it shows pretty good agreement between measure data and estimated data.

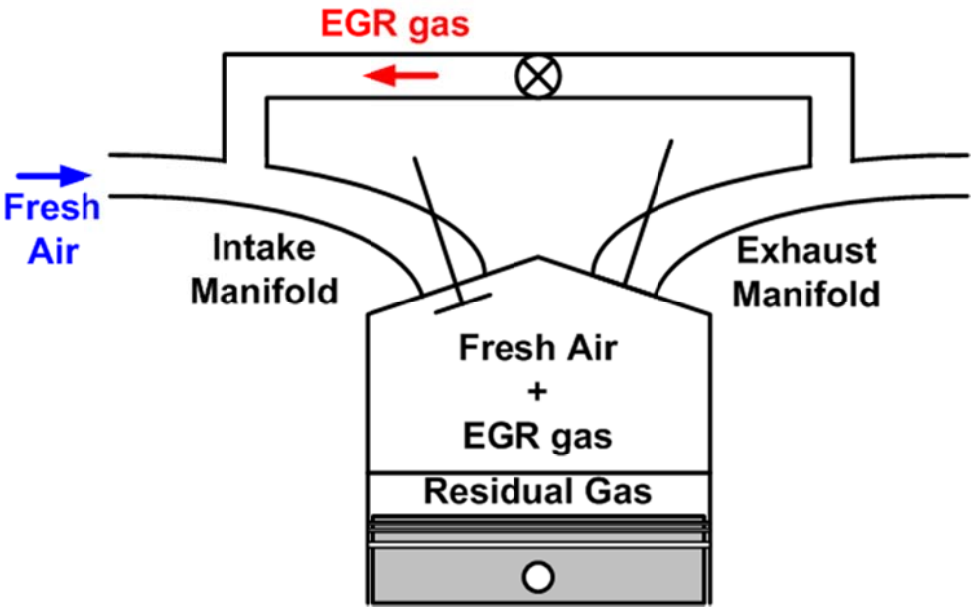

Figure 3.10 Gas composition of in-cylinder gas

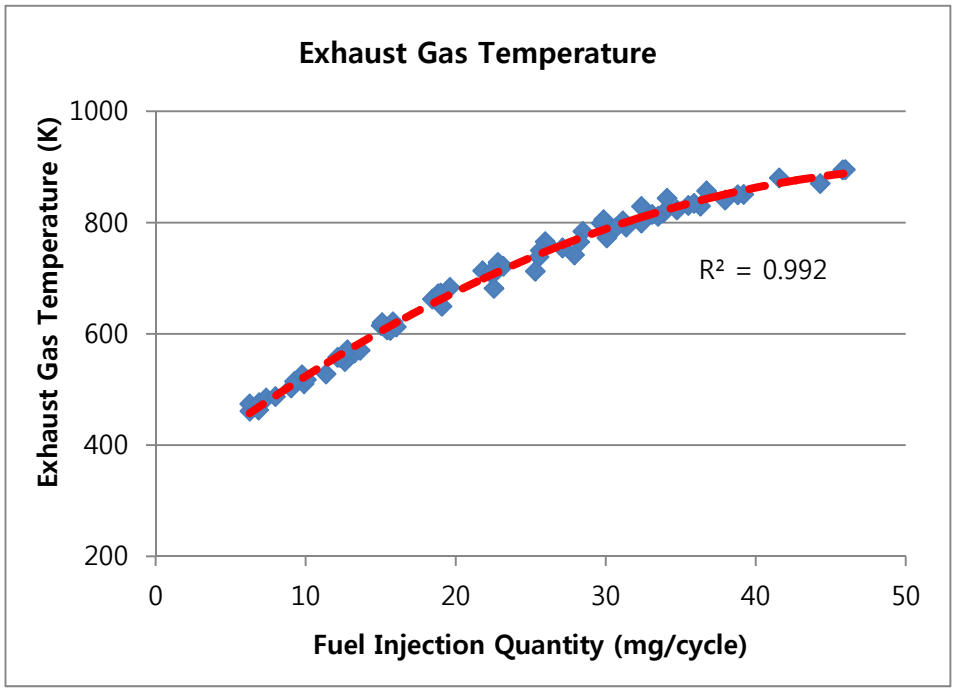

Figure 3.11 Deriving approximating equation of exhaust gas temperature

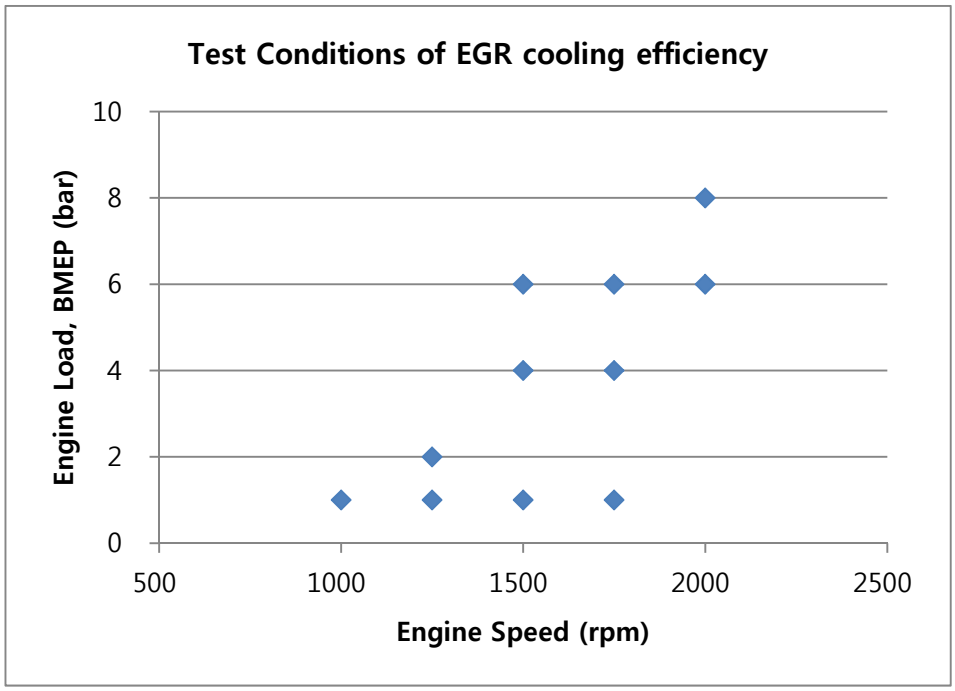

Figure 3.12 Test conditions of EGR gas cooling efficiency

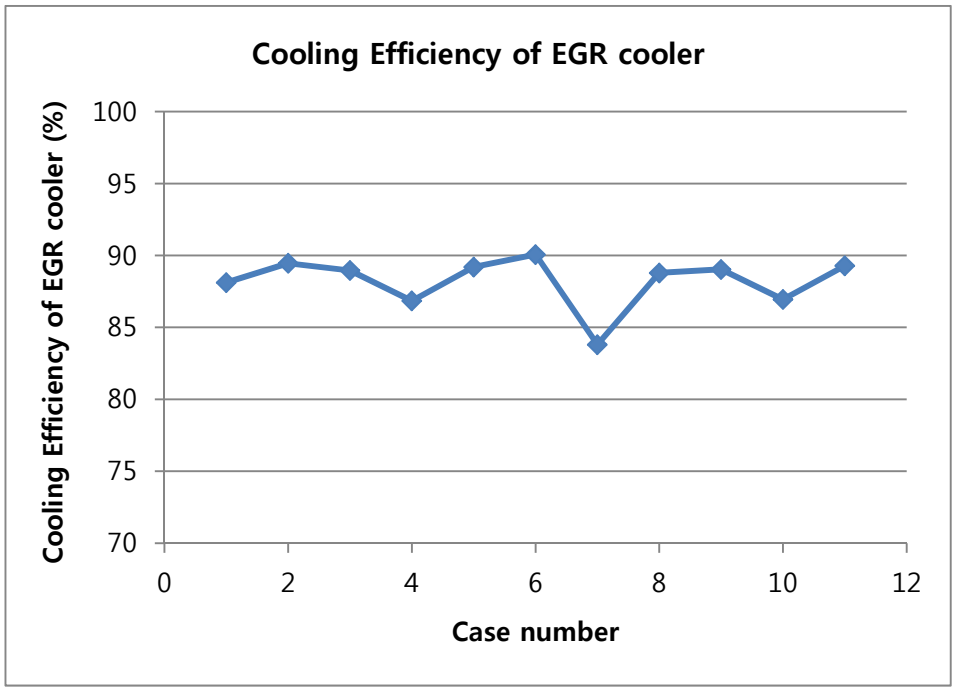

Figure 3.13 Cooling efficiency of EGR gas cooler

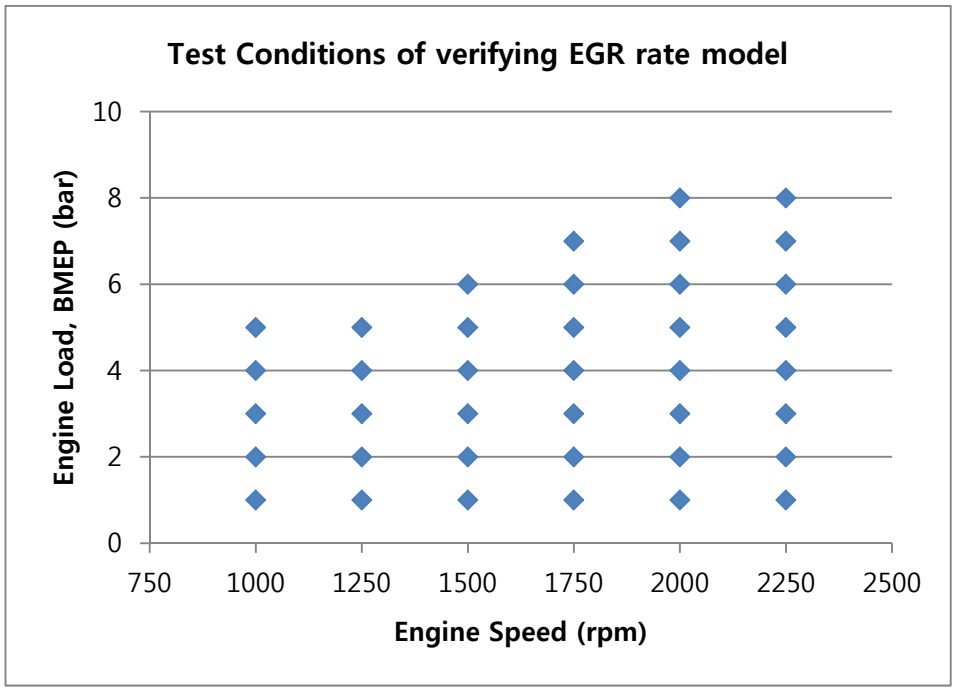

Figure 3.14 Test conditions of verifying EGR rate model

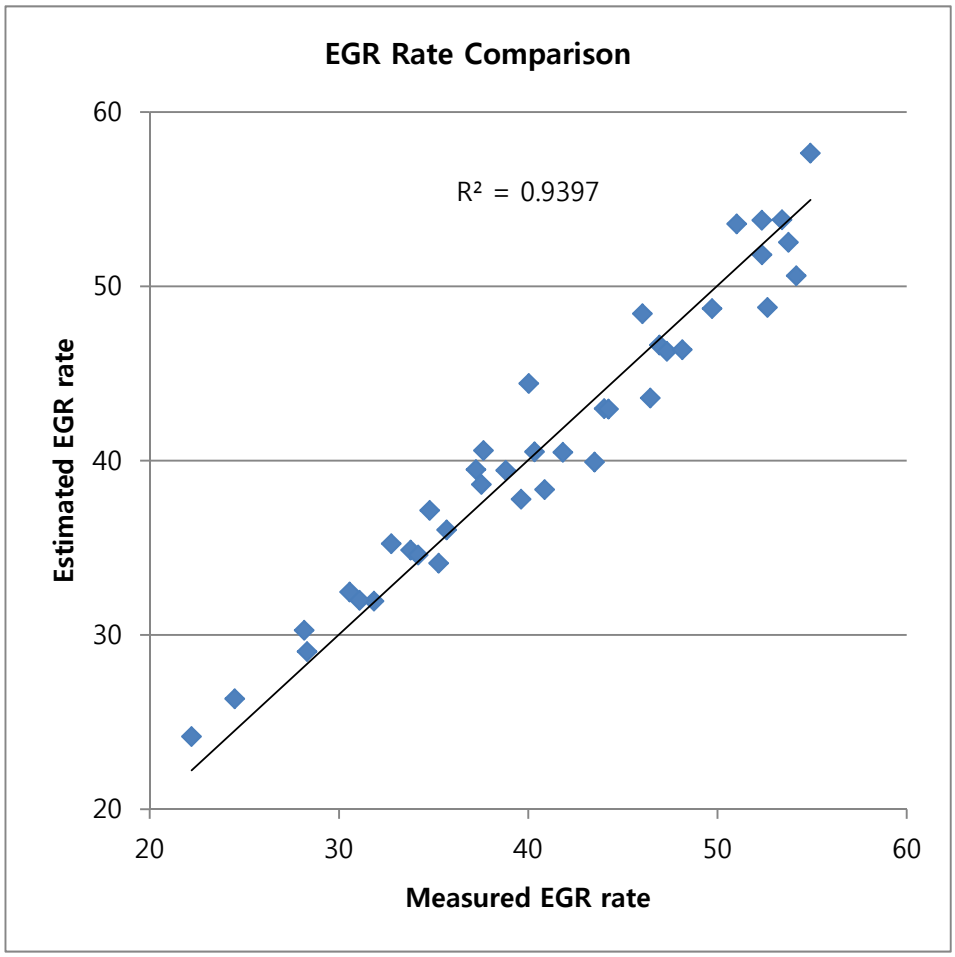

Figure 3.15 EGR rate comparison: Measured EGR rate vs. Estimated EGR rate

Chapter 4. Combustion control algorithm

4.1 Overall algorithm description

The objective parameters measured from the combustion analyzer are compared with the target value at the present operating condition and the difference is calculated. In the PID controller part, to minimize the difference, a change in the engine operating parameters are calculated and, then, added to the current engine operating parameters saved in the ECU. Finally, these new values are sent back to the ECU again and the ECU uses these new values for the engine operation. In addition, a calibration factor is set to encounter the changes caused by the coolant temperature, the environment and, etc, so that the precise target value can be set and controlled. Figure 4.1 shows the conceptual diagram of combustion control logic.

Taking MFB50 control logic as an example, the MFB50 value measured from the combustion analyzer and rpm / total amount of fuel injection determine the targeted MFB50 value. To minimize the difference between the target value and the measured value, the amount of a change in the main injection timing is estimated. When this value is added to the current main injection timing and sent back to the ECU, the engine works in accordance with that value.

4.2 **MFB50 Control algorithm**

4.2.1 MFB50 control parameter determination

In order to show validate performance to control MFB50 as a parameter of in-cylinder combustion, MFB50 should resist robustly to the noise. MFB50 usually appears where the heat release rate is high, in other words, the calculation terms are relatively high. Then the calculated results get more reliability. In addition, MFB50 also possess information about the start of combustion time and combustion speed, so it must be considered to choose engine parameters. The operating parameters that can affect MFB50 are main injection timing, pilot injection timing, EGR rate, boost pressure and etc. In this study, experiments were done to monitor the change in MFB50, when those 4 factors had been swung, and the results are determined as Figure 4.2.

In case of the boost pressure, there is almost no change in MFB50 while swinging the boost pressure. Although there are some changes in MFB50 due to a change in the pilot injection timing and the EGR rate, its linearity or the change are small. As it can be shown in the graph, there is a good linearity in MFB50 if there is a change in the main injection timing. Therefore, for this research, MFB50 is controlled by varying the main injection timing.

4.2.2 MFB50 weight-averaged filtering

In case of MFB50, a weight-average value of previous cycles is used rather than using the analyzed combustion data from the previous cycle for the control. There is a possibility that MFB50 value may change due to the noise while measuring pressure signals, so, for the sake of stability of the logic operation, the weight-average method is chosen. The following is the weight-average method used for the research.

$$\mathrm{MFB50_{filtered}} = (\mathrm{MFB50_n} \times f_1) + (\mathrm{MFB50_{n-1}} \times f_2) + \cdots + (\mathrm{MFB50_{n-k+2}} \times f_{k-1}) + (\mathrm{MFB50_{n-k+1}} \times f_k)$$

$$\mathrm{k} = f(\mathrm{RPM}, \mathrm{m_{fuel}}) \quad (4.1)$$

At the current logic, the value of weight-averaged factor or the number of cycles to be weight-averaged is fixed consistently, regardless of the operating conditions, but logic is formed to incorporate with variables in case of any need. In this study, 4 cycles of MFB50 are weight-averaged.

4.2.3 MFB50 target determination logic

Target MFB50 values are consisted as a map in function of RPM and the fuel injection quantity. The target MFB50 values for each operating condition are

based on the steady-state experiment results. Also, when the coolant temperature is different, the combustion characteristics inside the cylinders change, so a calibration factor is added to consider the change in the coolant temperature. MFB50 target correlation factor due to the coolant temperature is able to be turned on and off manually. MFB50 control target correlation factor due to EGR rate is applied as well.

The correlation factor is activated when the estimated EGR rate is lower than specific EGR rate. More NOx emission is expected where the actual EGR rate is lower than target EGR rate measured in steady states. The most effective way to decrease the NOx emission using injection strategy is retarding main injection timing [66]. Specific EGR target is determined by subtracting margin value from EGR rate map to maintain NOx emission in low level, especially at transient states. EGR map is made by performing steady state experiment where the map consists of engine speed and fuel injection quantity. If estimated EGR rate is lower than the target value, MFB50 target correlation factor which is multiplication of EGR rate gap and correction factor is activated. The calculated correlation factor is added to the target MFB50 and the correction factor affects the target MFB50 in retarding direction. Figure 4.3 is the example case that shows the MFB50 target correlation using EGR rate. The engine operating condition is changed from middle to low load and the gap of target EGR rate and estimated EGR rate is increased. Then, the target

MFB50 is corrected to retarding direction.

Before the exporting the target MFB50, a low-pass filter is applied to calculate target MFB50 to maintain the stability of control. Figure 4.4 shows the entire flow chart to determine the target MFB50.

4.2.4 Logic of PID gain determination

PID gain is determined by RPM and the fuel injection quantity, same as the determination of MFB50, and, the coolant temperature and the calibration factor to encounter the change in MFB50 are also added. In addition, a calibration factor is added to calibrate PID gain in accordance with the difference between the target MFB50 and the real MFB50. The flow chart to determine the PID gain. P, I and D gain are calculated individually for each cylinder is shown in Figure 4.5..

4.2.5 Control limit determination

There is a possibility that the engine operation becomes unstable under some operating conditions due to the control even though the PID gain in combustion control is set appropriately. Therefore, in this study, logic is added to limit the variation caused by the PID control within set boundaries shown in Figure 4.6. The limit applies firstly inside of the PID controller (Limit 1). The limit is determined by

choosing a smaller value between the limit value calculated by the map data consisted of RPM and the fuel injection quantity, and the limit value is calculated by taking an average value of MFB50 of four cylinders. The second limit is given outside of the PID controller and this limit is also determined by RPM and the fuel injection quantity (Limit 2). Lastly, the final limit is given just before the main injection timing, which is calibrated, is sent to the ECU (Limit 3).

4.2.6 PID controller

In the PID controller, a variation of the main injection timing is determined by the PID gain obtained previously and taking a difference between the target MFB50 and the current MFB50. A PID calculation is performed for every one cycle and calibrated main injection timing is extracted by adding variations of the main injection timing and the pre-control value. Control limit of PID gains and main injection timing, considered at the control limit determination, are applied to each calculation.

There are three modes that are able to provide the modified main injection timing to ECU as shown in Figure 4.7. First one is formed so that the new main injection timing calculated for each cylinder can be applied to the intake BDC of each cylinder by switching them in order. Second one is formed so that the new main

injection timing calculated for specific cylinder (user selective) can be applied to all cylinders. Final one is formed so that the new main injection timing for each cylinder can be input manually.

4.2.1 Overrun

For MFB50, appropriate values cannot be obtained during overrun period where the fuel is not injected. Therefore, wrong MFB50 values are exported in the combustion analyzer and wrong I gain values are accumulated as the PID controller is forced to operate once for every one cycle. Thus, after overrun is finished and fuel injection is re-activated, there is a problem related with the wrong I gain and, hence, MFB50 cannot be controlled properly which causes combustion instability.

In order to overcome this problem, logic is formed to find such operating condition where the overrun or the amount of fuel injection is very small and the PID control does not operate within that condition.

After detecting the overrun, the overrun signal should be considered. Usually overrun condition causes a problem that when the engine accelerates after the overrun. Figure 4.8 shows the unstable case without considering overrun that even though the real MFB50 is far advanced than the target value, it tends to be controlled in more advanced direction.

MFB50 control algorithm is modified to prevent from the abnormal control at the end of overrun. Figure 4.9 shows the modified algorithm. By looking over the control related parameters, it was confirmed that the control of the main fuel injection timing reached the max limit and this was caused by the accumulation of I gain error at the overrun range. Therefore, for the improvement, pre-control values of the main fuel injection timing are used over several cycles after the overrun exit and, until this cycle terminates, the logic is modified to reset the I gain. Logic is added to expand the range of the control of the main injection quantity with a step during the transient state which is followed after the cycles.

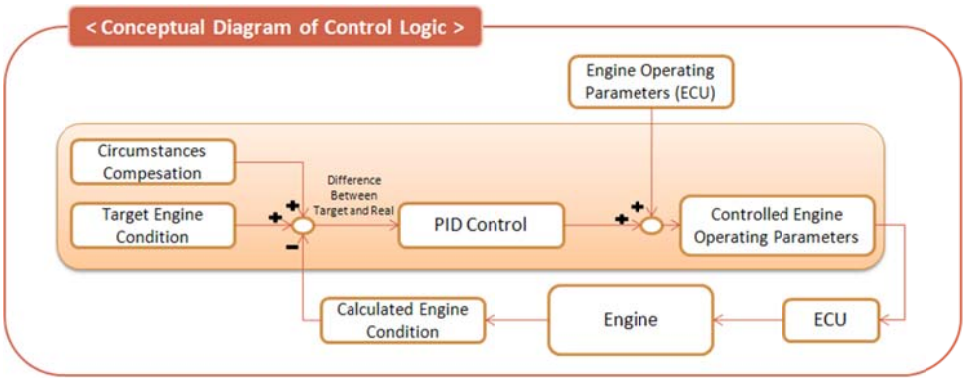

Figure 4.1 Combustion control logic concept

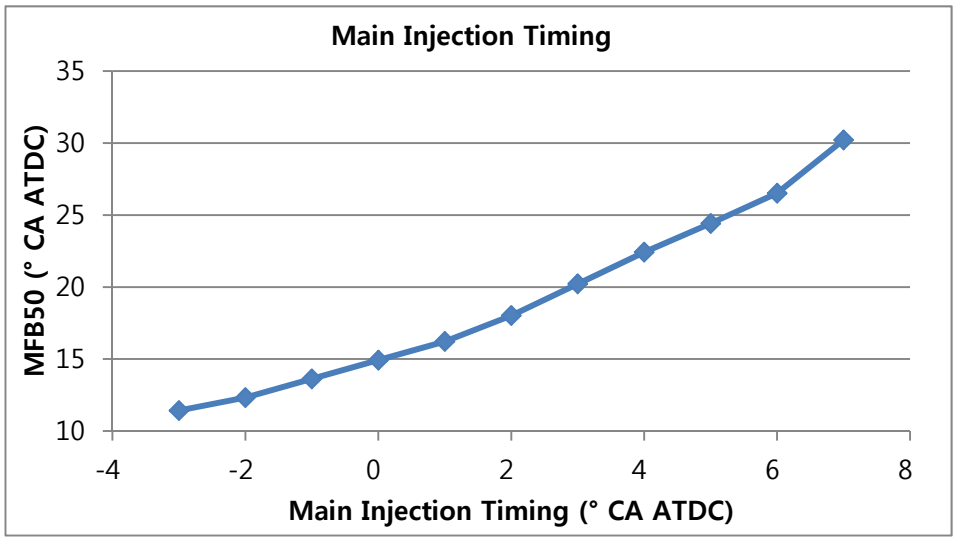

(a) Main injection timing

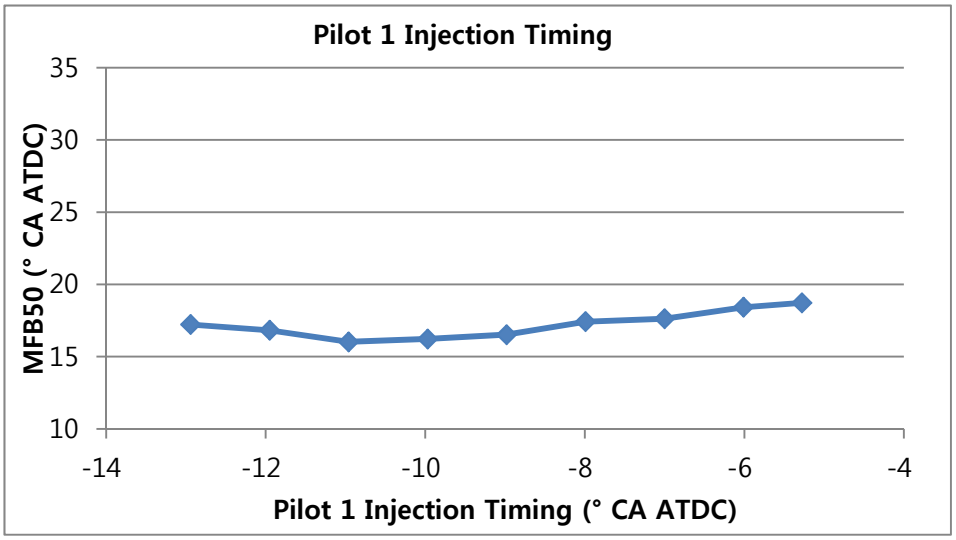

(b) Pilot 1 injection timing

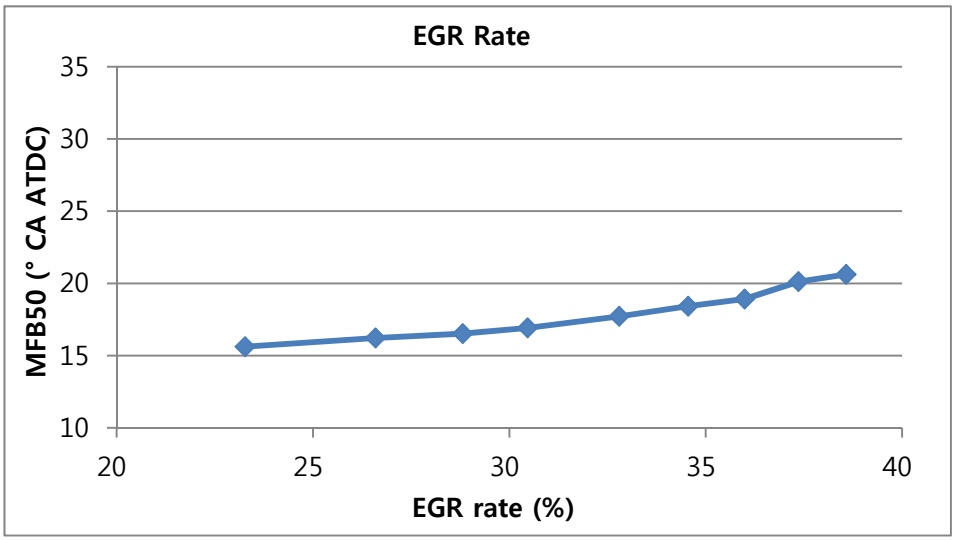

(c) EGR rate

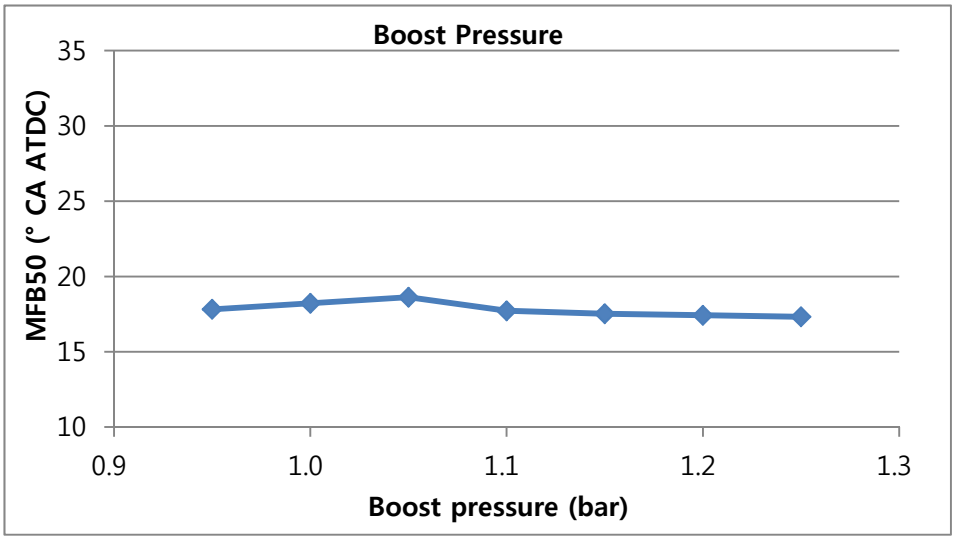

(d) Boost pressure

Figure 4.2 Experiment results showing the relationship between engine operating parameters and MFB50 at 1500 rpm and BMEP of 4 bar

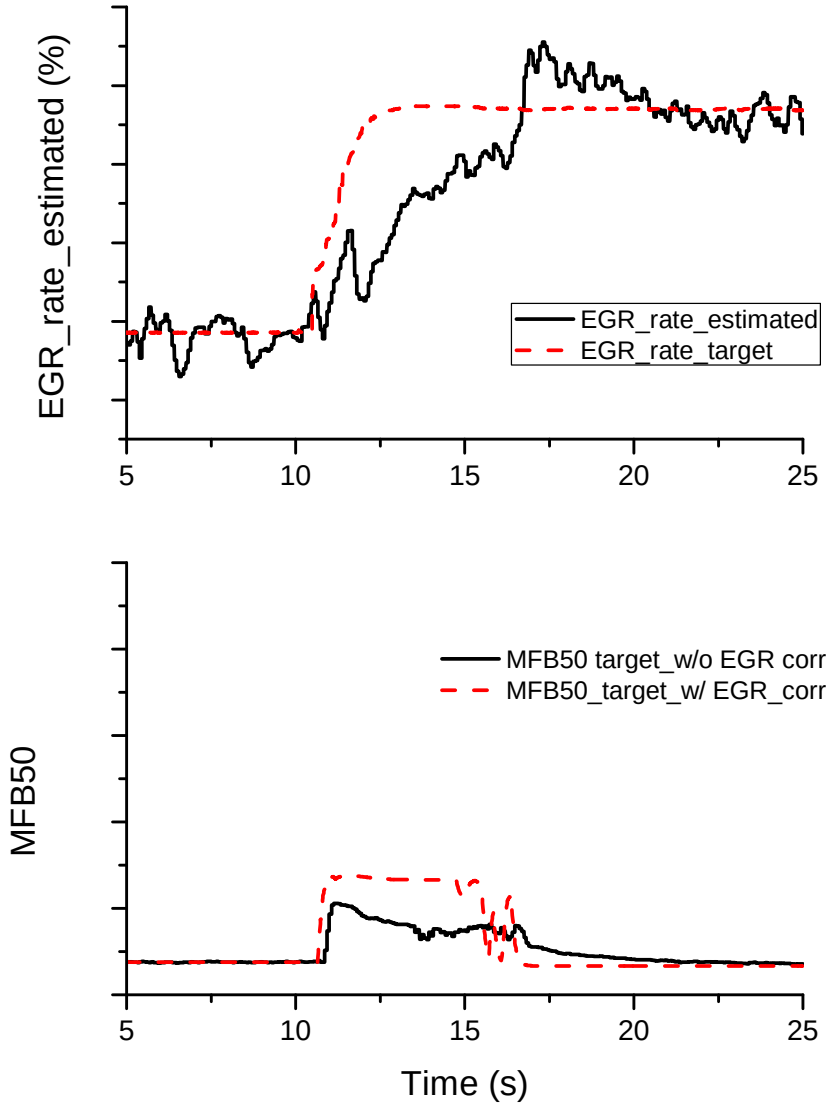

Figure 4.3 MFB50 target correlation using estimated EGR rate

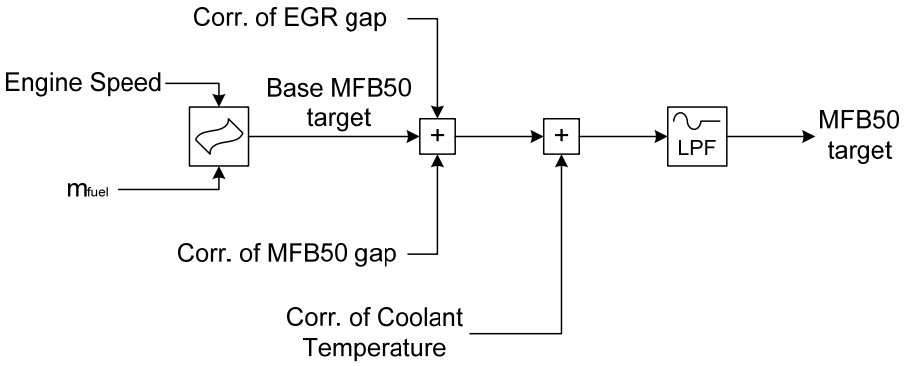

Figure 4.4 Determination of target MFB50

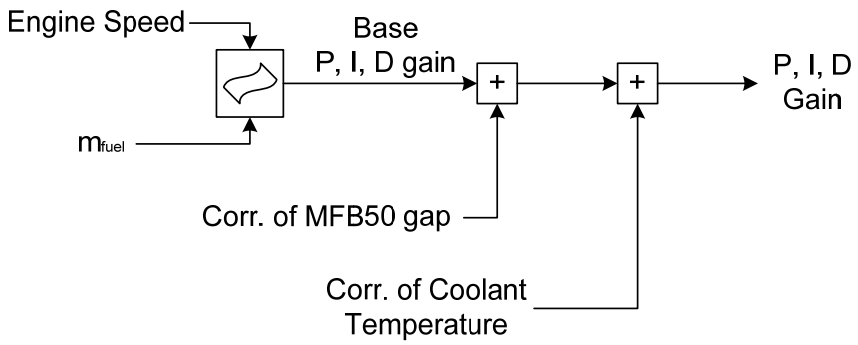

Figure 4.5 Determination of PID gain

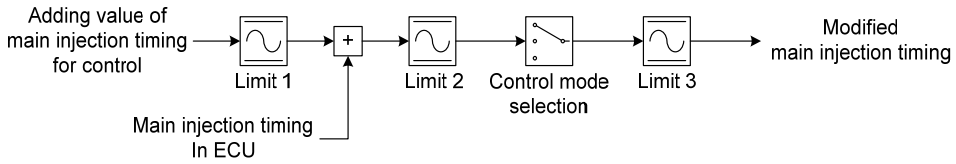

Figure 4.6 Applying the limit of MFB50 control

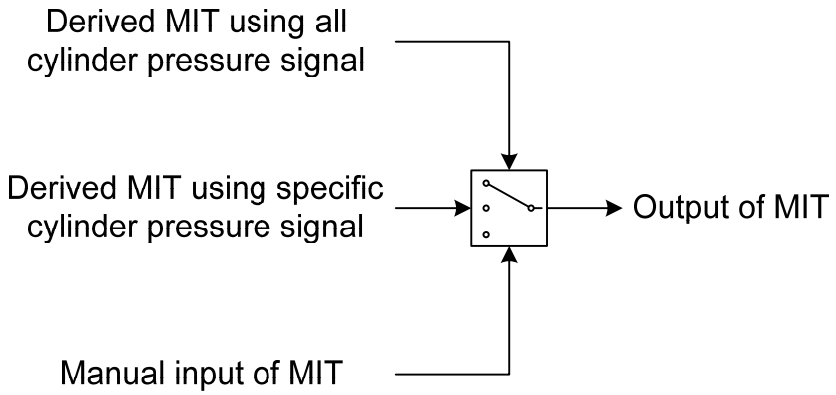

Figure 4.7 Control mode switching

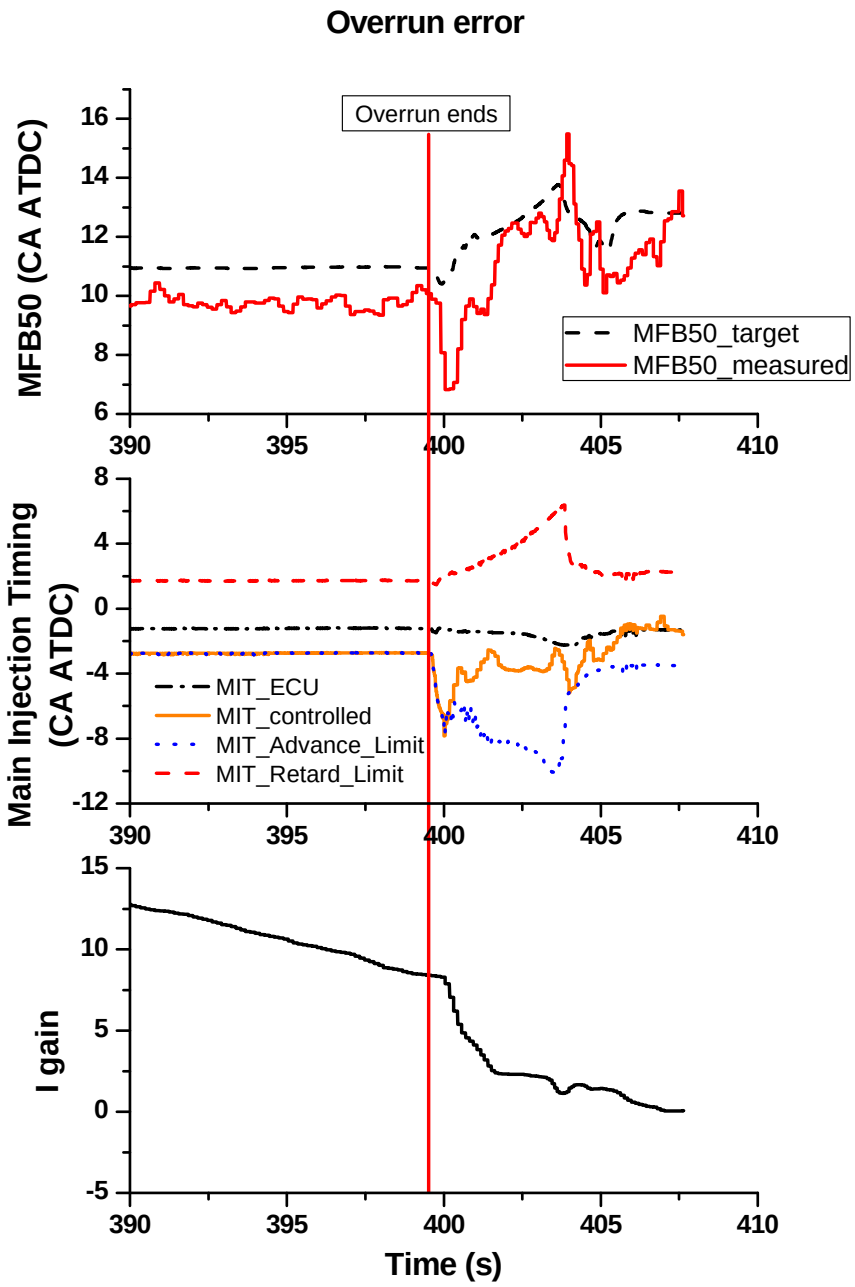

Figure 4.8 Abnormal operation of control logic at overrun

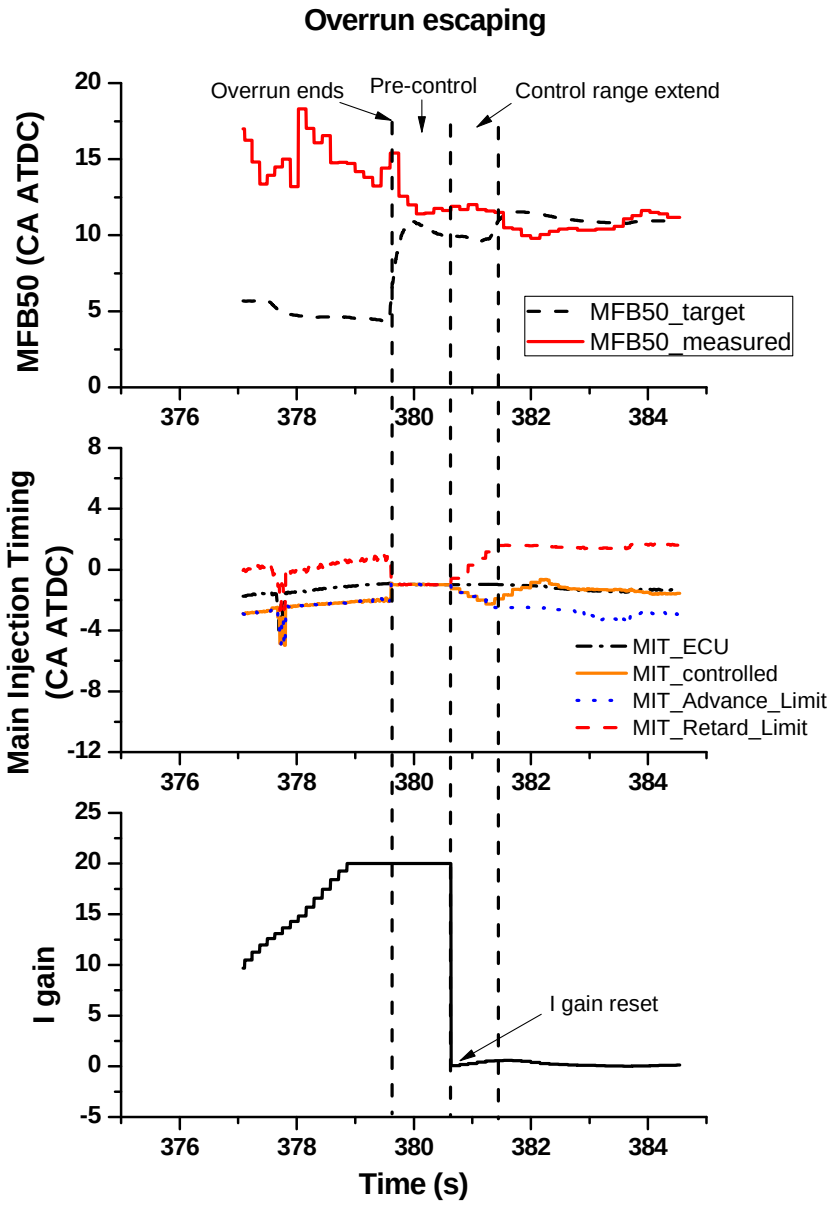

Figure 4.9 Performance verification of MFB50 control with the addition of overrun exit recognition logic

4.3 **IMEP Control algorithm**

4.3.1 Determination of IMEP control parameter

Engine operating parameters which control IMEP are fuel injection quantity and fuel injection timing. The fuel injection timing is already used for the control of MFB50, so if it is used for the control of IMEP along with MFB50, its performance gets worse. Therefore, the amount of fuel injection was chosen, instead of the fuel injection timing. Due to characteristics of engine control logic, if the amount of fuel injection is changed by the control, it affects the control of the intake system such that the entire engine control is affected. If the main injection quantity is used as a parameter to control IMEP, a change in the amount of the fuel injection controls the IMEP difference but the calibrated amount of fuel amplifies the difference between the amount of the fuel from ECU and the real amount of the fuel from the FMO logic. FMO logic is the correction algorithm between the target fuel injection quantity and calculated fuel injection quantity using air flow sensor and air-fuel ratio sensor. In order to solve this, the control logic is modified so that the FMO logic cannot indicate the calibrated amount of fuel which is used to trace IMEP.

Therefore, an engine control parameter which is the closest to the final fuel injection signal, if possible, must be chosen for the IMEP control. In case of the

engine control system used for the research, the duration of main injection is the last step of parameter to be able to bypass among the engine operating parameters about fuel injection quantity. As a result, energizing time is selected to control IMEP as an engine operating parameter.

4.3.2 IMEP input

The IMEP values from the combustion analyzer are passed through the limit for a stable operation of the combustion control logic for each cylinder and the weight-averaged values from the previous cycles are formulated according to the engine operating conditions which are then passed to the control logic.

$$\mathrm{IMEP_{filtered}} = (\mathrm{IMEP_n} \times f_1) + (\mathrm{IMEP_{n-1}} \times f_2) + \cdots + (\mathrm{IMEP_{n-k+2}} \times f_{k-1}) + (\mathrm{IMEP_{n-k+1}} \times f_k)$$

$$\mathrm{k} = f(\mathrm{RPM}, \mathrm{m_{fuel}}) \quad (4.2)$$

For the current logic, the weight-average is inactivated. IMEP values from the previous cycles are used for the control, regardless of the operating conditions.

4.3.3 IMEP Target determination

Target IMEP is also function of engine RPM and the fuel injection quantity, which

was obtained at the engine developing stage. c Also, when the coolant temperature is changed, the combustion characteristics inside the cylinders and friction are varid, so a calibration factor is added to encounter the change in the coolant temperature. IMEP target correlation factor due to the coolant temperature is able to be turned on and off manually. A low-pass filter is applied to calculate target MFB50 to maintain the stability of control. Figure 4.10 shows the flow chart to determine target IMEP.

4.3.4 Algorithm for PI gain determination

PI gain is determined by map data containing the number of revolutions of an engine and the amount of the fuel injection, same as the determination of IMEP. On top of that, a calibration factor for target IMEP values and a calibration factor for the coolant temperature are also included. Lastly, a calibration factor, which is determined by the current amount of fuel injection and the difference between the previously calculated IMEP and the real IMEP, is also set. As the difference gets larger, the calibration factor becomes smaller to prevent engine operating parameters from rapid change. P and I gain are calculated individually for each cylinder. Figure 4.11 shows the flow chart to determine PI gain for IMEP control.

4.3.5 Control range limit

There is a possibility that the engine operation changes rapidly under some operating conditions due to the control even though the PI gain in combustion control is set appropriately. Therefore, in this study, logic is added to limit the variation caused by the PI control within set boundaries as shown in Figure 4.12. The limit operates inside of the PI controller first. This limit is selectable among three types. First one is determined by the map data consisted of RPM and the fuel injection quantity, and second one is determined by the map data consisted of fuel injection quantity and rail pressure. The last limit mode is choosing a smaller value between the limit value calculated by the map data consisted of RPM and the fuel injection quantity, and, the limit value calculated by fuel injection quantity and rail pressure. The second limit is given outside of the PI controller and this limit is also determined by RPM and the fuel injection quantity. Lastly, the final limit, which is calibrated, is given just before the main injection duration and, then, sent to the ECU.

4.3.6 PI control

PI control is operated by using the determined PI gain value and the difference between the target IMEP value, and, the IMEP value from the previous cycle. Control limit of PI control and main injection duration, are applied to each calculation step. PI control is either activated or inactivated by bypass signal and control signal in accordance with the operating conditions.

PI control is set to operate once for every one cycle and IMEP control is implemented by a change in the energizing time, so the pre-control value is not included at this stage. A ramp interval is set to prevent a sudden change in the engine operating condition at the control entry and the control exit. At the control entry, the proportion of control interference is increased slowly for the specified cycle and, at the control exit, the opposite action is taken.

4.3.7 Control logic activation and inactivation

IMEP control must be inactivated at the overrun condition so that the engine control can operate promptly when a torque is generated after the overrun. Overrun is found by maintaining the amount of fuel and the throttle angle below a specified value

It is possible that drivability gets worse due to the IMEP control logic. Increasing rate of fuel injection quantity at acceleration state and decreasing rate of fuel injection at deceleration state could be blocked because of the control logic. IMEP control logic is inactivated when the throttle angle variation exceed minimum and maximum limit. IMEP control logic is also off, when vehicle speed is zero and acceleration pedal position is under specific value. Figure 4.13 shows the flow chart to determine driving condition for drivability.

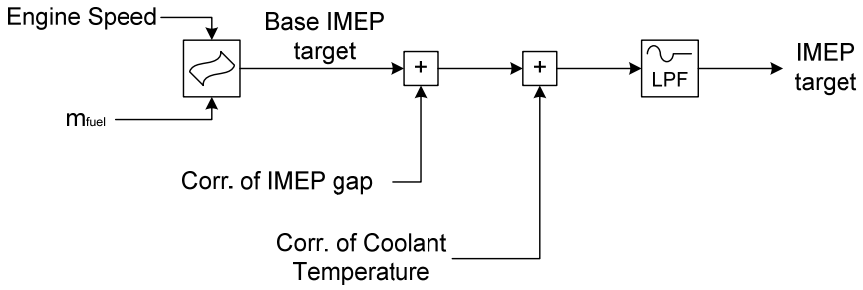

Figure 4.10 Determination of target IMEP

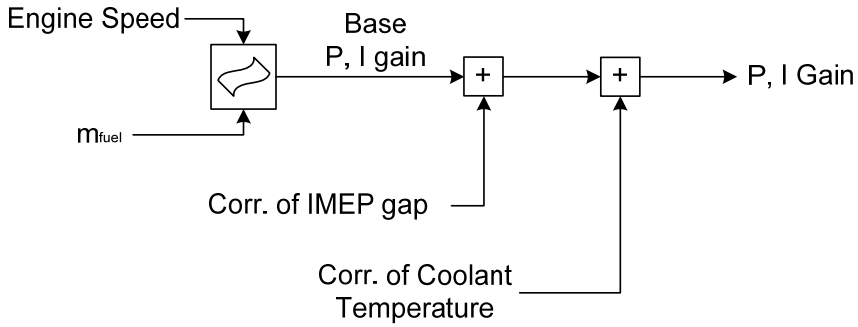

Figure 4.11 Determination of PI gain for IMEP control

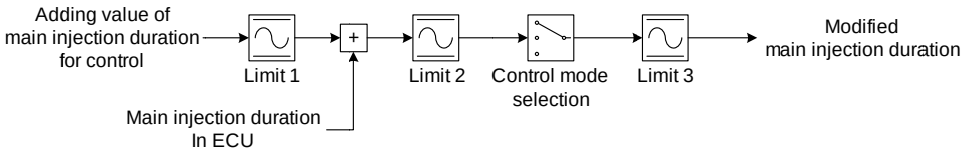

Figure 4.12 Applying the limit of IMEP control

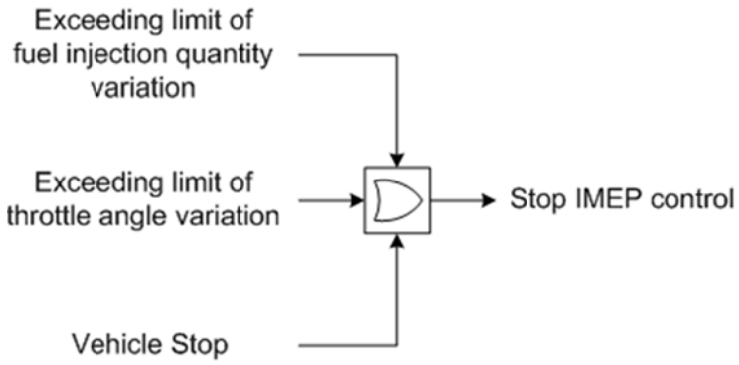

Figure 4.13 IMEP control inactivation for drivability

4.4 Control algorithm for maximum cylinder pressure

4.4.1 Operating condition hysteresis

In engine development stage, maximum in-cylinder pressure is a critical value for maximum power and torque. The maximum in-cylinder pressure is limited due to the durability of the engine components. Injection quantity and injection timing is adjusted while monitoring maximum pressure and exhaust manifold temperature. According to this process, the most effective engine parameter to control the maximum pressure is main injection timing. When maximum pressure control logic uses the main fuel injection timing to control the maximum pressure, it is necessary to separate the operating range from the MFB50 control. In addition, when an engine operates at such operating conditions where the operating range is separated, there would be a problem related to the stability since there is a frequent mode shift between the maximum pressure control and the MFB50 control. Hence, a hysteresis is installed between those two ranges to remove such problems. Actually, MFB50 control is more effective at low and medium load, and maximum pressure control is needed at high load. When the fuel injection quantity exceeds limit L_1, controlling main injection timing is used to control maximum pressure. On the contrary, when the fuel injection quantity is below the limit L_2, controlling main injection timing is used to control MFB50. L_1 is always higher than L_2. Figure 4.14 shows the

hysteresis between MFB50 and maximum pressure control. A limit of the maximum pressure is determined by RPM. The limit is considered by the durability such as thermal stress of component or stress of moving parts.

4.4.2 Limit of maximum pressure determination logic

The limit of maximum pressure is subtracted from the current maximum pressure for each cylinder. If the subtracted value is smaller than 0, maximum pressure control is unnecessary. Therefore, only if the subtracted value is greater than 0, then it is passed to the controller. A low pass filter is applied to cope with abnormal input fluctuation.

4.4.3 PID gain determination logic

The PID gain, which will be used for the maximum pressure control, is calculated by multiplying the weighting factor- determined from the exceeded value of the limit of maximum pressure- with the amount of fuel injection and the base value of the gain. As the difference of maximum pressure gets larger, P gain becomes larger to decrease the maximum pressure rapidly. Unlike the MFB50 control algorithm, the most important point is maintaining maximum pressure under the limit.

4.4.4 Control range limit

The limit style of the maximum pressure control range shares the main fuel injection timing and the limit of the MFB50 control. There is a possibility that the engine operation becomes unstable under some operating conditions due to the control even though the PID gain in combustion control is set appropriately. Therefore, in this study, logic is added to limit the variation caused by the PID control within set boundaries. The limit operates inside of the PID controller first. The limit is determined by choosing a smaller value between the limit value calculated by the map data consist of RPM and the fuel injection quantity, and, the limit value calculated by taking an average value of maximum pressure of four cylinders. The second limit is given outside of the PID controller and this limit is also determined by RPM and the fuel injection quantity. Lastly, the final limit, which is calibrated, is given just before the main injection timing and, then, sent to the ECU. Maximum pressure control logic operates in severe condition, thus, limit of maximum pressure control should be considered more carefully than MFB50.

4.4.5 PID control

As described in chapter 4.4.1, the control of the main fuel injection timing is used simultaneously for both MFB50 control and maximum pressure control. Thus, the logic is formed to shift the control mode in accordance with the control range hysteresis. The main fuel injection timing from the PID controller is checked by the

maximum/minimum control limit and, then, sent to the ECU.

The PID controller to control the maximum pressure has the same structure as the controller for the MFB50 control and if the maximum pressure value does not exceed the limit, then, PID gain for maximum pressure control is re-set to 0.

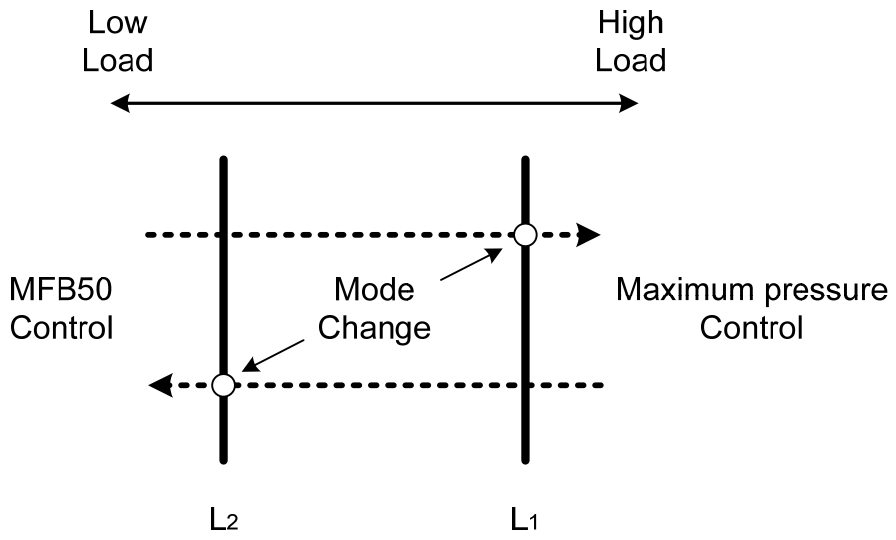

Figure 4.14 Hysteresis between MFB50 and maximum pressure control

4.5 Control logic verification

4.5.1 MFB50 and IMEP control

Table 4.2 is the results of the performance test at the steady-state where both MFB50 and IMEP control are applied simultaneously. Operating engine speed is 1500 rpm and engine load is BMEP of 4 bar. It is found out that the difference of MFB50 in the cylinders is reduced by 50 % when the MFB50 control operates. In addition, the difference of IMEP in the cylinders is reduced by 46 % when the IMEP control operates. Figure 4.15 shows the MFB50 and MFB50 difference at the steady state for each control condition, and Figure 4.16 shows the IMEP and IMEP difference at the steady state for each control conditions. Cylinder-to-cylinder variation of MFB50 and IMEP is decreased simultaneously, and the actual MFB50 and IMEP are tracking the target values of each parameters.

4.5.2 Maximum pressure control

In order to check the operating status of the maximum pressure control logic, a maximum pressure control experiment was performed under the full load condition. Maximum power of the engine used in this study is 200 hp at 3800 rpm. The maximum pressure limits are changed from 176 bar to 170 bar with a step of 3 bar

and it is confirmed that the main fuel injection timing is changed in accordance with a change of the maximum pressure limit as shown in Figure 4.17. Also, it is found out that there is a change in the maximum pressure in accordance with the change in the maximum pressure limit.

Table 4.1 Variation in MFB50 and IMEP at the steady state with the application of combustion control

	Base	MFB50 Control	IMEP Control	MFB50+IMEP Control
MFB50 Variation(%)	100.0	50.1	125.9	52.6
IMEP Variation(%)	100.0	103.2	53.8	84.7

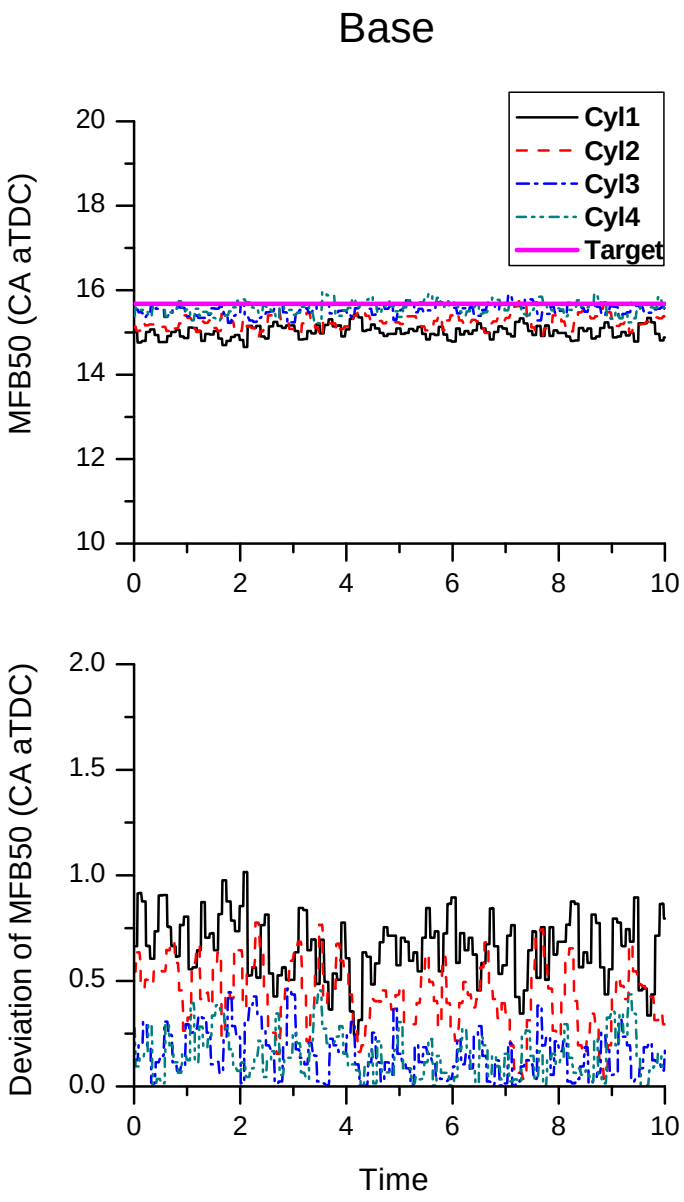

(a) Base condition

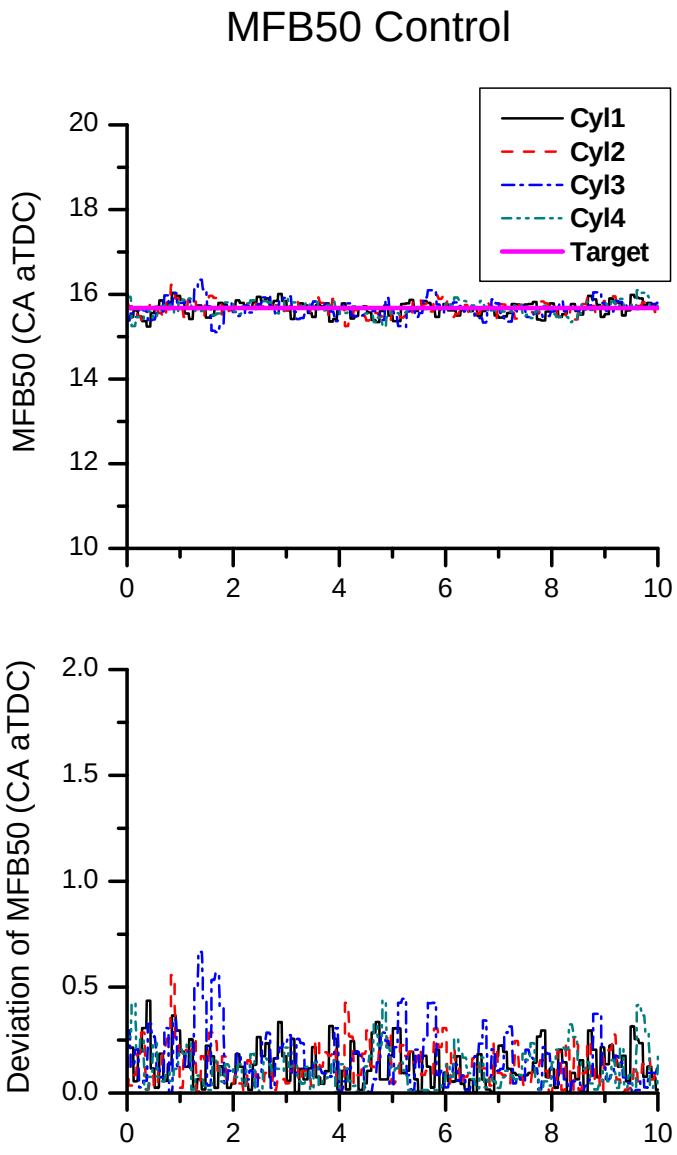

(b) With MFB50 control condition

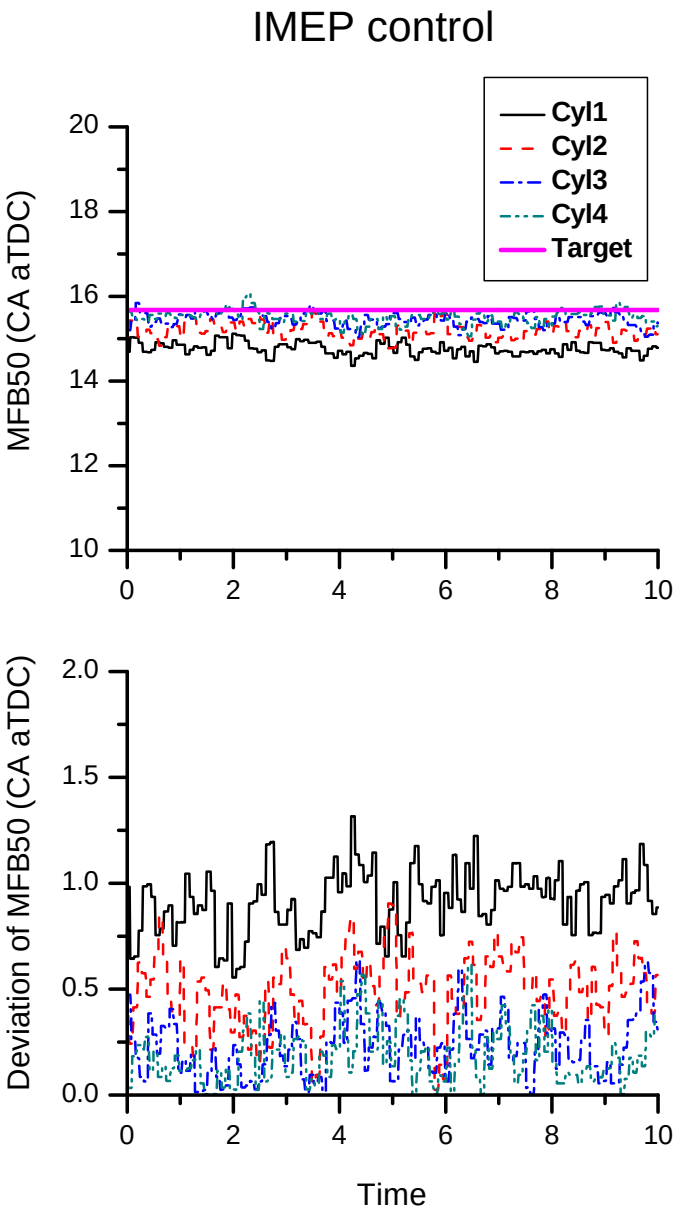

(c) With IMEP control condition

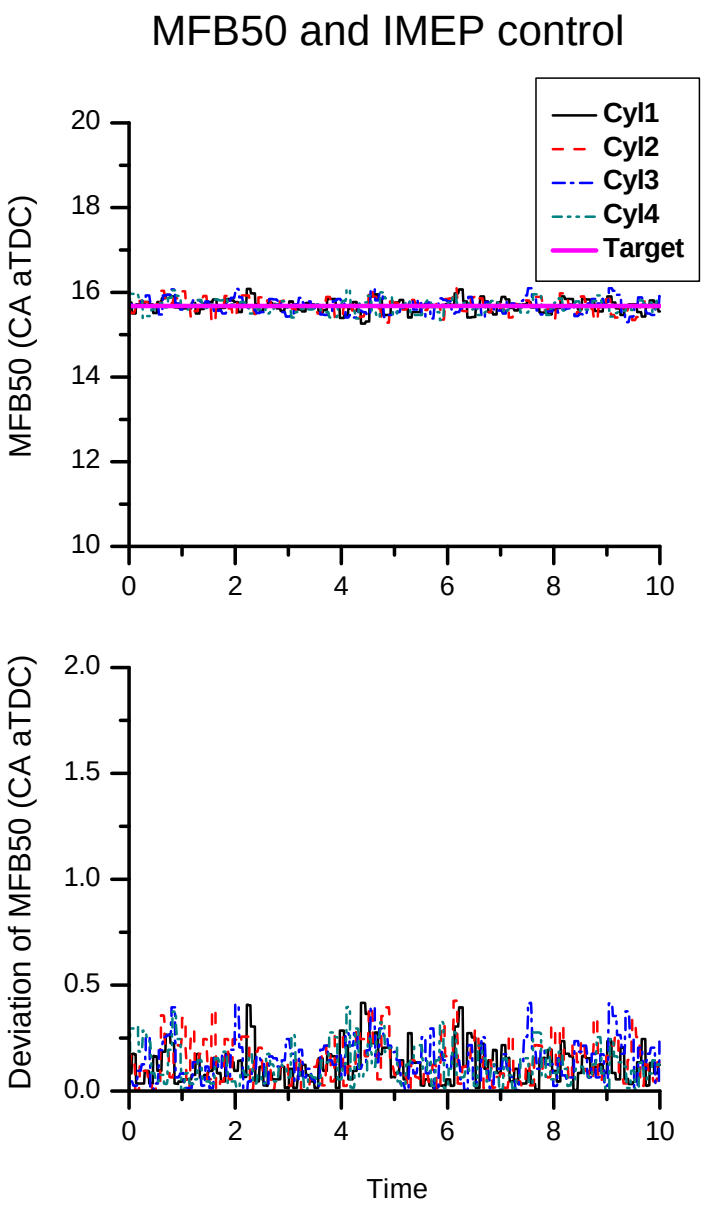

(d) With MFB50 and IMEP control condition

Figure 4.15 MFB50 and variation in MFB50 at the steady state (1500 rpm & BMEP of 4 bar) with application of different control conditions

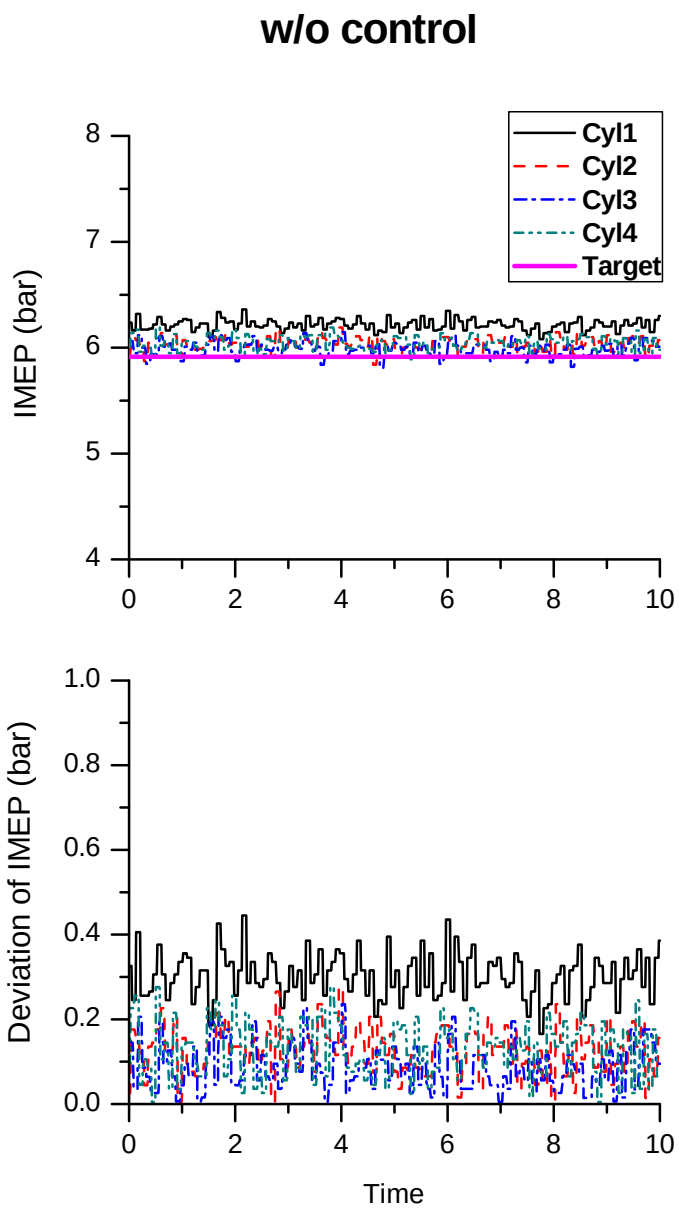

(a) Base condition

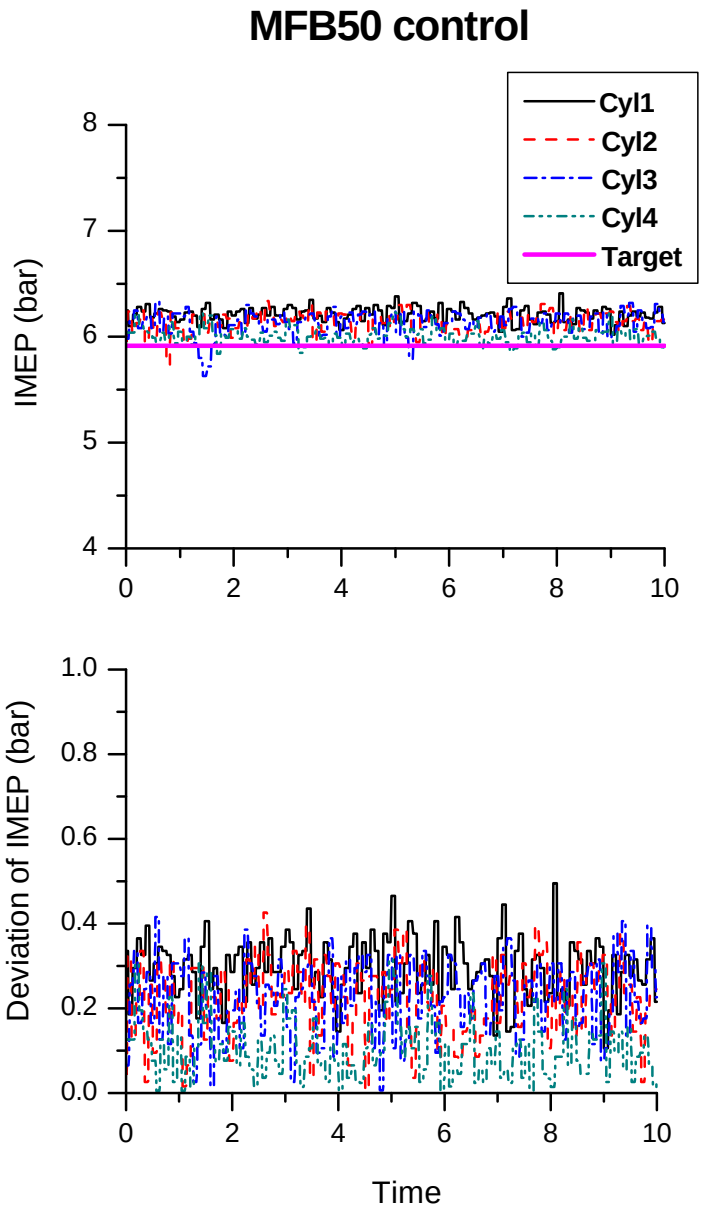

(b) With MFB50 control condition

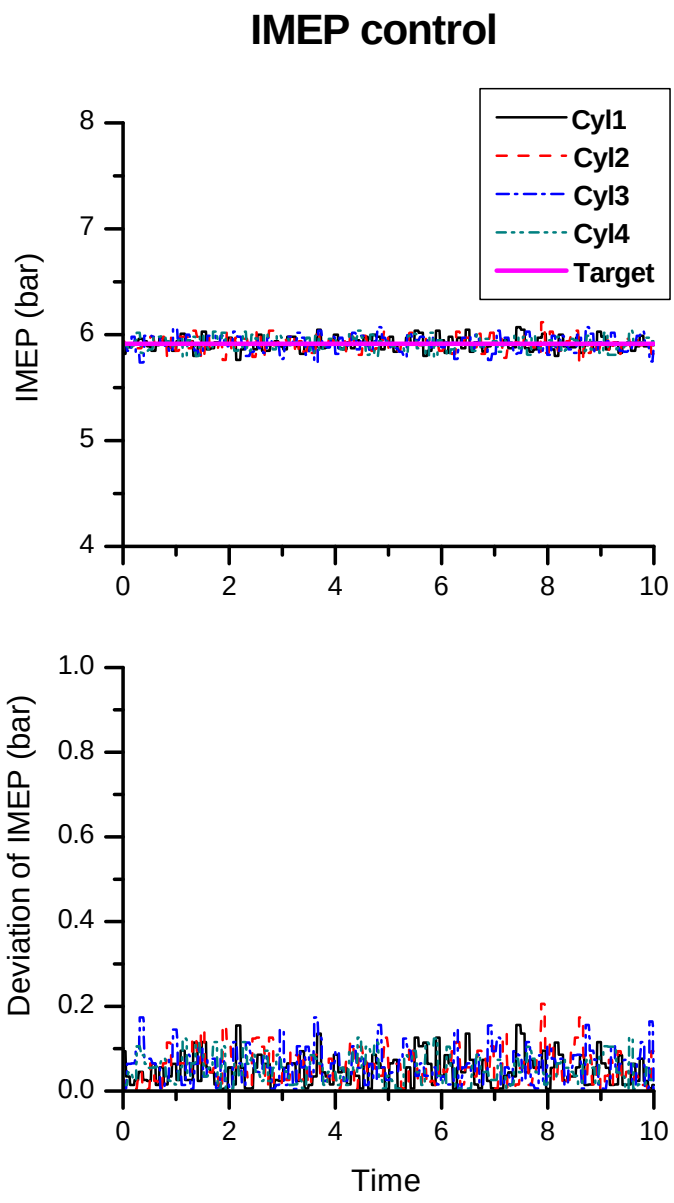

(c) With IMEP control condition

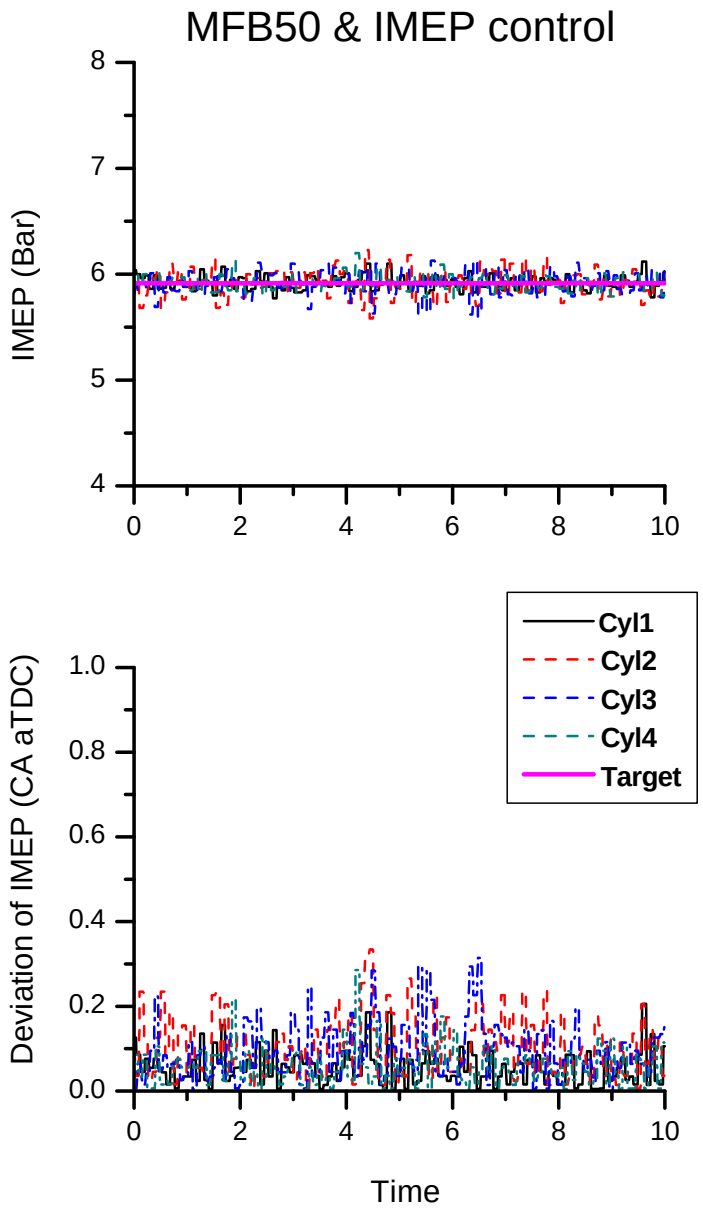

(d) With MFB50 and IMEP control condition

Figure 4.16 IMEP and variation in IMEP at the steady state (1500 rpm & BMEP of 4 bar) with application of different control conditions

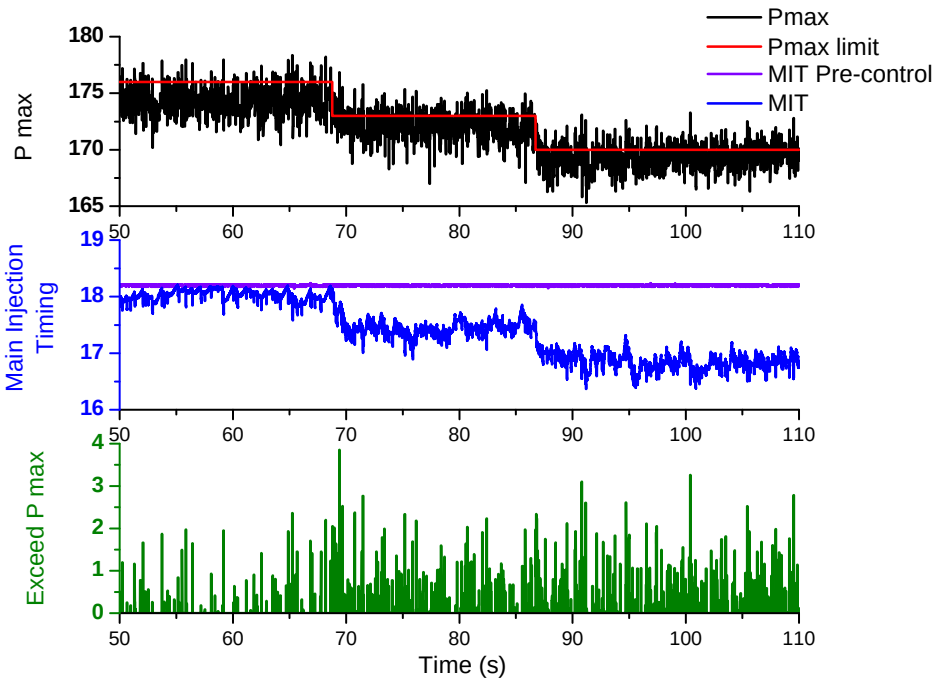

Figure 4.17 Verification of operation of the maximum pressure control algorithm

Chapter 5. Verifying the effect of Control Logic

NEDC mode driving test was performed with various control conditions to verify the effect of combustion control in transient conditions. Control conditions were divided into four which are open-loop control, MFB50 control, IMEP control, and, MFB50 and IMEP control. Additional experiment was performed to validate the effect of combustion control in engine load and speed decreasing conditions.

IQA code was modified to simulate the degradation of injector, representing deterioration of engine component. IQA code was modified to simulate injector which injects less and more fuel than injection signal. The effect of combustion control with modified IQA code was verified by performing NEDC mode test. Control modes were divided into four which are open-loop control, MFB50 control, IMEP control, and, MFB50 and IMEP control. Engine-out emissions of each control conditions were compared with each other.

5.1 Driving test at NEDC mode

A NEDC mode driving experiment was performed to measure the amount of emissions of the exhaust gas when control logic was applied. At this stage, MFB50 target compensating with using EGR rate model was not activated. In this chapter, the effect of tracking the MFB50 and IMEP target was verified solely. NEDC mode

is a driving mode, which is widely used in Europe, to measure the fuel efficiency and the emission of the exhaust gas. NEDC consists of ECE-15, which simulates the urban driving, and EUDC which simulates the high-way driving. In NEDC mode, a car travels the total distance of 11 km within 1180 seconds with an average speed of 33.6 km/h and the maximum speed of 120 km/h. Figure 5.1 shows the vehicle speed profile of NEDC mode [3].

The Table 5.1 represents the amount of emissions of the exhaust gas from an engine for each substance under no control; results are normalized to the base conditions. When MFB50 control is activated, the emission of soot is reduced by 10% at the same fuel consumption rate. The amount of soot emission is greater at the high speed range, EUDC, because the main injection timing is advanced to trace the MFB50 under acceleration. Also, when control is not applied, the emission of soot reaches the peak value, where the required torque drops sharply, but this phenomenon fades away under the control of MFB50 shown as Figure 5.2. In contrast, the amount of the emission of HC increases by 4~5 % because, when the injection timing is advanced, the ignition-delay gets longer [36]. The amount of emissions of CO and NOx remain almost constant.

Table 5.1 The amount of exhaust gas emissions at NEDC driving with the application of combustion control

	CO (%)	HC (%)	NOx (%)	Soot (%)	F.C. (%)
Base	100.0	100.0	100.0	100.0	100.0
MFB50 Control	99.7	104.6	100.0	89.2	100.4
IMEP Control	103.9	105.0	99.5	101.3	100.4
MFB50+IMEP Control	100.4	104.3	102.3	90.2	100.0

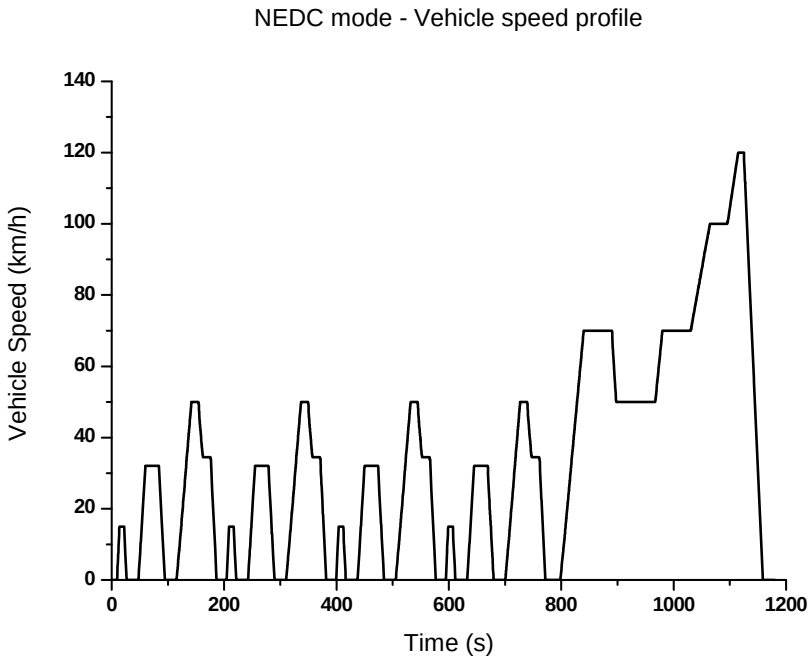

Figure 5.1 Vehicle speed profile of NEDC mode

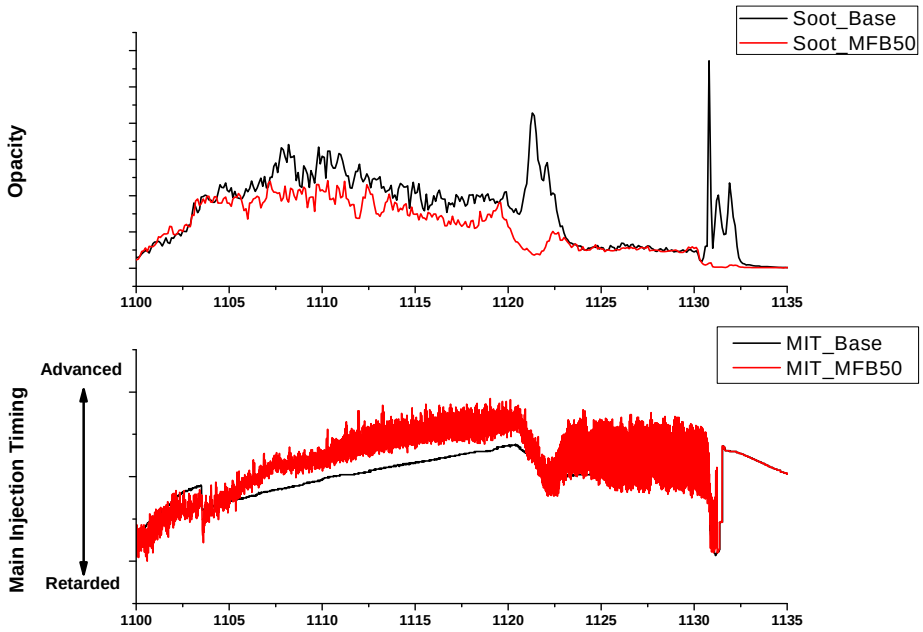

Figure 5.2 Analysis of reduction in the emission of soot under the application of MFB50 control

5.2 **Suppression of NOx emissions in transient condition**

When the engine load is in transient state, air and EGR supply system shows time lag [67, 68]. Then, EGR rate is not maintained like as steady state. It causes undesired in-cylinder gas condition, not same to the steady state, that generates more harmful emissions. This phenomenon is occurred by two sources, boost pressure delay and EGR gas supplying delay. Actual boost pressure is always slower than target boost pressure at transient condition because of the inertia of turbocharger turbine/compressor, filling the intake system. For example, if the engine load is decreased abruptly, declining of actual boost pressure is always slower than the declining of target boost pressure as in Figure 5.3. Engine load is dropped from BMEP of 5 bar to 1 bar while the engine speed is maintained at 1750 rpm. EGR gas flow rate is determined by the difference between exhaust manifold pressure and intake manifold pressure, and effective EGR valve area. At declining engine load state, exhaust gas pressure decreased as quickly as the decrease in fuel injection quantity. However, the decrease of intake manifold pressure is slower than exhaust manifold pressure. This blocks supplying the EGR gas to intake manifold [69]. Higher EGR rate is usually required when lower load output is required for the engine [70]. However, when the engine experiences sudden decrease of engine load, engine is always starving for EGR gas because of the above phenomenon. Then,

engine-out NOx emission shows a peak at this state as shown in Figure 5.4. One of the possible solutions is adjusting injection strategy according to actual EGR rate and, in this case, retarding combustion is effective solution. Therefore, as described in MFB50 control logic, target MFB50 is retarded when the actual EGR rate is lower than the target EGR rate. However the actual EGR rate is extremely hard to measure cycle-by-cycle, estimation model for EGR rate provides essential information to control NOx emission in transient condition.

Figure 5.5 shows the measured NOx emission and EGR rate during engine load decline. Target EGR rate rises while fuel injection quantity decreases and the gap between target EGR rate and actual EGR rate increases. However, main injection timing is retarded due to retarded target MFB50 and NOx emission peak is removed unlike the case without control. Controlling MFB50 with EGR rate information is effective to maintain NOx emission at low level in transient state.

Figure 5.6 shows the measured NOx emission and estimated EGR rate during simultaneous decline of engine load and speed. Similar to the load decreasing case, there is large gap between estimated EGR rate and target EGR rate. NOx peak is shown again without considering EGR rate but NOx peak is removed again when considering the EGR rate gap between estimated and target EGR rate.

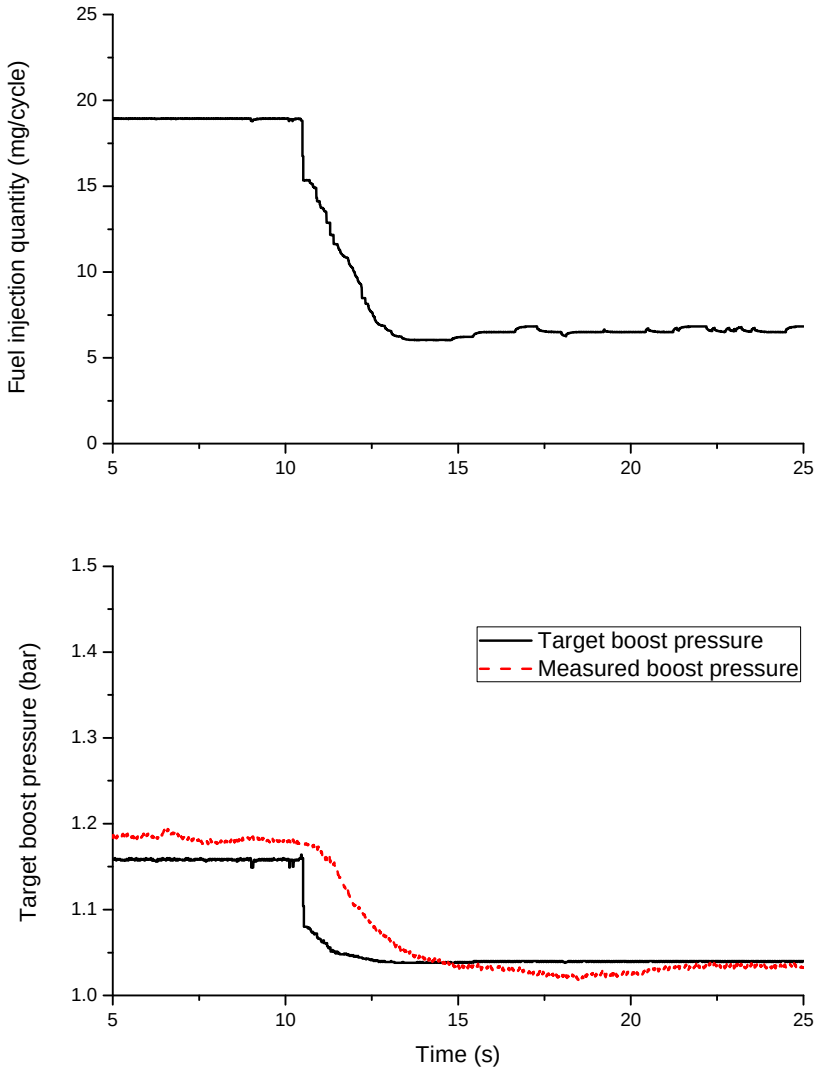

Figure 5.3 Behavior of target boost pressure and actual boost pressure at load decline

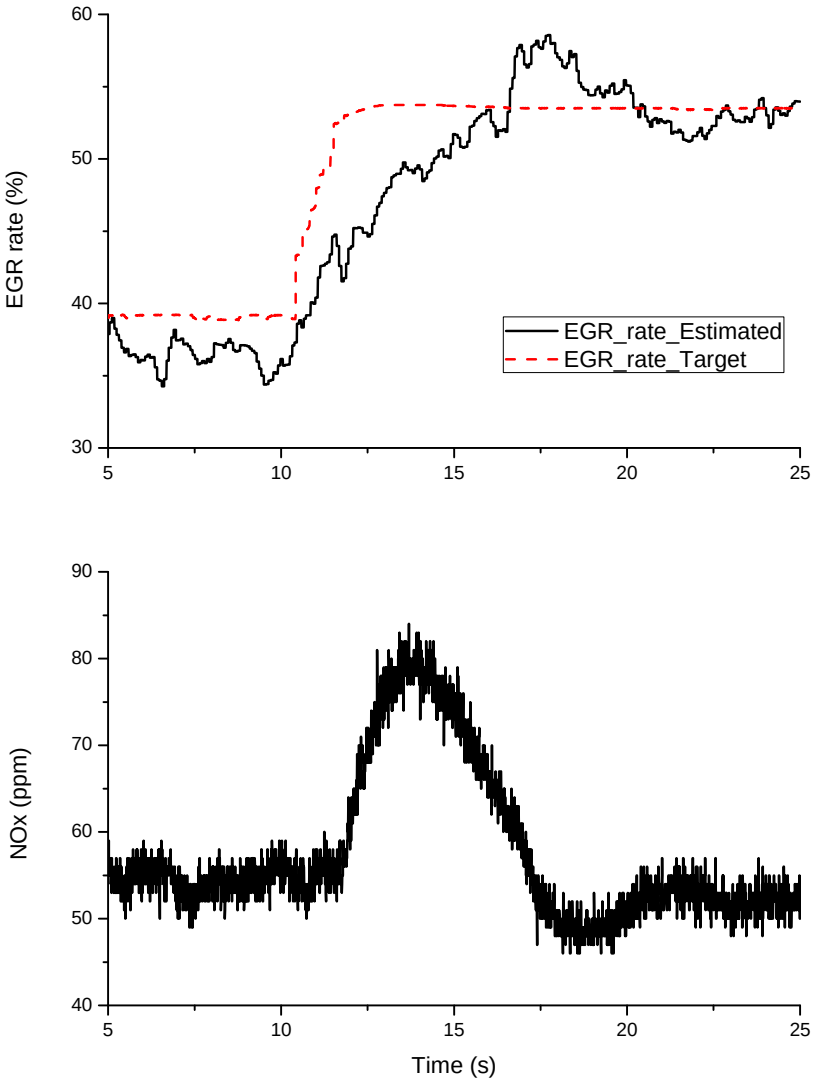

Figure 5.4 Behavior of target and estimated EGR rate, and NOx emission at load decline

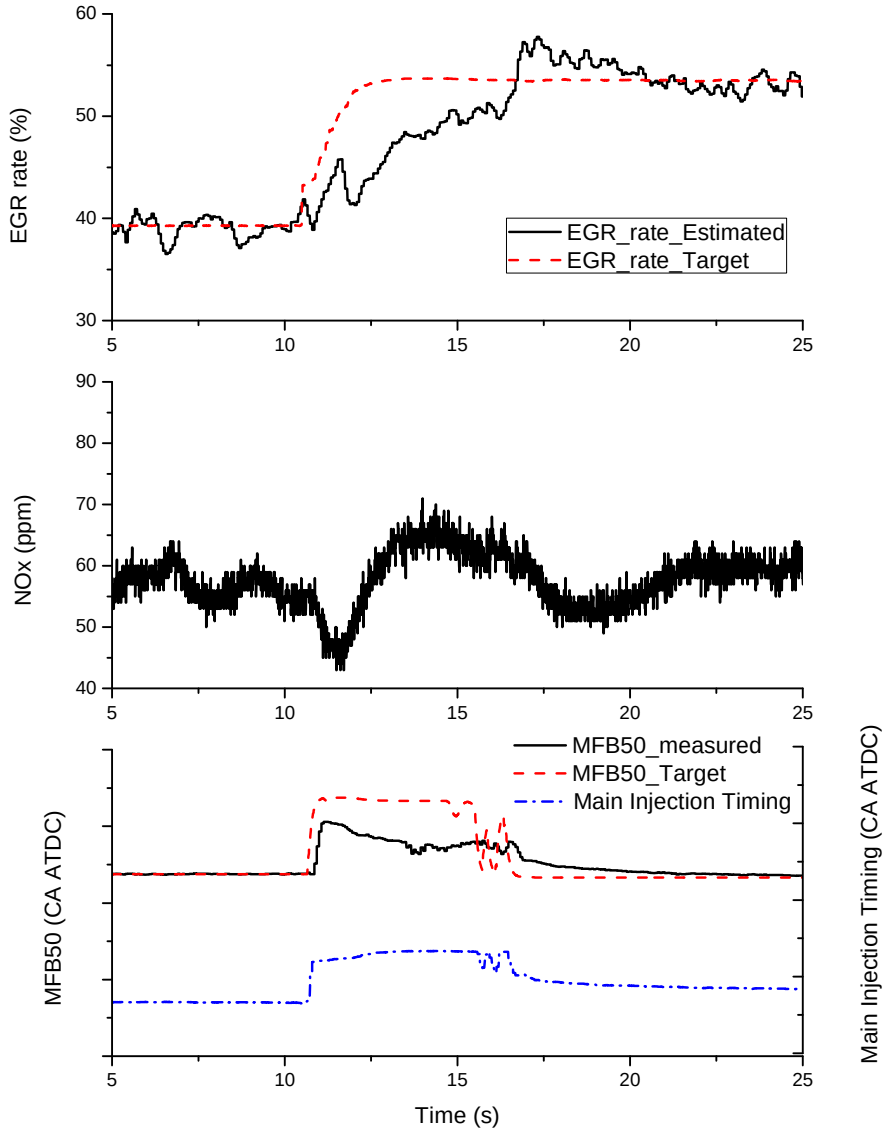

Figure 5.5 Removing of NOx emission peak with modified MFB50 target

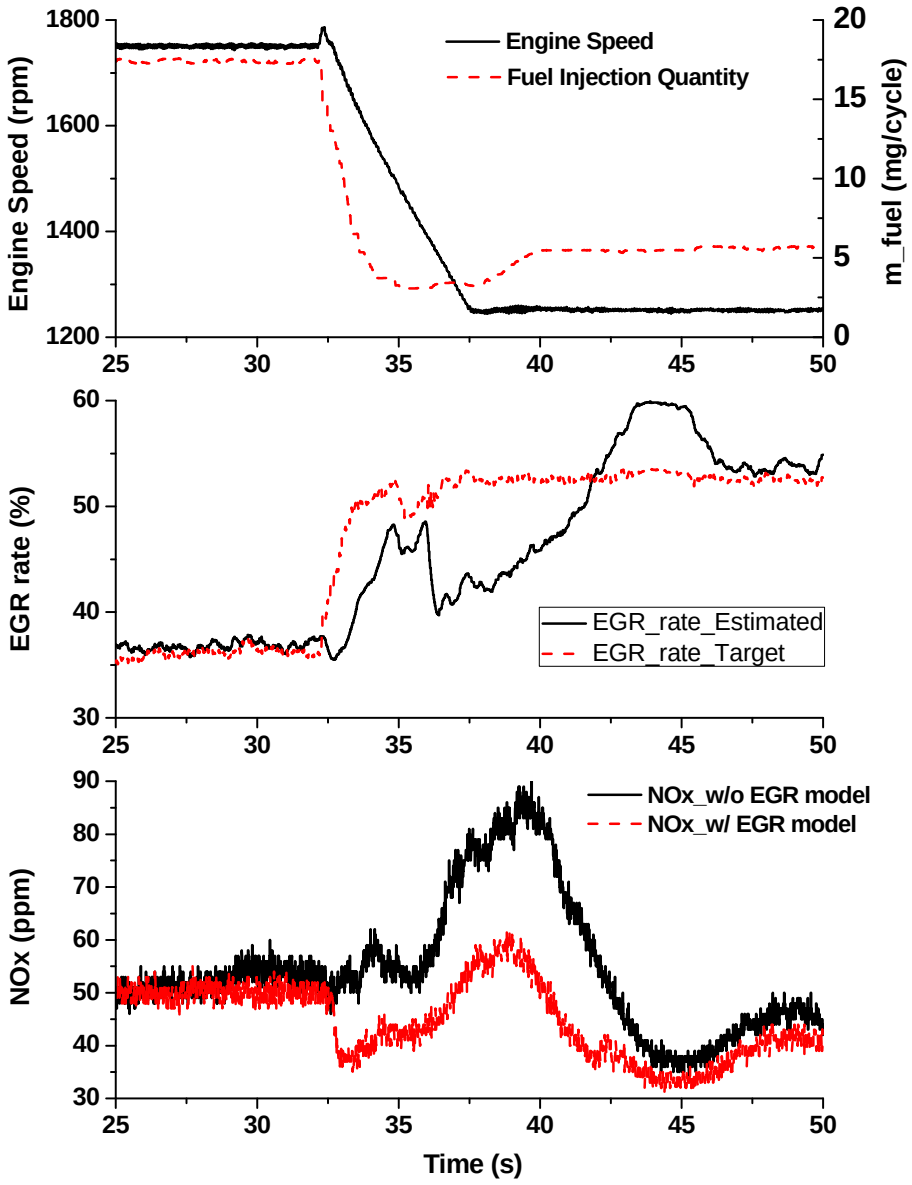

Figure 5.6 Removing of NOx emission peak with modified MFB50 target

5.3 **Injector deviation experiment**

Characteristics of emissions of exhaust gas of a diesel engine are largely affected by the characteristics of an injector. However, an injector operates at very severe conditions such as high temperature and high pressure, so the performance can vary depending on driving conditions of the vehicle [71]. A simultaneous control of MFB50 and IMEP is expected to encounter the performance variation and minimize deterioration of the performance caused by aging of the injector.

In this study, IQA code was modified to simulate injector deterioration. IQA code is a correction factor of tolerances at each point in the characteristics map for each injector. It influences on the fuel injection quantity by adjusting the energizing time of the individual injector. IQA code is composed of the correction factor at idle condition, pilot injection, emission point, part load and full load conditions. IQA codes for installed injectors were inputted to minimize the variation of each engine's emission performance [72].

The injector modified for less fuel injection than injection order using IQA code is called minimum injector and the injector modified for more fuel injection than injection order is called maximum injector. IQA code for minimum injector experiment forced ECU to recognize that installed injector injects more fuel than injection signal without IQA code. After this modification, ECU orders this injector

to inject less fuel than target fuel injection quantity determined by the map data. IQA code for maximum injector experiment is modified in the opposite way to inject more fuel than injection order.

By changing the IQA code of an injector, a minimum injector- which injects less amount of fuel than the ordered amount from the ECU- and a maximum injector- which works in the opposite way of the minimum injector- can be described, and, it is found out that the characteristics of emissions of exhaust gas are differ by a large margin, if NEDC mode driving is performed at the IQA code state for each. Also, comparisons made between different conditions for each injector conditions; no control, MFB50 control, IMEP control, and, simultaneous control of MFB50 and IMEP to measure the characteristics of emissions of exhaust gas under the NEDC mode driving. Especially in this study, the difference range in the amount of emissions of exhaust gas affected by a change in the characteristics of injectors is the main consideration.

Table 5.2 represents the difference in the amount of emissions of exhaust gas affected by the change in the characteristics of injectors under different control conditions. Under the base condition, where no control is applied, the difference in the exhaust gas according to three injector situations are 44.9 %, 67.1%, 10.1 % and 46.4% for CO, HC, NOx and soot, respectively. When MFB50 control is applied, the

difference in the exhaust gas tends to reduce for CO and HC. Deterioration of combustion due to the change in the characteristics of injectors is compensated and the combustion stability is secured by the MFB50 control which controls the main injection timing. When IMEP is controlled, not only the difference range in the amount of emissions of CO and HC are reduced but also the difference range in the amount of emission of soot is reduced. When both MFB50 and IMEP are controlled, the difference range in the amount of all measured exhaust gas reduces. The difference ranges in the amount of emission for CO and HC are reduced to less than 30 % and, for NOx and soot, are reduced to less than 5 %. In short, although the characteristics of injectors are changed, the characteristics of the combustion show more similar trend as a standard injector. The changes in the characteristics of torque generation of an engine and the ignition timing due to the deterioration of injectors are compensated by the combustion control logic.

The emissions ranges for each control conditions are summarized in Table 5.3. Range is the gap between maximum and minimum emission result among three injector tests. The results are normalized with the range of without control condition. As it can be seen, the range is decreased for all of measured emissions. Especially, reduction of soot emission range is remarkable when the MFB50 and IMEP control is activated. The result is re-displayed in Figure 5.7. Each axis means normalized

emissions data. Gray area is the emissions range result without control, and checker patterned area is the emissions range result with control logic. It is found that variations of emissions are decreased simultaneously. According to the results, control logic is effective to compensate injector variation or to overcome defect of injector.

Emission characteristics with the minimum and the maximum injectors are normalized by emission results with the base condition of the base injector. Figure 5.8 shows the emission results with the minimum injector. CO and HC emissions with the minimum injector are increased due to the excessive air supply and deterioration of combustion. However, NOx emission is decreased because of low flame temperature with deteriorated combustion. Soot emission is diminished because soot oxidation is enhanced by intense air-fuel mixing due to the overcharged air. With the MFB50 and IMEP controls, CO and HC emissions are decreased about 20~30 %, and, NOx and soot emissions are slightly increased. In other words, in-cylinder combustion characteristics are recovered back to the base injector condition.

Figure 5.9 shows the emission results with maximum injector. Soot emission with maximum injector is increased due to dense fuel droplets and an air-starved condition. Soot emission is increased about 25 % with the maximum injector and air-fuel mixing is deteriorated due to the increase in the amount of fuel. Soot

emission is stabilized with the IMEP control logic and less soot emission is generated than the base condition of the base injector. IMEP control logic is holding the fuel injection quantity to the base injector. NOx emission is increased about 3 %. Flame temperature is higher when the A/F ratio approaches to stoichiometric ratio. A diesel engine is operated usually under a lean condition and a rich injector leads to richer A/F ratio adjacent to the stoichiometric condition. Higher A/F ratio generates higher flame temperature and more NOx emission is formed. NOx emission is decreased to the base level with the control because the A/F ratio is returned to the base condition. On the other hand, CO and HC emissions of maximum injector are maintained the same level to that of the base injector and these levels were maintained regardless of control conditions.

Table 5.2 Variation in exhaust gas emissions under different control conditions caused by different injectors

Control	Injector Type	CO	HC	NOx	Soot	Fuel Consumption
Base	Minimum Injector	144.0	162.5	92.7	78.8	99.3
	Base Injector	100.0	100.0	100.0	100.0	100.0
	Maximum Injector	99.2	95.4	102.8	125.2	100.0
	Range	44.9	67.1	10.1	46.4	0.7
MFB50 Control	Minimum Injector	128.8	110.0	89.8	93.4	98.6
	Base Injector	100.0	100.0	100.0	100.0	100.0
	Maximum Injector	97.4	90.7	101.7	136.3	99.9
	Range	31.3	19.3	11.8	42.8	1.4
IMEP Control	Minimum Injector	125.0	124.1	95.8	87.0	98.5
	Base Injector	100.0	100.0	100.0	100.0	100.0
	Maximum Injector	92.4	90.6	104.5	105.7	99.9
	Range	32.7	33.5	8.6	18.7	1.5

MFB50 + IMEP Control	Minimum Injector	123.7	121.0	95.5	95.2	99.5
	Base Injector	100.0	100.0	100.0	100.0	100.0
	Maximum Injector	94.5	93.1	97.9	95.3	100.5
	Range	29.1	28.0	4.5	4.8	1.1

Table 5.3 Emission ranges for each control conditions which is normalized by the base condition

Control	CO (%)	HC (%)	NOx (%)	Soot (%)
Base	100	100	100	100
MFB50 Control	69.7	30.1	116.6	82.3
IMEP Control	75.7	52.4	84.9	40.9
MFB50+IMEP Control	65.3	43.5	45.5	9.3

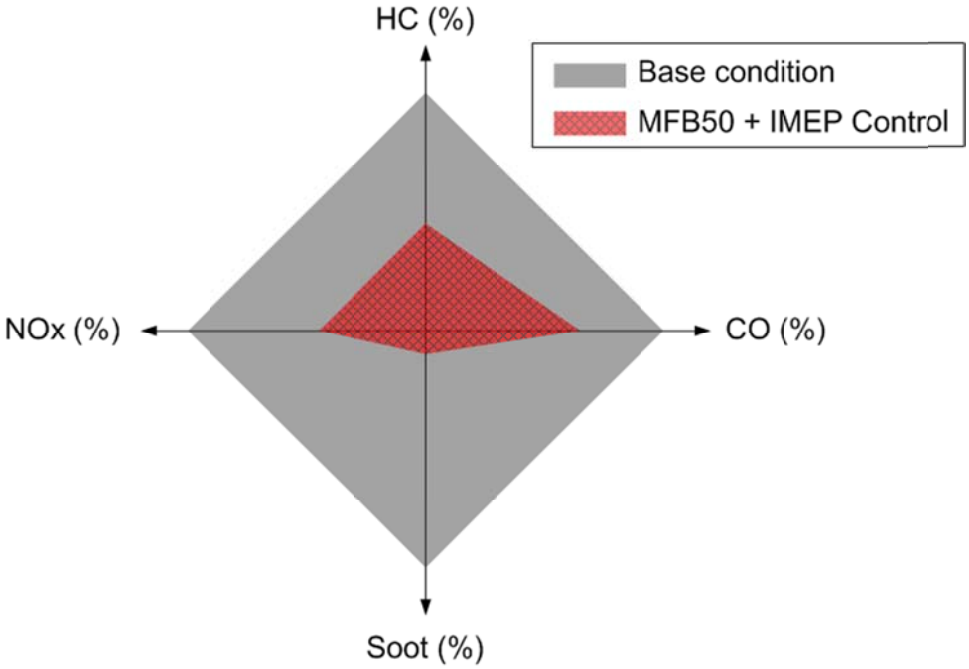

Figure 5.7 Emission ranges for each control conditions which is normalized by the base condition

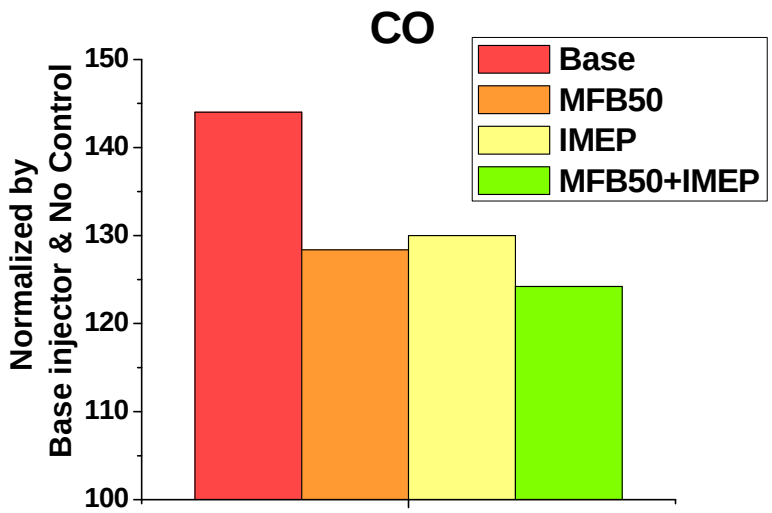

(a) CO emission

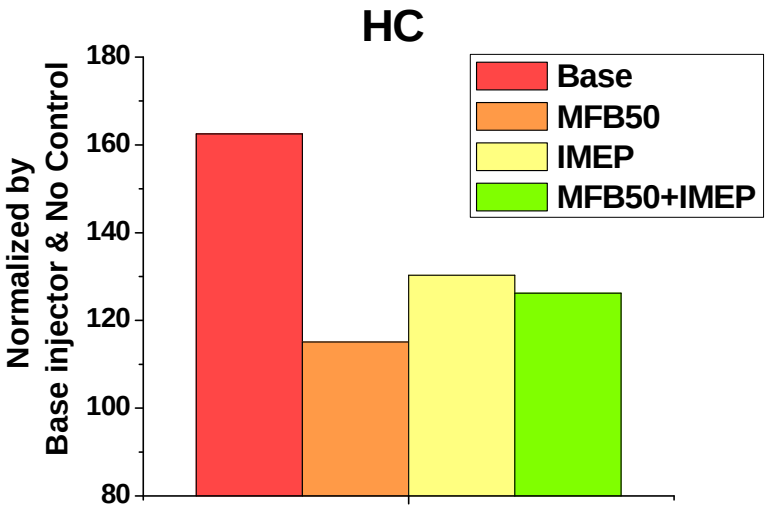

(b) HC emission

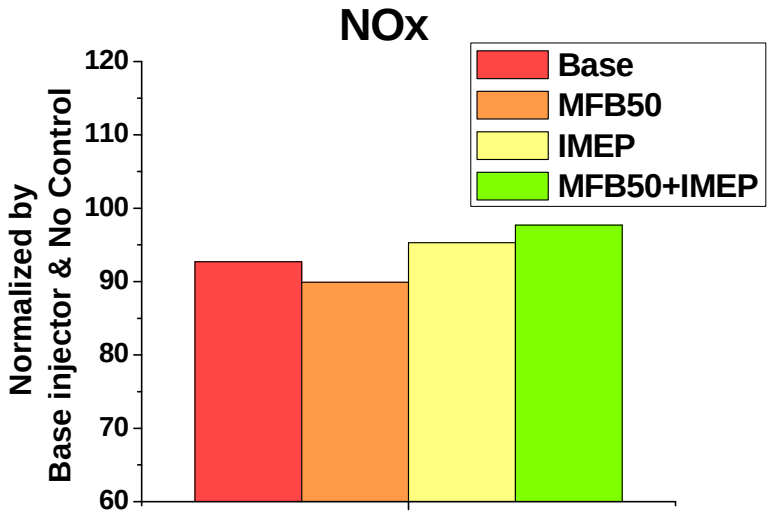

(c) NOx emission

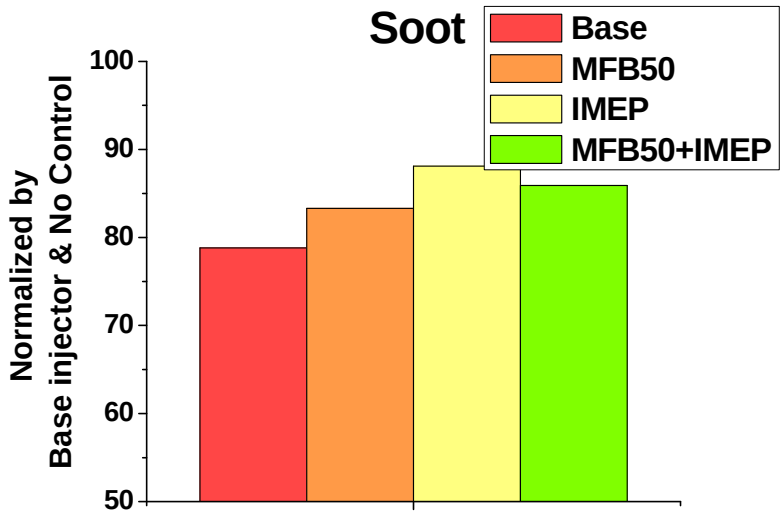

(d) Soot emission

Figure 5.8 Emissions characteristics with the minimum injector

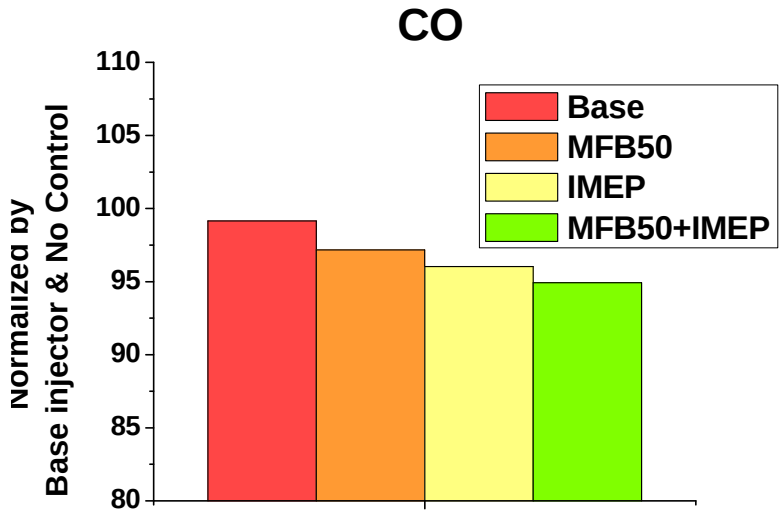

(a) CO emission

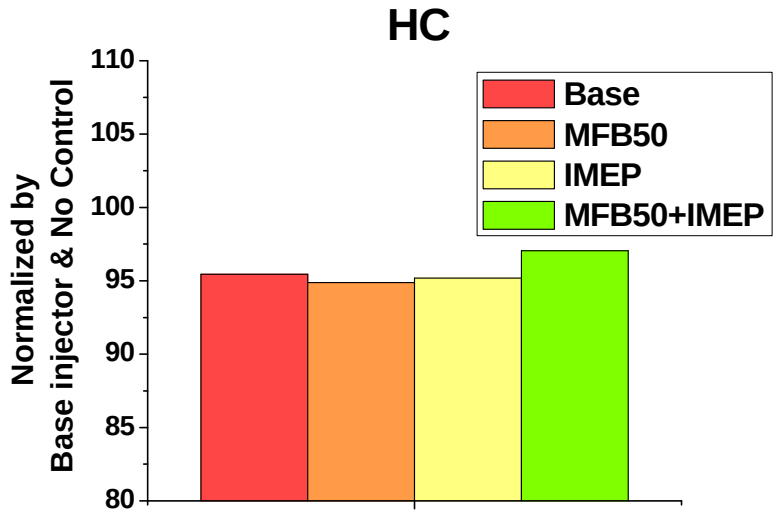

(b) HC emission

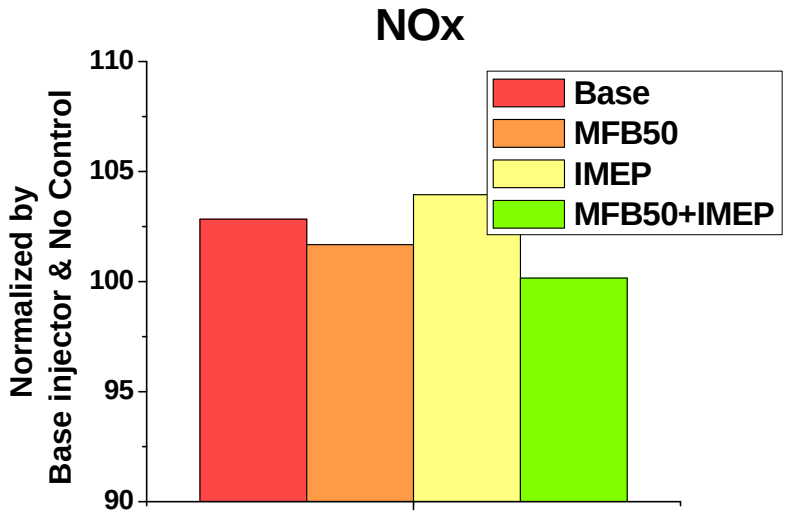

(c) NOx emission

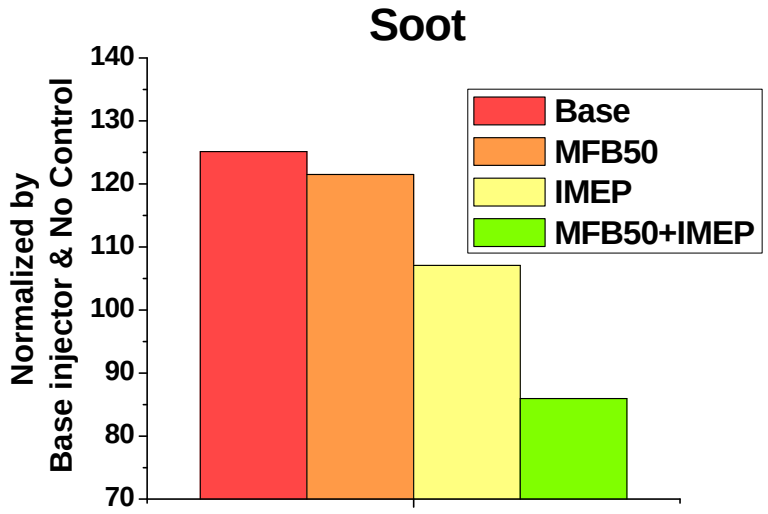

(d) Soot emission

Figure 5.9 Emissions characteristics with the maximum injector

Chapter 6. Conclusions

In this study, the effect combustion control using in-cylinder pressure signal on emission characteristics and deterioration of engine components were examined by multi-cylinder diesel engine experiments in transient state.

To control MFB50 and IMEP in real-time, a real-time combustion analyzer based on the in-cylinder pressure was built at the first time. The operating process of the analyzer was to finish its analysis at the end of each cycle and the analysis results were successfully applied to the control of next cycle. To finish the analysis in time, the analysis range and the calculation process were optimized. Heat release rate analysis window was limited from 40 ° BTDC to 90 ° ATDC and the heat loss to the cylinder wall was ignored. IMEP calculation begins at BDC after the firing, exhaust stroke, but pressure data acquisition for one cycle is not completed at this state. To calculate IMEP using pressure data of 720 °CA, pressure data at exhaust stroke of the previous cycle was used. In addition to the MFB50 and IMEP, maximum cylinder pressure and pressure data at intake valve closing was sent to the combustion control operator. By using this calculation scheduling and optimizing, the combustion analyzer developed in this study can export when the cycle terminates, all the analyzed combustion parameters are extracted to be used for the next cycle.

EGR rate prediction model was developed based on the ideal gas equation of state. Input data was acquired from the ECU variables except for the cylinder pressure. There are several assumptions to calculate the EGR rate with limited engine information, such as constant residual gas ratio and ignoring heat transfer in the intake manifold. The EGR rate model was verified in several engine operating conditions, where the EGR gas supplying is activated. The coefficient of determination between measured EGR rate and estimated EGR rate is derived as 0.9397 and it shows meaningful agreement between measurement and estimation.

The controlled variables in this research were MFB50, IMEP and maximum pressure which are calculated by developed combustion analyzer. MFB50 and IMEP are representing the combustion phase and the engine-out torque, respectively. The real MFB50 was adjusted to the target MFB50 by controlling the main injection timing and the IMEP was controlled via the energizing time of the main injection quantity. Maximum cylinder pressure was controlled to maintain target level by controlling main injection timing. Control areas of MFB50 and maximum cylinder pressure are divided using hysteresis. The closed-loop control was based on PID control and the difference between the target engine operating condition and the measured operating condition was diminished by means of the logic. The control logic was verified through steady-state, and, step load and engine speed change

experiments. Even though the engine operating condition was changed stepwise, the actual MFB50 and IMEP followed the target values with the control logic in a short time.

The effect of the combustion control logic was tested through the NEDC mode driving, experiment of transient state. Soot formation decreased about 10% with activating both MFB50 and IMEP control, while the amount of other emissions remains almost constant. Correction factor derived by the EGR rate shows another effect on NOx emission in transient state. Target MFB50 was retarded when the estimated EGR rate is lower than target EGR rate, determined by steady state experiment. Main injection timing was retarded to track the modified target MFB50 and NOx emission peak at deceleration state was removed due to the retarded main injection timing.

The beneficial effect of the control logic increased with defective fuel injector conditions. Engine-out emissions with defective injectors showed wide ranges of variation from the normal injector condition, for example, HC emission was increased 62.5 % with the minimum injector. However, the emissions ranges were reduced with the MFB50 and IMEP control logic, and soot emission range with combustion control was decreased to one tenth of the soot emission range without

combustion control. The combustion control logic was effective to prevent deterioration of emission performance with the defected injectors.

From the conclusions above, engine control using the in-cylinder pressure data has a function to control emissions peak at transient conditions. It can also compensate the deterioration of engine components during the operation due to the aging or damaging. However, stability and accuracy of the in-cylinder pressure transducer over time, and reliability of pressure sensor itself is still a fundamental requirement to be proven for enabling an exact combustion analyzing, EGR rate estimation or combustion control at transient state.

Bibliography

1. Choi, S., “The Effects of In-Cylinder EGR Stratification on Combustion and Emission Characteristics in a Diesel Engine”, Ph.D. thesis, School of mechanical and Aerospace Engineering, Seoul National University, 2010.
2. Guillemin, F. Grodin, O. Chauvin, J. and Nguyen, E., “Combustion Parameters Estimation Based on Knock Sensor for Control Purpose Using Dedicated Signal Processing Platform”, SAE paper 2008-01-0790, 2008.
3. http://www.dieselnet.com/standards/
4. Punater, A. Ripley, G. and Schten, K., “Controller for Rapid Development of Advanced Mode Combustion Algorithm using Cylinder Pressure Feedback”, 2008 Convergence Transportation Electronics Association, 2008.
5. Ministry of Knowledge Economy, Republic of Korea. “Long term roadmap for regulation of vehicle fuel economy to cope with United Nation Framework Convention on Climate Change (UNFCCC)”, 2009.
6. Johnson, T., "Diesel Emissions in Review," SAE Int. J. Engines 4(1):143-157, 2011.``
7. Mori K., Matsuo S., Nakayama S., Shiino S., Kawatani T., Nakashima K. and Takeda Y., “Technology for Environmental Harmonization and Future of the Diesel Engine”, SAE paper 2009-01-0318, 2009.
8. Yoon, M., Lee, K. and Sunwoo, M. “A method for combustion phasing control using cylinder pressure measurement in a CRDI diesel engine”, Mechatronics 17, pages 469-479, 2007.
9. Ohyama, Y. “Engine control using combustion model”, IJAT, Vol 2, No.2, pages 53-62, 2001.
10. Kirchen P., Obrecht P. and Boulouchos K., “Soot Emission Measurements and Validation of a Mean Value Soot Model for Common-Rail Diesel Engines during Transient Operation”, SAE paper 2009-01-1904, 2009.

11. Hagena J.R., Filipi Z.S. and Assanis D.N., “Transient Diesel Emissions: Analysis of Engine Operation During a Tip-In”, SAE paper 2006-01-1151, 2006.
12. Kang H. and Farrell P. V., “Experimental Investigation of Transient Emissions (HC and NOx) in a High Speed Direct Injection (HSDI) Diesel Engine”, SAE paper 2005-01-3883, 2005.
13. Youssef B., Guillemin F., Solliec G. L. and Corde G., “In Cylinder Trapped Mass Estimation In Diesel Engines Using Cylinder Pressure Measurements”, 2011 IEEE International Conference on Control Applications, 2011.
14. Worm J., “An Evaluation of Several Methods for Calculating Transient Trapped Air Mass with Emphasis on the “Delta P” Approach”, SAE paper 2005-01-0990, 2005.
15. Mladek M. and Onder C. H., “A Model for the Estimation of Inducted Air Mass and the Residual Gas Fraction using Cylinder Pressure Measurements”, SAE paper 2000-01-0958, 2000.
16. Colin G., Giansetti P., Chamaillard Y. and Higelin P., “In-Cylinder Mass Estimation using Cylinder Pressure”, SAE paper 2007-24-0049, 2007.
17. Desantes J.M., Galindo J., Guardiola C. and Dolz V., “Air mass flow estimation in turbocharged diesel engines from in-cylinder pressure measurement”, Experimental Thermal and Fluid Science 34, pages 37-47, 2010.
18. Klein P. and Gruter R., “Real-Time Estimation of the Exhaust Gas Recirculation Ratio Based on Cylinder Pressure Signals”, SAE paper 2007-01-0493, 2007.
19. Chauvin J., Petit N. and Rouchon P., Corde G. and Vigild C., “Air Path Estimation on Diesel HCCI Engine”, SAE paper 2006-01-1085, 2006.
20. Park Y., Lee H., Kim J., Lee K. and Sunwoo M., “Cylinder Air Charge Estimation for a Diesel Engine Equipped with VGT, EGR, and SCV”, SAE paper 2011-01-1148, 2011.
21. Lee H., Park Y., Kim J., Lee K. and Sunwoo M., Development of model based

EGR mass flow rate estimation algorithm in a diesel engine", KSAE 2010 annual conference KSAE10-A0005, 2010.

22. Wahlstrom J. and Eriksson L., "Modeling of a Diesel Engine with VGT and EGR including Oxygen Mass Fraction", Vehicular systems, Department of Electrical Engineering, 2006.
23. Park Y., "Mean Value Air Path Modeling for High Speed Direct Injection Diesel Engine Equipped with VGT and EGR", Master thesis, Automotive Engineering, Hanyang University, 2009.
24. Eck C., Konigorski U., Cianflone F., Landsmann G., "Fault Detection System for the Air Path of Common Rail Diesel Engines with Low Pressure EGR", SAE paper 2011-01-0701, 2011.
25. Darlington A., Collings N. and Glover K., "Diesel Cylinder Charge Properties: Feed-Forward Control and Cycle-by-Cycle Analysis Using an In-Cylinder Gas Sampling System", SAE paper 2011-01-0709, 2011.
26. Welling O. and Collings N., "UEGO Based Measurement of EGR Rate and Residual Gas Fraction", SAE paper 2011-01-1289, 2011.
27. Han Y., Liu Z., Zhao J., Xu Y., Li J. and Li K., "EGR Response in a Turbo-charged and After-cooled DI Diesel Engine and its Effects on Smoke Opacity", SAE paper 2008-01-1677, 2008.
28. Kim D., Oh B., Ok S., Lee K. and Sunwoo M., "Cylinder Pressure based Real-Time IMEP Estimation of Diesel Engines", KSAE paper, Vol. 17, No. 2, pages 118-125, 2009.
29. AVL, "Cylinder Pressure Based Engine Control System, CYPRESS", 2008.
30. Carlucci A. P., Chiara F. F. and Laforgia D., "Block Vibration as a Way of Monitoring the Combustion Evolution in a Direct Injection Diesel Engine", SAE paper 2006-01-1532, 2006.
31. Goldwine G., G.deBotton, Rivin B. and Sher E., "Studying the Relationship between the Vibration Signature and the Combustion Process in Diesel Engines", SAE paper 2004-01-1786, 2004.

32. Hariyanto A., Bagiasna K., Asharimurti I., Wijaya A. O., Reksowardoyo K. I. and Arismunandar W, “Application of Wavelet Analysis to Determine the Start of Combustion of Diesel Engines”, 2007-01-3556, 2007.
33. Arnone L., Boni M., Manelli S., Chiavola O., Conforto S. and Recco E.,” Diesel Engine Combustion Monitoring through Block Vibration Signal Analysis”, SAE paper 2009-01-0765, 2009.
34. Payri F., Broatch A., Tormos B. and Marant V., “New methodology for in-cylinder pressure analysis in direct injection diesel engines - application to combustion noise” Measurement Science Technology 16, pages 540-547, 2005.
35. Asannis D. N., Filipi Z. S., Fiveland S. B. and Syrimis M., “A Predictive Ignition Delay Correlation Under Steady-State and Transient Operation of a Direct Injection Diesel Engine”, ASME J.Eng. Gas Turbines Power 125, pages 450-456, 2003.
36. Heywood J. B., “Internal Combustion Engine Fundamentals”, Mc-GrawHill, New York, 1988.
37. Katrasnik T., Trenc F. and Opresnik S. R., “A New Criterion to Determine the Start of Combustion in Diesel Engines”, ASME J.Eng. Gas Turbines Power 128, pages 928-933, 2006.
38. Cowell L. H. and Lefebvre A. H., “Influence of Pressure on Autoignition Characteristics of Gaseous Hydrocarbon-Air Mixtures”, SAE Paper 860068, 1986.
39. Glavmo M., Spadafora P. and Bosch R., “Closed Loop Start of Combustion Control Utilizing Ionization Sensing in a Diesel Engine”, SAE paper 1999-01-0549, 1999.
40. Pischinger F., Reuter U. and Scheid E., “Self-Ignition of Diesel Sprays and Its Dependence on Fuel Properties and Injection Parameters”, ASME J.Eng. Gas Turbines Power 110, 399-404, 1988.
41. Smith, J., Schulte, C., and Cabush, D., "Individual Cylinder Fuel Control for Imbalance Diagnosis," SAE Paper 2010-01-0157, 2010.

42. Rackmil, C. and McKay, D., "Sensor- Less Individual Cylinder Pressure Estimation and Closed Loop Control for Cold Start and Torque Balancing," SAE Int. J. Engines 3(1), pages 1042-1052, 2010.
43. Guillemin, F., Grondin, O., Chauvin, J., and Nguyen, E., "Combustion Parameters Estimation Based on Knock Sensor for Control Purpose Using Dedicated Signal Processing Platform," SAE Paper 2008-01-0790, 2008.
44. Byttner S. and Holmberg U., “Closed-loop control of EGR using ion currents”, 27th IASTED International Conference Modeling Identification and Control, 2008.
45. Thomas S. and Sharma R.P., “Model Based Control of Engines”, SAE transactions 2007-26-025, 2007.
46. “Audi diesel targets Bin 5, Euro 6 “, SAE Technical News Letter, http://www.sae.org/automag/technewsletter/080129DieselTech/04.htm, 2008.
47. “Honda prepares i-DTEC diesel for 2009“, SAE Technical News Letter, http://www.sae.org/automag/technewsletter/080129DieselTech/01.htm, 2008.
48. “New GM V6 diesel has cylinder-pressure monitoring”, SAE tech briefs, http://www.sae.org/automag/techbriefs/04-2007/1-115-4-22.pdf, 2007.
49. “VW Jetta SportWagen Scores High”, http://www.greencar.com/articles/vw-jetta-sportwagen-scores-high.php, 2008.
50. Haraldsson G., Tunestal P., Johansson B. and Hyvonen J., “HCCI Combustion Phasing with Closed-Loop Combustion Control Using Variable Compression Ratio in a Multi Cylinder Engine”, SAE paper 2003-01-1830, 2003.
51. Reitz R. and Ehe von der J., “Use of in-cylinder pressure measurement and the response surface method for combustion feedback control in a diesel engine”, IMechE Vol. 220 Part D: J. Automobile Engineering, 2006.
52. Hasegawa, M., Shimasaki, Y., Yamaguchi, S., Kobayashi, M., "Study on Ignition Timing Control for Diesel Engines Using In-Cylinder Pressure Sensor," SAE Paper 2006-01-0180, 2006.
53. Yoon, M., Lee, K., Sunwoo, M., and Oh, B., "Cylinder Pressure Based

Combustion Phasing Control of a CRDI Diesel Engine," SAE Paper 2007-01-0772, 2007.

54. Schnorbus T., Pischinger S., Korfer T., Lamping M., Tomazic D. and Tatur M., “Diesel Combustion Control with Closed-Loop Control of the Injection Strategy”, SAE paper 2008-01-0651, 2008.
55. Liebig, D., Krane, W., Ziman, P., Garbe, T., "The Response of a Closed Loop Controlled Diesel Engine on Fuel Variation," SAE Technical Paper 2008-01-2471, 2008.
56. Audet A. and Koch C. R., “Actuator Comparison for Closed Loop Control of HCCI Combustion Timing”, SAE paper 2009-01-1135, 2009.
57. Willems, F., Doosje, E., Engels, F., and Seykens, X., "Cylinder Pressure-Based Control in Heavy-Duty EGR Diesel Engines Using a Virtual Heat Release and Emission Sensor," SAE Technical Paper 2010-01-0564, 2010.
58. Ryan T., “HCCI—update of progress 2005”, 12th Annual Diesel Engine Emissions Reduction (DEER) Conference, Detroit, U.S.A., 2006.
59. Akihama K., Takatori Y., Inagaki K., Sasaki S. and Dean AM., “Mechanism of the smokeless rich diesel combustion by reducing temperature”, SAE paper 2001-01-0655, 2001.
60. Kimura S., Aoki O., Kitahara Y. and Aiyoshizawa E., “Ultra-clean combustion technology combining a low temperature and premixed combustion concept for meeting future emission standards”, SAE paper 2001-01-0200, 2001.
61. Olsson J., Tunestal P. and Johansson B., “Closed-Loop Control of an HCCI Engine”, SAE paper 2001-01-1031, 2001.
62. Ohmura T., Ikemoto M. and Iida N., “A Study on Combustion Control by Using Internal and External EGR for HCCI Engines Fuelled with DME”, SAE paper 2006-32-0045, 2006.
63. Kumar, R., Zheng, M., Asad, U., and Reader, G., "Heat Release Based Adaptive Control to Improve Low Temperature Diesel Engine Combustion," SAE Paper 2007-01-0771, 2007.

64. Husted, H., Kruger, D., Fattic, G., Ripley, G., "Cylinder Pressure-Based Control of Pre-Mixed Diesel Combustion," SAE Paper 2007-01-0773, 2007.
65. Guzzella L. and Onder C. H., “Introduction to Modeling and Control of Internal Combustion Engine Systems”, Springer, 2010.
66. Hong K. “A Study on the Effect of Multiple Injection on Common Rail HSDI Diesel Engine Performance and Emissions”, Master thesis, Mechanical and Aerospace Engineering, Seoul National University, 2008.
67. Yokomura, H., Kouketsu, S., Kotooka, S., and Akao, Y., "Transient EGR Control for a Turbocharged Heavy Duty Diesel Engine," SAE Paper 2004-01-0120, 2004.
68. Kalsi, K., Collings, N., Heaton, D., and Faulkner, S., "Study of Steady State and Transient EGR Behaviour of a Medium Duty Diesel Engine," SAE Paper 2008-01-2438, 2008
69. Reifarth, S. and Angstrom, H., "Transient EGR in a High-Speed DI Diesel Engine for a set of different EGR-routings," SAE Int. J. Engines 3(1), pages 1071-1078, 2010.
70. Pontoppidan, M., Demaio, A., Bella, G. and Rotondi, R., "Parametric Study of Physical Requirements for Optimization of the EGR-rate and the Spray Formation for Minimum Emissions Production Over a Broad Range of Load/Speed Conditions," SAE Paper 2006-01-1120, 2006.
71. Bright, C., Faidley, L., Witthauer, A., Rickels, E., "Programmable Diesel Injector Transducer Test Results," SAE Paper 2011-01-0381, 2011.
72. http://www.scribd.com/doc/65176553/Classe-de-Injetor-Bosch

초 록

전 세계적으로 각종 자동차 관련 배기 규제 및 지구 온난화로 인한 CO_2 규제가 한층 강화되고 있다. 이러한 규제에 대응하기 위하여 여러 엔진 부가 장치 및 제어 기술이 소개되고 있다. 이 중 HSDI (High Speed Direct Injection) 디젤 엔진에 대해서는 연소제어 기술이 배기가스 저감은 물론 엔진 구성품의 열화에도 대응할 수 있는 기술로서 주목받고 있다. 또한 최근 실린더 내 압력 측정 기술의 발전으로 기술 적용에 의한 비용 상승 폭이 점차 줄어들고 있다.

본 연구에서는 실린더 내 연소 압력을 기반으로 한 엔진 제어 로직을 개발하였다. 실린더 내 연소 현상을 대표하는 변수로서는 MFB50과 IMEP를 선정하였다. 이에 더하여 연소 제어 기술을 이용하여 실린더 내 최고 압력을 제한하는 알고리즘 구성하여 엔진 내구성 및 최대 출력 향상에 기여할 수 있도록 하였다. 또한 실시간 EGR률 예측 모델을 적용하여 실린더 내 가스 조성을 연소 제어 로직에 반영할 수 있도록 하였다.

MFB50을 제어하기 위한 변수로서 주 연료 분사시기를 선정하였고, 저부하 영역부터 중부하 영역 구간에서 목표 MFB50을 추종하도록 PID

제어를 이용하였다. 최고 부하 영역에서는 주 연료 분사시기를 조절하여 실린더 내 최고 압력을 지정한 수준 이하로 제어하는 로직이 구현되었다. IMEP를 제어하기 위한 변수로서는 주 연료 분사의 분사 기간을 선정하였고, 연료 분사 기간을 제어하여 목표 IMEP를 추종하는 것을 확인하였다. 완성된 연소 제어 로직은 NEDC 모드 등의 과도 상태 운전 조건에서 성능 검증을 수행하였다. 연소 제어 로직을 통하여 과도 상태 운전에서 배기 배출물의 급격한 증가를 제거하고 일정한 수준을 유지하는 것을 확인하였다. 또한 연소제어 로직을 이용하여 연료 분사계의 열화에 의한 배기배출물 특성 악화 현상을 완화시킬 수 있는 것을 확인하였다.

주요어 : 직접분사식 디젤 엔진, 모델 기반 제어, 폐회로 제어, 배기가스 유해 물질, 과도 상태, 연료 분사계 열화

학번 : 2005-23445